ENGINEERING AND OPTIMIZING PHYSIOLOGICAL CELL ISOLATION VIA THE SECONDARY ANCHOR TARGETED CELL RELEASE SYSTEM

BY

ALI ANSARI

DISSERTATION

Submitted in partial fulfillment of the requirements
for the degree of Doctor of Philosophy in Bioengineering
in the Graduate College of the
University of Illinois at Urbana-Champaign, 2018

Urbana, Illinois

Doctoral Committee:

Assistant Professor Princess Imoukhuede, Chair
Professor Catherine J. Murphy
Professor Rohit Bhargava
Professor Rashid Bashir

ABSTRACT

Cancer treatment regimens, such as chemotherapies are fundamentally limited through patient drug resistance, as patients respond differentially due to these individualized resistances and differences in biomarker expression on cells. Quantification of these biomarkers, then, would allow a methodology for designing personalized treatments and regimens that the patients would no longer be resistant to. However, techniques designed to purify or isolate cells to quantify these biomarkers are not designed to maintain physiological cell expression. In order to develop an isolation modality to preserve receptor numbers, I have developed and optimized the Secondary Anchor Targeted Cell Release (SATCR) system to separate out cells of interest for downstream analysis. The SATCR enables both capture and release of cells through the targeting of the secondary anchor- streptavidin- through the introduction of 4mM biotin into the system. The system has been optimized to preserve physiological wall shear stress, receptor quantity and cell diameter of cells isolated through the system. This allows for our system to create a more physiologically faithful modality for downstream analysis- potentially opening the door to more physiological analyses of purified cell samples for personalized medicine.

Surface functionalization allows for the customization and adaption of surfaces for a variety of needs and applications. We have used surface functionalization to adapt glass and PDMS surfaces with the SATCR surface, but there exists a great deal of mineable space for surface functionalization and its adoption in existing modalities. This space includes moving the SATCR surface from static glass based systems into dynamic microfluidic glass and PDMS systems, and possibly even further to non-standard functionalized materials such as polyvinyl chloride. The functionalization of alternate materials would allow further customization and easier adoption of the capture surface into other substrates, further increasing the utility and

degrees of freedom for the SATCR capture surface. In addition to substrate alteration, further adaptions and modifications can advance and optimize the SATCR technology to enable more effective and selective isolation of cells through SATCR integration.

I want to dedicate this work to my dear family and friends, and most especially to those who have become both. All of you inspire me daily to work harder and to be a better person and overall researcher. Without you all, none of this would have been possible. Thank you.

ACKNOWLEDGEMENTS

I am thankful to the many funding sources that have funded us throughout this project, specifically the National Science Foundation CBET (1512598), the NSF CAREER Award CBET (1653925), Mexico's National Council of Science and Technology (CONACyT), and the American Heart Association Grant (16SDG26940002).

Thank you so much Dr. Imoukhuede, for your wonderful mentorship and example both professionally and personally. I can honestly say that I am a better teacher and researcher under your tutelage and I cannot thank you enough. Without your guidance and support, I could not have gotten to this point. I also would like to thank both the late Scott Maclaren and Dr. Dianwen Zhang from the University of Illinois Fredrich Seitz Material Research Laboratory and Beckman Institute for AFM and microscopy training. Thank you as well to the Imoukhuede Lab, in which I have found not only a work place, but also a secondary home. All of you have been the most wonderful lab mates and I am truly honored to call you my friends. A special thanks to Dr. Jared Weddell, Stacie Chen, Spencer Mamer, and Wendy Woods from the Imoukhuede Lab, as well as Stefan Gentile and Mohammad Usama Zahid from our neighbor labs for being my sounding board and emotional support throughout this doctorate. You all are wonderful, and I am forever in your debt. I would also like to thank the countless mentors and teachers that have helped me throughout my career, as well the innumerable friends that I have made here who have all helped to push me to become the researcher that I am today. I could not have made it without all of your guidance, and lessons. I strive to be the kind of teacher that you all were to me. Thank you all for everything you all have done. Additionally, I would like to thank all of my undergraduate and graduate students for your assistance with experiments, but also for teaching me how to be a better mentor and researcher. A special thank you to Reema Patel and Kinsey Schultheis for all of your assistance and research, and I wish the best for both of you in all of your future endeavors.

Lastly, I wish to thank my parents and family for their undying support and being my moral, spiritual, and academic compasses. In addition, a significant and huge thank you to my greatest and bestest friends- Dr. Ritu Raman and Corinne Matthews for your advice, assistance, and constant presence in both my personal and professional lives. Thank you for being my emotional lifelines, my role models, as well as my constant mentors. I truly appreciate it.

TABLE OF CONTENTS

CHAPTER 1

INTRODUCTION

1.1 Motivation:

One of the largest remaining problems with chemotherapies and cancer drug regimens is the fact that patients exhibit differential responses (T. T. Batchelor et al., 2007) based on individual susceptibilities or acquired resistances (De Castro, Clarke, Al-Lazikani, & Workman, 2013; Mamer et al., 2017; Saunders et al., 2012; Schneider & Sledge, 2007; Weddell & Imoukhuede, 2014). This problem of drug resistance is one of the largest contributors to inefficient chemotherapies regimens or even toxicity from incorrect dosages (De Castro et al., 2013). Indeed, many leading national laboratories (ACS, NCI, AACR, etc.) agree that personalized medicine is a critical need for confronting the problem of drug resistance and ultimately advance cancer treatment (Ansari, Lee-Montiel, Amos, & Imoukhuede, 2015; Doroshow, 2009; Hansen, 2015; Salwitz, 2012) . Personalized medicine allows for the individualized design of treatment regimens based on specific patient resistances. One methodology for quantifying resistances is through the quantification of cell surface receptors on relevant cells of interests such as tumoral cells. Profiling these cell receptor numbers would not only give valuable insight about the cell's response when exposed to drugs but also would enable quantification of resistances and susceptibilities of these cells to therapeutics such as chemotherapies. Thus, it is necessary to advance technology that precisely isolates these cells of interest for analysis without altering their cellular receptor expression. However, several isolation schema typically either are too slow (Wynick & Bloom, 1990)- which alters receptors that are dynamically changed in response to non-physiological environmental stimulus- or they

are rapid but destructive- which alters cell receptor numbers and viability of the cells through the destruction of the cells (Wynick & Bloom, 1990). Thus, it is necessary to develop an isolation modality that is able to isolate cells while retaining physiological expression (Ansari et al., 2015; Ansari, Patel, Schultheis, Naumovski, & Imoukhuede, 2016).

In our previous publications, we introduced the Secondary Anchor Targeted Cell Release System (Ansari et al., 2015, 2016) (SATCR) in order to address this critical need for cell isolation that preserves physiological expression. We use surface functionalization to modify a glass and PDMS surface to isolate cells from single and multi-cell samples. This functionalization captures cells through the interaction of the streptavidin functionalized surface with biotinylated antibodies (Ansari et al., 2015)that target the cells of interest. These biotinylated antibodies can be customized for whichever cell of interest is required, and are incubated with the cell sample prior to exposure to the capture surface. Once incubated with the cells, the antibody laden cells are pulled down between the interaction between the streptavidin and biotin proteins, as avidin and biotin family proteins have very specific binding (Ansari et al., 2015; Holmberg et al., 2005; M Wilchek & Bayer, 1990; Meir Wilchek & Bayer, 1987). Once pulled down, the cells can be competitively released from the surface through the competitive replacement of the desthiobiotin in the SATCR surface with excess biotin, as desthiobiotin is a less effective binding partner to streptavidin than the biotin itself. Thus, cells can be isolated without directly interacting with the primary antibody-cell tether, reducing the stress on the cells directly.

This dissertation presents the rationale behind both functionalization as well as cell isolation as it pertains to personalized medicine and drug resistance. Additionally, this

dissertation will advance this SATCR capture surface into not only PDMS microfluidics, but also polymer tubing in an attempt to optimize the technology. These adaptions improve throughput, and are much more efficient in time and reagent usage. Through the advancement and application of this technology to multiple modalities and platforms, we can create a completely customizable platform for cell isolation that can be used to isolate cells while retaining physiologically relevant cellular information.

1.2 Overview

Chapter 2 covers a comprehensive review of surface functionalization as well as its applications. This is followed by the adaption of the technology to microfluidic devices and the optimizations conducted within that system. Chapter 4 covers the further implementation of this chemistry into polymer tubing to capture and release cells in non-glass modalities as well as further applications that are possible through this implementation.

CHAPTER 2

SURFACE FUNCTIONALIZATION AND CELL ISOLATION

Plenty more room on the glass bottom: Surface functionalization and Nanobiotechnology for cell isolation

Ali Ansari and P. I. Imoukhuede, PhD

2.1 Introduction:

As the great Richard Feynman once immortalized in his lectures (Feynman, 2011), "*There's plenty more room at the bottom."* This scientific optimism can also be applied to surface functionalization, which is the modification and addition of chemical functional groups, on materials. Currently, there remain worlds of minable space for surface functionalization to enable completely new avenues of biomedical research. This is due to the flexibility that surface functionalization has in what it can be designed to do. Surface functionalization can modify surfaces to do something as simple as altering the hydrophobicity or hydrophilicity of a substrate to make it more or less biocompatible, to something as chemically complex as modifying a surface with a multi-layered cellular capture and release modality. As such, surface functionalization can further advance existing biomedical research, as biocompatibility is crucial for techniques that interface with biological materials such as cells and tissues. Additionally *in vivo* techniques such as cell patterning, which conjugate cells to a surface in specific orientations, or cell isolation, which reversibly captures cells of interest for further downstream analyses both require methodologies to increase the biocompatibility of the capture substrate in order to

promote cell adhesion and reduce cell death. Additionally, though both of these techniques differ in design objectives, they use the same basic chemistries and designs, and thus the chemistries can be applied for either experimental design once understood. In this review we aim to present opportunities that exist to adapt it and integrate surface functionalization for one's own needs by first discussing the extant techniques of surface functionalization for cell patterning and isolation and presenting the advantages and disadvantages of functionalization.

2.2 Surface Functionalization and Affinity Based Pull Down

Surface functionalization spans many scientific fields in the literature. To be thorough, we sub-classified several different types of surface functionalization that pertains to both cellular patterning as well as cell isolation. This will allow for the readers a more complete knowledge of the techniques at their disposal, and allow them to be able to apply any and all of them into their research. Cell isolation and cell patterning are very similar in design- both compartmentalize and separate out certain targeted cells and attach them preferentially onto a functionalized surface- pulling them out of a larger sample. In this sense, the "capture" portion of both processes are near identical in design and intent. However, cell isolation based techniques aim to release or recollect the captured cells into a more purified sample. This allows for downstream analyses and further experimentation. Cell patterning does not typically recapture or release cells, as the cells are typically patterned for drug testing (Ingber, 2016; Jiang, Ferrigno, Mrksich, & Whitesides, 2003; Khademhosseini et al., 2004; H.-W. Wu, Lin, & Lee, 2011) or other experimental design (Bacakova, Filova, Parizek, Ruml, & Svorcik, 2011; Compton, Luo, Ma, Botvinick, & Venugopalan, 2014) (Fig. 1). As these two processes differ, they are described separately below. Lastly, surface functionalization can be done to alter or improve substrate

properties or biocompatibility. While this does not typically involve recollection of captured cells such as cell isolation techniques, it is not the same as patterning specific cells-rather improving environment- and as such they are further separated as well. The distinction between cell patterning and cell isolation is important, as no conversation about tools is complete without first talking what uses they have. Cell enrichment has already been well established as a methodology for purifying samples (Gao, Li, & Pappas, 2013) for profiling techniques such as flow cytometry (both regular (S. Kuntaegowdanahalli & Bhagat, 2009; Mizuarai, Takahashi, Kobayashi, & Kotani, 2005; Nolan, Condello, Duggan, Naivar, & Novo, 2013) and quantitative flow cytometry (S. Chen et al., 2017; P. I. Imoukhuede & Popel, 2011; Princess. I. Imoukhuede & Popel, 2014; Princess I Imoukhuede & Popel, 2012)), and protein analyses such as ELISA (Ariyasu et al., 2012; Regehr et al., 2009; Vermette et al., 2003), or Next Generation sequencing (Lin et al., 2014). Higher purity samples will give more consistent and meaningful information, with less cellular noise due to non-homogeneous cell types. The more consistent and more accurate these downstream analyses become, the closer that personalized medicine will be able to move towards individually tailoring drug regimens to specific patient profiles. Thus, recollection of cells via cell isolation techniques serves as a distinctive alternative use of surface functionalization to cell patterning.

Additionally, while other authors such as den Toonder et al and Song et al. have already gone into great depth about the importance of isolating cells physiologically (Ansari et al., 2015, 2016; den Toonder, 2011; M. Yu, Stott, Toner, Maheswaran, & Haber, 2011), as well as non-capture based cell enrichment techniques for isolation (Song et al., 2017), we shall focus on techniques that center on surface chemistries and affinity based capture. In addition, while a large percentage of these techniques may currently be currently used for positive enrichment, as the

chemistry is identical for both modalities, they can all be customized for negative enrichment with ease.

2.2.1: *Self assembled monolayer chemistry:* Surface Functionalization can be defined as the chemical modification of a surface to add some functional group or function (Aswal, Lenfant, Guerin, Yakhmi, & Vuillaume, 2006; Jiang et al., 2003; Kutsenko et al., 2017; Mrksich et al., 1996; Shaporenko, Cyganik, Buck, Terfort, & Zharnikov, 2005), and one of the most widely adopted methodologies to surface functionalize substrates is using self-assembled monolayers (SAMs). SAMs are very widely used as they independently self-orient and establish even monolayers on surfaces spontaneously without the use of complex mechanisms (Muskal, Turyan, & Mandler, 1996). These SAMs are substrate dependent and can be tailored in composition and length to correspond with the necessary functionality desired (Shaporenko et al., 2005). SAMs of silanes (which consist of silicon and oxygen groups) are formed on silicon based substrates such as glass or wafers. These silanes are appended with tail groups of unique functional groups such as amines depending on the experimental design (Aswal et al., 2006)(Fig. 2) .As substrates of glass and silicon are relatively cheap and inert, silicon based devices are gaining popularity with the movement to glass based microfluidic devices. On the other hand, SAMs of thiols (containing sulfur and hydrogen groups) have been functionalized on a diverse set of well-established metal substrates such as copper (Laibinis et al., 1991), palladium (Carvalho, Geissler, Schmid, Michel, & Delamarche, 2002; Love et al., 2003; Love, Estroff, Kriebel, Nuzzo, & Whitesides, 2005), platinum (Z. Li, Chang, & Williams, 2003; Love et al., 2005), mercury (Love et al., 2005; Muskal et al., 1996), gold (C. D. Bain & Whitesides, 1988; Colin D. Bain et al., 1989; Biebuyck, Bain, & Whitesides, 1994; Dubois, Zegarski, & Nuzzo, 1993; Kutsenko et al.,

2017; Su, Wu, Robelek, & Knoll, 2005), and silver (Fenter et al., 1991; Laibinis et al., 1991; Love et al., 2005; Walczak, Chung, Stole, Widrig, & Porter, 1991) enabling the addition of specific functional groups to these substrates(Love et al., 2005). As a result thiol chemistry is one of the most commonly adapted SAMs, as its flexibility in substrate design allows easy integration in existing systems. Additionally, gold and silver can also be functionalized with SAMs made of selenides or selenoates which consist of selenide groups (Shaporenko et al., 2005). This enables substrates such as a gold and silver to be functionalized with different SAMs depending on the necessary experimental design. This could enable more complex functionalization schema, if need be. These methodologies are by no means exhaustive and are meant to provide the basis for the chemistries expanded on within the paper.

2.2.1.1 *Thiol Chemistry applications and design*:

As metals are very well characterized in the field, they are very commonly used. A Web of Science literature comparison showed gold was as much as three times more commonly listed as a key term than glass in papers in functionalization, cell release and even surface functionalization. As such, it is important to begin with their chemistries and applications to understand how to integrate them with your experimental design.

Thiol SAMs enable tunable cell patterning and integration with existing technologies:

Self –Assembled thiols allow for tunable cell patterning on gold and other metallic based substrates. Thiol based systems have been used in microfluidic systems to pattern cells (Dillmore, Yousaf, & Mrksich, 2004; Y. Li et al., 2007; Yousaf, Houseman, & Mrksich, 2001; Zhang et al., 2013). Li et al has used thiols to direct and aid in the deposition of their ECM proteins by using the gold surface as the cathode. Li et al used (($HS(CH_2)_{11}(OCH_2\ CH_2\ )_6\ OH$),

more commonly known as E_6.,to activate the surface for deposition with more typical cell patterning materials such as ECM and fibronectin proteins. After functionalizing the gold surface with the E_6 thiol, Li et al. was able to use the ECM and fibronectin solution as the electrolytic solution for the electrochemistry. Through the introduction of an electric potential, the E_6 thiol was desorbed and replaced with the ECM proteins selectively- fully activating those regions for cell adhesion. As the gold is extremely conductive to these electrical charges, they were able to easily activate only those specific environments for cell adhesion. Conversely, thiol chemistry can also be used to create regions to prevent cell binding for cell patterning (Jiang et al., 2003; Mrksich, 1998). Jiang et al micro-printed two different types of thiols, HS $(CH_2)_{11}(OCH_2OCH_2)_3OH$ ($C_{11}EG_3$) and HS $(CH_2)_{17}CH_3$ (C_{18}), which differed in their adherence to cells. The $C_{11}EG_3$thiols resisted protein deposition as well as the attachment of cells. In contrast the (C_{18}) thiol served as the protein absorbing thiol, and the thiol that cell attachment would be directed to. Through selectively patterning regions with the different thiols, they could confine the cells into directed patterns. Using a small cathodic voltage pulse of -1.2 volts for 30 seconds, they then were able to release the EG_3 thiols from the surface of the gold, enabling migration of the cells into this de-functionalized region. Jiang et al was then able to observe differential migration capability across cell types, through the release of these thiols. Thus, thiol chemistry can be used to tune the activation or deactivation of surfaces for cell patterning.

Researchers such as Jiang et al. and Dillmore et al. were able to integrate this surface functionalization with extant quantitative technologies such as Surface Plasmon Resonance (SPR) or printing techniques such as photolithography in order to append further adaptability to their cell patterning modalities. SPR was used in the capture chip to quantify deposition of protein as the cells migrated into the un-thiolated gold regions (Jiang et al., 2003; Sigal, Mrksich,

& Whitesides, 1998). The ability to quantify protein deposition enables parameterization of cell migration in response to multiple chemical stimuli. Indeed, Jiang et al was able to show an abolishment of migration after the treatment of the cell surface with different migratory inhibitory drugs(Jiang et al., 2003). Taking this thiol based cell patterning a step further, Dillmore et al patterned photo-cleavable thiols with a reactive conjugate (Dillmore et al., 2004). This conjugate then is what then attaches to the ligands needed for cellular attachment such as an RGD domain. Through the use of a light source or even a photolithographic mask, the surface could be adaptably patterned to allow attachment of cells in specific regions. Another combinational methodology uses the conductive properties of gold, as well as adaptable thiol chemistry. Adapting all of these techniques together- researchers even created a patterned surface on gold with hydroquinone that will be oxidized through electrical current through the gold substrate and then will allow for the subsequent reaction with a conjugate which then can be attached to the ligand of choice (Yousaf et al., 2001). This can be integrated with a functionalization scheme that has hydroquinone on multiple sections of the gold surface, and only the regions that are electrically active will be oxidized and will eventually promote cell attachment.

Electrical conductivity of thiol patterned metal substrates enable cell recollection:

While the above chemical functionalizations have been used for cell patterning, these modalities can be integrated with supplementary chemistry to allow for the recollection of the isolated cells. The recollection of these isolated cells would provide the ability to analyze the cells downstream, or allow for subsequent passaging of the cells. As such, thiol based cell isolation typically harnesses the electrical conductivity of the gold or other metals used as a

substrate to release the bound thiols from the surface. By introducing an electrical voltage of -1.2 V to the gold surface the thiol modified molecule was desorbed from the surface (Inaba, Khademhosseini, Suzuki, & Fukuda, 2009; Jiang et al., 2003; Yousaf et al., 2001; Zhang et al., 2013). As the cells were attached directly to the thiol, the desorption of the thiols resulted in the release of the cells from the surface. Once lifted from the surface, the recollected cells could be re-cultured as large sheets, individualized cells, or even analyzed separately using other downstream techniques.

2.2.1.2 *Silane Chemistry applications and design*:

Another commonly used SAMs are silanes, which self-assemble spontaneously on substrates that contain silicon. As both glass (silicon dioxide) and PDMS (poly-dimethylsiloxane) are very versatile and well established as modalities for microfluidics, they are very prominently used in the literature-a footprint consisting of thousands of papers when using a Web of Science literature search. Additionally, glass is widely adopted for functionalization as it is optically clear and can be used cheaply (Berthier, Young, & Beebe, 2012). In microfluidic devices, glass is typically bonded to PDMS (an elastomeric substrate which also contains additional silicon groups) (Berthier et al., 2012; Bhattacharya, Datta, Berg, & Gangopadhyay, 2005; Gervais, El-Ali, Günther, & Jensen, 2006; Hassan et al., 2017; Kuddannaya & Chuah, 2013; Kurkuri et al., 2011; Regehr et al., 2009; Séguin, McLachlan, Norton, & Lagugné-Labarthet, 2010; Wan et al., 2012; Watkins et al., 2013), and can be further functionalized.

Silane SAMs functionalization enables patterning of low population circulating cells

Amino silanes such as APTES have been integrated with affinity based capture modalities in both cell patterning and cell isolation applications. In both cell isolation and cell

patterning, these technologies focus on rare cell types of interest to allow for the most application of their device. This is due to the idea that if the device is able to resolve cell pull-down of low expressed cells in solution, than when the cells are expressed at higher populations; their device would not have a problem resolving them. One type of these low population cells of interest are circulating tumor cells (CTCs) due to the vital information about tumoral activity (Adams et al., 2008; Alunni-Fabbroni & Sandri, 2010; Cohen et al., 2008; Karabacak et al., 2014; Kim, Yoon, Stella, & Nagrath, 2014; Mikolajczyk et al., 2011; Myung, Launiere, Eddington, & Hong, 2010; O'Flaherty et al., 2012; Pecot et al., 2011; Song et al., 2017; Wan et al., 2012). Many researchers developed functionalization schemes to target the CTCs in a variety of different modalities. Researchers developed a CTC separation modality in glass and PDMS which is functionalized with a self-assembled chlorinated silane before adding in epoxy functionalized layers that allow them to conjugate the Anti-EpCAM antibodies that the systems uses to isolate the CTCs (Kurkuri et al., 2011). Similarly, several iterations of the NanoVelcro system has been developed which uses silane chemistry to functionalize silicon nanowire substrates with streptavidin and biotinylated anti-EpCAM to pull down CTCs (Lin et al., 2014). Both of these techniques use antibodies as a targeting technique with the surface functionalization techniques acting as a tether to hold the antibodies and then ultimately the cells that attach to them to the surface.

In contrast, physical modification techniques have been used to improve the pull down percentages through increase of surface area or roughness. For example, Mahmood et al used acids to micro-rough the surface of the glass prior to amino silane functionalization with later anti-EGFR conjugation to pull down CTCs (M A I Mahmood et al., 2014). The increase in surface area allowed higher interaction between the capturing moiety and the cells of interest, the CTCs. This allowed for higher percentages of isolation than a flattened glass version. Instead of

altering the base substrate surface, Diéguez et al acid roughened the PDMS surface, rather than the glass, before conjugating with CD45 antibodies (Diéguez, Winter, Pocock, Bremmell, & Thierry, 2015) which also showed improvements in cell pull down. For both of these modalities, the surface roughness allowed for greater surface area for cell capture and for cell attachment, while the silane functionalization pulled the cells down to the surface and tethered them to the surface.

Silane SAMs enable integration of cell patterning with other extant technologies

Further evolving this chemical functionalization, the silane functionalized system has been integrated with alternative architectures and modalities to widen the ability of the technology to pattern cells. Saneinejad et al. implemented glass based silane functionalization with sputtered gold to create a hybridized system for patterning cells. As previously described, the gold could be functionalized with a thiol to pattern PEG repulsive or peptide adhesive regions for cell growth, based on the configuration of the chemistry, while the silane could allow for the opposite set of proteins for patterning design (Saneinejad & Shoichet, 1998).This would allow tuning of the binding locations for the cells, as well as allow for separating regions if multiple cell binding locations were needed. Saneinejad et al. also implemented a different capturing technology with this silane chemistry that differed from more typical antibody targeting. Saneinejad et al. used folded sequences of DNA called aptamers to target the cells of interest. These aptamers would allow for directed affinity pulldown of cells without using specific antibodies, as the sequences could be tailored to fit the receptor in question perfectly (Bunka & Stockley, 2006; H. W. Chen et al., 2008; Gotrik, Feagin, Csordas, Nakamoto, & Soh, 2016; M A I Mahmood et al., 2014; Sheng et al., 2012; Wan et al., 2010, 2012; William Chen et al., n.d.). Mahmood et al experimented with directly conjugating silanes with these aptamers

specific to the EGF receptor. This EGF receptor targeting pulled down glioblastoma cells to investigate differences in behavior between the cancer cells and healthy ones (Mohammed A.I. Mahmood, Arafat, Kim, & Iqbal, 2013).

Silane SAMs enable recollection of cells through reactive additives or environmental changes

Complex systems have been constructed to facilitate cell release through various additives to recollect the cells that the silane based surfaces captured. One such system is our lab's Secondary Anchor Targeted Cell Release System (SATCR) (Ansari et al., 2015, 2016). This system uses a SAM of an aminosilane which then attaches to the glass and PDMS surface. We then bind a desthiobiotin protein to the amine group on the APTES layer. Desthiobiotin is a protein that is a functional analog to another protein named biotin. Biotin family proteins bind exclusively with avidin family proteins, and are known as one the most selective and powerful natural binding partners out there (Coad et al., 2012; Gonzá et al., n.d.; González et al., 1997; Holmberg et al., 2005; Kobayashi et al., 1995; Lee-Montiel & Imoukhuede, 2013; G. U. Lee, Kidwell, & Colton, 1994; T. T. Nguyen, Sly, & Conboy, 2012; M Wilchek & Bayer, 1990). The capture surface uses streptavidin to pull down biotinylated antibody to the functionalized surface. Release is initiated through the use of outcompeting the desthiobiotin protein's binding to the streptavidin which a more effective binding partner- the biotin protein itself. Through the introduction of 4 mM biotin, the cells are released from the surface (Ansari et al., 2015). This system allows for customizable capture and release through the adaption of different biotinylated antibodies, but still is limited through the effectiveness of the binding strength of the antibody. To address this binding affinity problem, integrated aptamers have been integrated to improve this binding affinity between the cellular targets and their silicon functionalized capture surface

(L. Chen et al., 2011; Swaminathan et al., 2013; Wan et al., 2012). Through the use of a mercapto-silane, the aptamer is conjugated to the silicon nanowires promoting cell capture. The cells are released through the introduction of an exonuclease which then degrades the aptamers and releases the cells from the wires themselves for recollection (L. Chen et al., 2011). Along similar lines, aptamer conjugated silanes were implemented into a microfluidic device which used an assay with pits that would involve the pulldown of cells via aptamers attached to glass beads (Wan et al., 2012). These cells were subsequently released with an antisense RELease molecule that would unravel the aptamer structure and result in the release of the cells. Both of these techniques use these aptamers to supplant the use of antibodies in the capture modality, and thus preventing the antibody affinity from limiting capture of the cells.

In contrast, environmental changes have been used to promote cell release rather than adding a release inducing molecule. For example, a thermally responsive iteration of Lin et al. 's NanoVelcro cellular release system does not use protein binding competition to release cells but rather uses environmental changes to release the cells from the aptamers attached to the biotin streptavidin complex (Lin et al., 2014). Like the SATCR System, the NanoVelcro system uses the interaction between streptavidinated protein and biotinylated aptamers to release the cells of interest for recollection. Through the conjugation of a thermally reactive polymer PIPAAM, the NanoVelcro CTC system was able to release cells when the temperature was lowered to 4C as the PIPAAM would unravel which would release the cell receptors from the biotinylated anti-EpCAM antibodies. Thus the environmental change was the trigger for the conformational changes releasing the cells from the surface rather than a competitive binding partner. Another methodology of environmental change based release was the implementation of a photo-responsive linker (Ariyasu et al., 2012). A photo-cleavable linker responsive to 330 nm of light

photo irradiation was implemented with an anti-HEL-IgG antibody to release cells of interest. Once light was introduced into the system, the linker was cleaved and the cells were released from the surface. Besides the addition of light energy, electrical energy has also been used to release captured cells. Cells that were isolated by a biotinylated antibody conjugated to functionalized nanofiber mats on glass (C. C. Yu et al., 2017)were exposed to an electrical current. The electrical current caused the capture surface to be repulsed by the charged nanofibers and resulted in the captured cells to be recollected from the nanofibers. Systems even exist which respond to the environmental pH and glucose in tandem to release cells of interest from mercapto-silane functionalized silicon nanowires (Liu et al., 2013). Cells are pulled down using specific polymers which bind to sialic acid on cells, but are outcompeted through the environmental change of pH and the addition of glucose into the environment. The use of a magnetic field to isolate and release cells in a microfluidic device (Kwak et al., 2018) has also even been designed. The magnetic nanoparticles were functionalized with silanes and then with an anti-EpCAM antibody to pull down the cells of interest to the surface of the microfluidic device. The magnetic field would hold the labeled cells while the other cells flowed through, and then when the magnet was turned off, the cells were released and could be recollected. All of these techniques use environmental changes to facilitate the cell release, and are also implementable with silane based chemistry.

2.2.2 ECM Mimicking Functionalized Surfaces and Hydrogels*:* In addition to the substrate dependent SAM functionalization, there are functionalization schemas that use chemistries that are substrate independent and thus can be conserved across substrates. However, as these techniques do not involve self-assembled layers, the chemistries tend to be more complex than

the monolayer chemistries mentioned above. These substrate independent functionalization schema can be applied to both solid substrates (Custódio, Frias, del Campo, Reis, & Mano, 2012) as well as hydrogels (Kato, Sato, & Iwata, 2007; Miyazaki, Kato, Teramura, & Iwata, 2008; Raman et al., 2016) to mimic 3D cellular environment more physiologically. Several of these functionalization schemas involve mimicry of the extracellular matrix (ECM) to preserve physiology for the cells. This has been shown in one dimension by through research in functionalizing glass with chitosan molecules (Custódio et al., 2012) which then are then subsequently conjugated with antibodies onto the chitosan. The adipose stem cells tested would not natively attach to the chitosan without the recognizing the antibody, which allowed for selective cell patterning. Similarly, thermally responsive plant cell wall polysaccharides such as xyloglucan that expressed RGD domains has also been used to isolate human malignant skin melanoma A375 cells through the creation of stable films on glass 24 well plates (Silva et al., 2013). As the A375 cells over express the integrin for binding to the RGD domains, the cells were able to be cultured readily onto the xyloglucan functionalized surfaces. Once captured, cells were released through heating the well plate to room temperature - showing the ability of these ECM mimicking "smart" surfaces to respond to stimuli. Bridging the gap between the single dimensional glass based system and the three dimensional hydrogel environment are systems such as the single dimensional hydrogel surface functionalized with heparin to promote cell adherence and proliferation (Camci-Unal et al., 2013). Heparin has previously been integrated with materials to make implantation of hydrogels such as poly(methyl methacrylate) more biological inert and reduce inflammation (Lai & Fan, 1996). Additionally, as glycosaminoglycans such as hyaluronic acid are expressed natively within the body (Burdick & Prestwich, 2011), they are popular bases for hydrogel creation. Hydrogels of hyaluronic acid

were created and crosslinked before functionalizing them with CD34 antibodies via EDC conjugation to pull down endothelial progenitor cells. Heparin methacrylate was tested against the hyaluronic acid methacrylate to test the benefits of heparin to cell adhesion on top of the hydrogel, with the heparin modified hydrogels promoting significantly higher cell growth with and without the antibody functionalization. This system showed the importance of substrate modification to modify cell growth, and ties neatly to the implementation of Raman et al.'s full three dimensional hydrogel system which more fully mimics physiological environments for cellular systems (Raman et al., 2016). This system is of note as it encapsulates and polymerizes the hydrogel with cells already laden in the system, rather than seeding them after polymerization. Indeed, this system eliminates the problem of cells settling to the bottom of the gel through a clever inversion of typical fabrication setups. The hydrogel was polymerized via UV in a high resolution custom built projection stereolithographic apparatus, and was able to polymerize different layers into a multi-material structure using alternating resin types. This design is similar to other previously mentioned functionalization schema in which additional layers of chemicals were used to add properties to a material. Furthermore, the different types of cell types encapsulated could allow for a co-culture sample that would be designed to even further recapitulate the cell microenvironment. These systems all allow for the creation of more physiological extracellular environment and do so regardless of the substrate functionalized. As such, these all show the adaptability of surface functionalization, as it allows for several disparate and sometimes multidimensional substrates to all reach similar functional activity.

2.2.3: Alternative Surfaces and Absorbed Protein Chemistry: Moreover, there are a few alternative methodologies or rarely used materials that may be also functionalized to capture or pattern cells. One alternative methodology for cell capture is the adsorption of proteins onto a

surface without any functionalization. This has been used extensively with different microfluidic devices for antibody adsorption on PDMS surfaces (Hassan et al., 2017; Watkins et al., 2013). These adsorbed antibodies pull down cells of interest to the surface for quantification. One distinct weakness of this method is as these antibodies are not specifically tethered, they lack an established orientation (Welch, Scoble, Muir, & Pigram, 2017). To get around this, some protocols add an excess of protein into the immobilization techniques, such that even if some are non-functional, they will still immobilize enough functional material that it will not matter. Self-assembled monolayers require more complex chemistry, but guarantee orientation. Studies even show that oriented antibody immobilization with long spacers resulted in as much as 10x the signal intensity (Kusnezow & Hoheisel, 2003; Peluso et al., 2003). As a potential evolution of this concept, aortic valve have been de-cellularized to become the substrate for functionalization, and used the proteins that are natively composing the valve as a structural target for functionalization (Ye, Zhao, Sun, & Li, 2009). By using the free amine groups on these proteins, they are able to functionalize the aortic valve with biotin to pull down avidin conjugated fluorophores as well as avidin conjugated antibodies. This allows for the flexibility of using natively adsorbed proteins as a target, while still using more complex chemistry to orient the capturing modality. Yet another adaption on this idea involves the functionalization of a thermally sensitive Poly(N-isopropyl acrylamide)(PIPAAm) onto polystyrene dishes via laser irradiation to create a responsive system that can alternatively culture and release cells at will (Okano, Yamada, Sakai, & Sakurai, 1993; Yamada et al., 1990). As the cells do not need a specific orientation of the PIPAAm for attachment, it is a non-issue whether they are oriented correctly or not. However, as the temperature is lowered to 4C, the surface will release the cells

and allow for recollection. In this way, the more complex chemistry is used to release the cells, than used to attach the cells to the PIPAAm functionalized surface.

2.3. Advantages/Disadvantages of Surface Functionalization:

2.3.1: *Advantages of surface functionalization*: Surface Functionalization has many advantages for substrate modification as it can customize and integrate different materials in addition to imparting utility to otherwise non-functionalized platforms. While there are many researchers that do absorb proteins to glass without functionalization (Bashir et al., 2001; Hassan et al., 2017), surface functionalization preserves the functional orientation of the protein, which allows for more efficient usage of the adhered protein. Furthermore, surface functionalization can allow for customizable passivation or inactivation of surfaces, which simple protein adsorption cannot do (Jiang et al., 2003; Mrksich et al., 1996). Additionally, surface functionalization can also enable layered architectures of proteins for more specific applications such as cell recollection (Ansari et al., 2015, 2016; Ariyasu et al., 2012). Through the use of specific tail groups and established conjugation chemistries such as EDC/NHS, proteins and chemical moieties can be conjugated to each other to impart more function (Andree et al., 2016; Ansari et al., 2015, 2016; Camci-Unal et al., 2013; Lippert et al., 2016). Even more still, functionalization can be used to change the surface properties of a material to make it more or less interactive with a moiety. Adding oxide groups or amine groups to a surface to change hydrophobicity is very useful when patterning cells or even binding proteins. All of these customizations can allow for a more interactive and responsive system. These changes have been appended into materials to make smart materials (Raman et al., 2016; Raman & Bashir, 2015) that are able to respond to environmental changes(Raman et al., 2017; Raman & Bashir, 2017). Surface functionalization, and the chemistries that it utilizes, can all enable this reactivity and responsiveness.

2.3.2: *Disadvantages of surface functionalization*: Despite all of the applications and advantages surface functionalization affords, there are three typical weaknesses that surface functionalizations schemas typically have. Firstly, certain chemistries are limited by substrate as mentioned above. When using glass surfaces, SAM modification is primarily restricted to silanes, as they self-assemble most effectively on the substrate. Similarly, as mentioned above, gold tend to be restricted to SAMs of thiols and selenoates primarily. This limits the chemistries slightly, as it requires one specific type of head group to react with it. Of course, this does not constrain the choice of tail groups that are possible, as you can append anything from amines to disulfides (Kutsenko et al., 2017) onto the thiol head groups. This is more of an issue if the thiols that are used require some higher level of chemical safety such as a chemical hood or fume hood. Similarly, certain silanes can be dangerous as well, and being constricted into their use can be limiting. Lastly, one concern of using complex chemistry to functionalize substrate is the risk or cross-reactivity or chemical reactions of the materials with another usually innocuous chemical downstream. Most SAMs are fairly non-reactive, however with surface functionalization schema that may involve more complex chemistries such as substitution reactions, it is possible that either the functionalizing chemical itself can react with another downstream chemical, or a reaction byproduct can re-react with it. For example in the functionalization of a non-standard material such as PVC(Balakrishnan, Kumar, Yoshida, & Jayakrishnan, 2005), chlorine groups released from silanization can result in the reaction of these chlorine groups with other downstream reactants. To mitigate this, many sequenced functionalization protocols involve long incubation steps with excess of the reactants to try to fully react with each subsequent layer. In addition, many multi-step functionalization protocols (Ansari et al., 2016) involve long and frequent wash steps. However, even this cannot completely remove the risk of cross-reactivity,

and thus strict chemical design of the functionalization is paramount to a fully optimized surface functionalized protocol.

2.3.3: *Substrate chemistry selection*: When deciding which substrate chemistry is ideal for a project, the most important things to consider are the parameters that are worth studying in the system that you are designing. Based on the experimental design, there will be certain parameters that will be tested or investigated. Deciding which parameters to study optimizes the system for measurement of those parameters. For instance, if the system designed requires optically clear material for binding quantification, then a substrate that is optically clear will be required for surface functionalization. Similarly, if multiple systems are able to resolve those parameters, then the decision becomes more up to personal preference or further parameterization. If material cost is a parameter that is valued, you may decide to opt for a cheaper system like silicon or glass as the substrate, if it is not necessary for the system to be integrated with another technique or cleavable systems to have gold or other pure metal based functionalization. Silicon substrates such as glass are easily obtained, cheap, and disposable. Moreover, silane chemistry has been very well established and there is a wealth of literature on it. Silicon based nanowires were even adapted To allow for higher conductance and more metallic properties for silicon based systems, however, gold affords an easier implementation of such parameters such as electrical conductance. If however, the testing modality requires an electrical conduction or integration with a measurement modality such as SPR which requires the conductance of the metal, using thiol chemistries will allow for the addition of alternate functionality to the metal surface for customization. Furthermore, since both the tail group and the functional group on the both thiol and silane chemicals can be customized completely, any sort of chemical functionality could be appended, from amine groups for conjugation via NHS and EDC, or even specialized protein

tags such as streptavidin or biotin. This affords complete customizability based on what parameters are necessary for each system. Ultimately each material has specialties and weaknesses associated with it, so choosing a substrate in order to optimize your experimental design should be the first step to choosing which surface chemistry SAM to utilize.

2.3.4: *Further applications for surface functionalization techniques*: Surface functionalization can be applied to practically any field to improve selectivity, stability, or even compatibility of different surfaces. By tuning the hydrophobicity of surfaces, cell capture or culture can be done more effectively and with more physiological environments (Dillmore et al., 2004; Saneinejad & Shoichet, 1998; Séguin et al., 2010; C. C. Yu et al., 2017). This research can be used with imaging modalities as well to functionalize fluorophores or even quantum dots with chemistries such that they bind to aptamers or even antibodies (Lee-Montiel, Li, & Imoukhuede, 2015b) to enable multiplexing of signals(Lee-Montiel & Imoukhuede, 2013; Lee-Montiel, Li, & Imoukhuede, 2015a). Surface functionalization can even be applied to improve biocompatibility of materials that are implanted into the body (Harris, Tosatti, Wieland, Textor, & Richards, 2004) to resist degradation, rejection and even reduce inflammation. As previously mentioned, the most important parameter for deciding whether to implement surface functionalization into a research modality that you are considering, is what sort of function that you want to impart onto it and for what purpose. From there, picking substrate and subsequent chemistry will come much more easily, as the form will fit the function.

2.4 Conclusions:

This review discusses surface functionalization and the applications that it has to a variety of fields of science. Through the presentation of the research of our lab as well as many of the luminaries in several disparate fields, we demonstrate that surface functionalization is a very powerful tool for appending utility to substrates that may not natively contain such capability. This functionality can be easily designed to interface with many different substrates and measurement modalities and can be implemented by researchers of practically any field based on their application. Through the flexibility and customizability that functionalization affords us, hopefully we can start to chip away at the great plenty of room that is left for us at the glass bottom- harkening back to the spirit of what Dr. Feynman spoke of in his lectures urging us to embrace the unknown. It is only through this acknowledgment of the long distance that we have yet to go, and the things that we have yet to know that we are able to move forward and truly revolutionize the field.

2.5 Acknowledgements:

We would like to thank the National Science Foundation CBET (1512598), the NSF CAREER Award CBET (1653925) and the American Heart Association (16SDG26940002) for funding support. Finally, we would also like to thank Stacie Chen and Spencer Mamer for stimulating conversation and advice about the paper.

2.6 Figures:

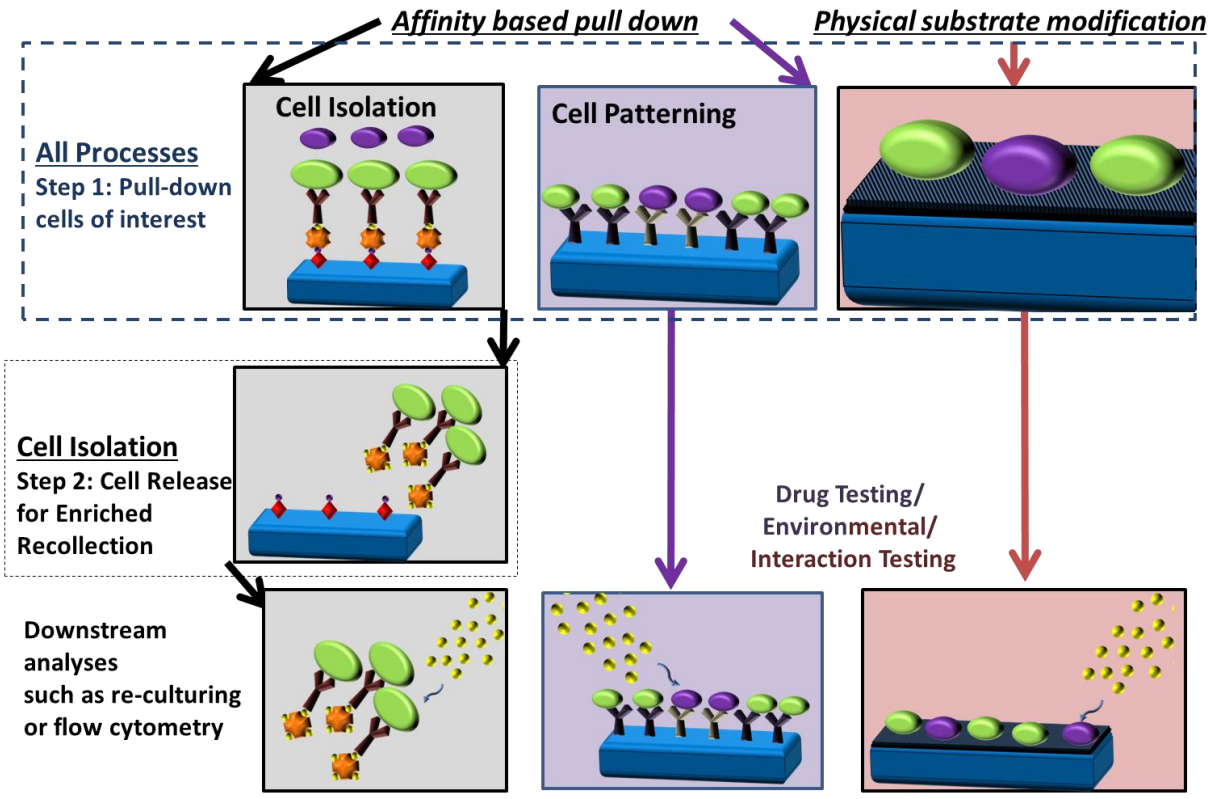

Figure 2.1: Categorization of Surface Functionalization Techniques. Each technique can broadly be classified into different categories based on the application of the technique. Both cell isolation and cell patterning are predominantly affinity based in their pull-down of cells but differ when it comes to the intent of the cells that are pulled out of the sample. Cell isolation typically aims to take the enriched sample and release them for recollection, while cell patterning techniques use the cells that are pulled down to experiment on directly. Similarly, physical substrate modification uses non-affinity based pull down to change the surface parameters of a material allowing it to be more conducive to cell capture, but typically does not aim to recollect cells once captured. Each of these techniques has their advantages and applications, and knowing what they are allows researchers to better design their own experiments.

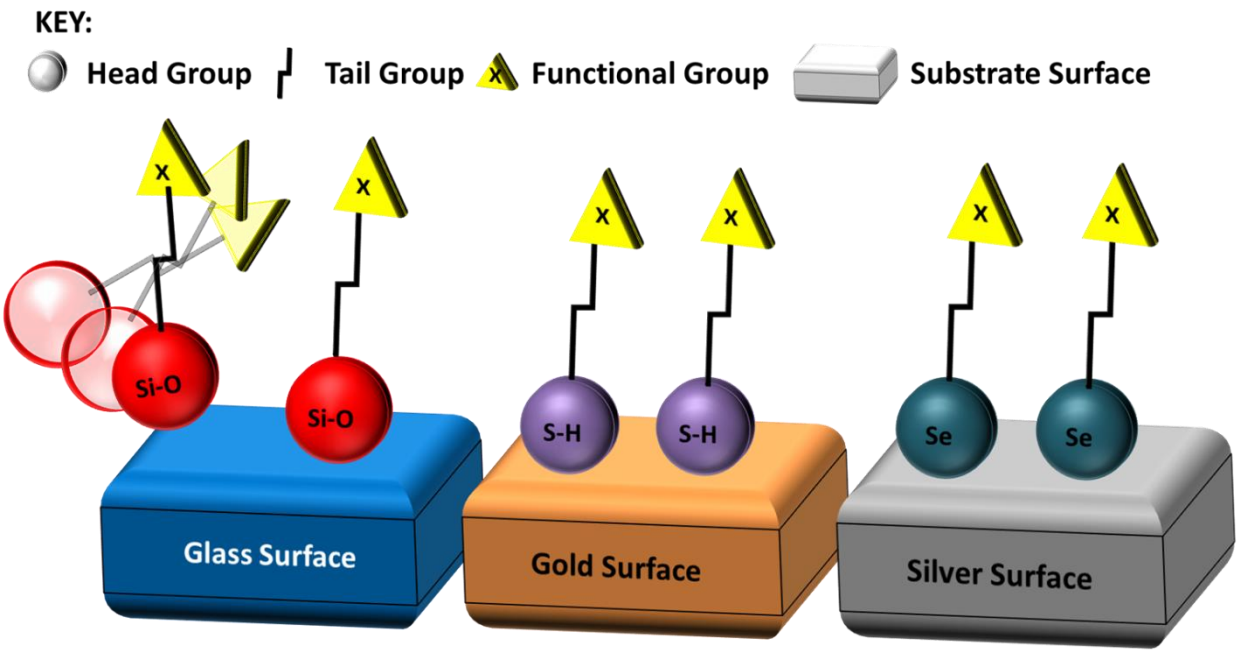

Figure 2.2: Schematic of Self Assembling Monolayers on Different Substrates: These chemicals self-orient themselves such that the head group bonds to the substrate without the need for complex experimental design. Thus, these materials expose the functional groups on the tail groups for further chemical modification and reaction. These substrates and SAMs are examples of substrate/SAMs pairs, but there are several other SAMs that are widely used throughout literature, allowing for a great deal of customizability in experimental design.

CHAPTER 3

MICROFLUIDIC ADAPTION OF THE SATCR SURFACE

Cell Isolation via a Spiral Microfluidic Adaption of the Secondary Anchor Targeted Cell Release System

Ali Ansari, Kinsey Schultheis, Reema Patel, Kareem Al-Qadi, Cassandra Jensen, Samantha R. Schad, Si Chen, Jared C. Weddell PhD, Surya P. Vanka PhD, P. I. Imoukhuede PhD

3.1 Introduction:

Developing diagnostic tools that enable accurate measurement of plasma membrane receptors, or "biomarker preserving diagnostics" is a necessary step towards precision medicine (Alunni-Fabbroni & Sandri, 2010; S. Chen et al., 2017; S. Chen, Guo, Imarenezor, & Imoukhuede, 2015). Indeed, several cancers are marked by overexpression of receptors, second messaging signaling molecules, and other deregulated biomarkers (Hanahan & Weinberg, 2011, 2000). Towards the goal of biomarker-preserving diagnostics, physiological cell isolation is needed. Current methodologies pose challenges of time-intensiveness or protein disruption (Ansari et al., 2015; De Spiegelaere et al., 2011; Nagrath et al., 2007). We recently applied magnetic beads to isolate endothelial cells from mouse skeletal muscle (Princess I Imoukhuede & Popel, 2012), endothelial cells from ischemic mouse tissue (P I Imoukhuede, Dokun, Annex, & Popel, 2013a), and both endothelial cells and tumor cells from mouse breast cancer xenografts (Princess. I. Imoukhuede & Popel, 2014). We found that magnetic bead isolation of 1-2 cell types could take upwards of five hours, which limits the clinical translation of these approaches (Nagrath et al., 2007; Naranbhai et al., 2011). Many lab-on-a-chip approaches offer faster cell isolation (Dittrich & Manz, 2006; Nagrath et al., 2007; Watkins et al., 2013). However, these

approaches often involve physical (De Spiegelaere et al., 2011; Nagrath et al., 2007; Privorotskaya et al., 2010; Watkins et al., 2013; Wynick & Bloom, 1990) or chemical methods (Adams et al., 2008; Shields et al., 2015) of manipulating cells, which may cause irreversible cell damage to plasma membrane proteins and signaling pathways (Alunni-Fabbroni & Sandri, 2010; Blann et al., 2005; S. Chen et al., 2017, 2015; De Spiegelaere et al., 2011; P.I. Imoukhuede & Popel, 2011; Mizuarai et al., 2005; van Beijnum, Rousch, Castermans, van der Linden, & Griffioen, 2008; Wynick & Bloom, 1990). Therefore, there is a need for rapid cell isolation techniques that preserve the physiological expression of proteins and genes on and within the cells (Alunni-Fabbroni & Sandri, 2010).

In pursuit of physiological cell isolation, we recently developed an affinity-based approach, Secondary Anchor Targeted Cell Release (SATCR) (Ansari et al., 2015, 2016). This system has two components (1) cell capture via the target desthiobiotin antibody to the streptavidin coated surface and (2) cell release via high-affinity biotin competition to the reversible desthiobiotin-streptavidin interaction (Fig. 3.1).

Here we achieve physiological rapid isolation by combining the SATCR onto a spiral microfluidic device. We determine how buffer supplementation stabilizes cell morphology. We examine whether selected plasma membrane receptor concentrations are preserved through our device and investigate the theoretical effects of the wall shear stress generated by the microfluidic device to ensure biologically faithful capture and release of cells. We apply our optimized buffers and device to isolate both primary human endothelial cells and a human breast cancer cell line. Altogether, the development of the coupled SATCR-spiral microfluidic device

for cell isolation, and the optimization that we present advances us towards the rapid receptor preserving technologies needed for cancer precision medicine.

3.2 Materials and Methods:

3.2.1 Computational fluid modeling: Fluid dynamics within the microfluidic device were simulated based on the incompressible Navier-Stokes equations for Newtonian fluids:

$$\rho \boldsymbol{v}_{,t} + \rho \boldsymbol{v} \cdot \nabla \boldsymbol{v} - \mu \nabla^2 \boldsymbol{v} + \nabla p = 0 \tag{1}$$

$$\nabla \cdot \boldsymbol{v} = 0 \tag{2}$$

Equations (1) and (2) are the momentum-balance and incompressibility equations respectively, where ρ is the density, $\boldsymbol{v}$ is the velocity field, $\boldsymbol{v}_{,t}$ is the time derivative of the velocity field, μ is the fluid viscosity, and p is the pressure field. The fluid is assumed to be Newtonian with fluid properties of blood: $\rho = 1060 \text{ kg/m}^3$ and $\mu = 0.0035 \text{ Pa} \cdot \text{s}$ (Weddell, Kwack, Imoukhuede, & Masud, 2015).The 3-dimensional microfluidic device geometry was developed as a rigid wall geometry with 6 concentric cylindrical spirals in Autodesk Inventor (Fig. 3.2) and meshed using Abaqus/CAE. No-slip boundary conditions were prescribed along the walls of the microfluidic device. The traction-free boundary condition is applied along the outlet of the microfluidic device. Inlet velocity is applied along the inlet of the microfluidic device with a parabolic profile given by:

$$v = v_{\max}(1 - \frac{r^2}{R^2}) \tag{3}$$

where v is the velocity at radial distance r from the center line of the microfluidic device, R is the radius of the microfluidic device $(R = 2.5 \text{ mm})$, and $v_{\max}$ is the maximum (centerline) velocity within the microfluidic device. The maximum velocity is calculated as twice the average velocity across the inlet of the microfluidic device:

$$v_{\max} = 2v_{average} = \frac{2Q}{\pi R^2} \tag{4}$$

where Q is the applied flow rate. Simulations quantifying fluid velocity and pressure profiles were carried out with the FEAP software modified with the stabilized finite element method for shear-rate dependent fluids, as described previously(Weddell et al., 2015). Post-processing and visualization of numerical data were carried out with Paraview. The stress tensor $(\boldsymbol{\sigma})$ and wall shear stress (Wall Shear Stress) are calculated in Paraview from the fluid velocity and pressure profiles as:

$$\boldsymbol{\sigma} = -pI + 2\mu\varepsilon \tag{5}$$

$$WSS = (\boldsymbol{\sigma} \cdot \mathbf{n}) - ((\boldsymbol{\sigma} \cdot \mathbf{n}) \cdot \mathbf{n})\mathbf{n} \tag{6}$$

where I is the identity matrix, ε is the strain rate tensor, and $\mathbf{n}$ is the surface normal vector.

3.2.2 Mold creation: The spiral master molds were designed and constructed using AutoCAD 2015 software (Autodesk, San Rafael, CA) and are comprised of two parallel connected spirals of 1 mm width x 217 mm length. Molds were then 3D printed using a Stereo Lithographic Apparatus at the Rapid Prototyping lab at the University of Illinois at Urbana-Champaign. Straight microchannels were printed using the same technique with 1 mm width and 40 mm length. Once printed, the molds were submerged in Sylgard polydimethylsiloxane (PDMS) (Dow Corning, Midland, MI) at a ratio of 1:10 by volume with its cross-linker, poured into the 3D printed molds then placed in a desiccator (Bel-art, Wayne, NJ) to remove bubbles. Once all bubbles were removed, the PDMS submerged mold was placed in a 55° C preheated oven (Thermo Fisher, Waltham, MA) for 60 min. The molds were removed and cooled overnight before cutting. Once set, the PDMS was removed from the molds and bonded irreversibly to 75 *x* 38 mm glass (Dow Corning, Midland, MI) using oxygen plasma treatment via Diener Plasma Cleaner Pico (Royal Oak, MI).

3.2.3 Cell culture: MCF7-GFP cells, a luminal breast cancer cell line (Corominas-Faja et al., 2013), were obtained from Cell Biolabs (San Diego, CA), as previously described (Ansari et al., 2015). Briefly, MCF7-GFP cells were grown in high glucose Dulbecco's modified Eagle medium (DMEM) supplemented nonessential amino acids (University of Illinois Cell Media Facility, School of Chemical Sciences, Urbana, IL), 10% fetal bovine serum (Invitrogen, Carlsbad, CA), and 1% Penicillin–Streptomycin (Invitrogen). HUVEC-GFP cells were obtained from Angio-Proteomie (Atlanta, Georgia). HUVEC-GFP cells and HUVECs were grown under normal HUVEC conditions, as previously described (S. Chen et al., 2015; P.I. Imoukhuede & Popel, 2011). Briefly, EGM-2 was supplemented with Bullet kits (Lonza, Basel, Switzerland). All cells were maintained at 37°C in 95% air, 5% CO2. Cells were grown to confluence before

the experiment, with HUVECs not being used beyond passage 6. For routine cell passaging, cells were detached from flasks using TrypLe (Life Technologies, Carlsbad, CA). For capture experiments, CellStripper cell dissociation solution (Corning, Manassas, VA) was applied for 5–7 min at 37° C then re-suspended in 10 mL stain buffer, containing 1% BSA and 0.09% Sodium Azide in PBS without calcium and magnesium (S. Chen et al., 2015). Cells were centrifuged at 500xg for 5 min at 4° C, supernatant was aspirated, and cells were re-suspended in cold Hanks Balanced Salt Solution without calcium, magnesium, or phenol red to a final concentration of $1x10^6$ cells/mL.

3.2.4 Poly-L-Lysine titration: PLL was titrated into cell stock solutions, HBSS wash, and biotin release solution at concentrations ranging from0.005 mg/mL to 5 mg/mL. HBSS was made as previously described (Ansari et al., 2016). Briefly, 500 mL of HBSS contained 4.0 g NaCl, 0.2 g KCl, 0.0402 g Na2PO4*7H2O, 0.03 g KH2PO4, and 0.5 g Glucose. DI water was added to get to 500 mL, filtered, and then refrigerated.

3.2.5 Biotin viability: Biotin was titrated between 20 mM to 20 nM in HBSS with trypan blue to test cell viability. Live eluted cells were counted via hemocytomer.

3.2.6 Biotin osmolarity analysis: Osmolarity of 0-4 mM biotin solutions in PBS, HBSS, DI water, and DMEM media were tested using an Wescor Vapor Pressure Osmometer Vapro 5520 (Wescor, South Logan, Utah).

3.2.7 Spiral integration: Spirals were functionalization using the previously described Secondary Anchor Targeted Cell Release System (Ansari et al., 2016). Glass 75 x 35 mm glass slides were

cleaned using Diener Plasma Cleaner Pico (Royal Oak, MI) for 5 min at 50% power and quickly placed in contact with a similarly cleaned spiral PDMS mold - forming an irreversibly bonded device. 2% (3-Aminopropyl) triethoxysilane (APTES) (Acros Organics, Geel, Belgium) in ethanol was applied to the spiral device's glass surface and placed on the Heidolph Titramax 1000 (Schwabach, Germany) vibrating platform shaker at 300 Hz for 50 min and then rinsed with ethanol. The spirals were then cured in a Thermo Scientific Precision (Thermo Scientific, Pittsburg, PA) oven for 1 hours at 90° C and rinsed with 2- (N-morpholino) ethanesulfonic acid (MES Buffer). Desthiobiotin (DSB) (Sigma, St. Louis, MO) was solubilized with 10 µL of dimethyl sulfoxide (BDH, Radnor, PA) per mg of DSB. The DSB carbonyl group at 1.5 mg/mL was activated and combined with 1-Ethyl-3- (3-dimethylaminopropyl) carbodiimide (EDC) (Thermo Scientific, Pittsburg, PA). The activated DSB was first dissolved in pH 6.0, 2- (N-morpholino) ethanesulfonic acid (MES buffer) for 15 min and quenched using mercaptoethanol and then applied to the spiral. Following overnight incubation at 4° C in a refrigerator, excess DSB was washed with phosphate buffered saline (PBS). 0.4 mg/ml streptavidin (Proteochem, Loves Park, IL) in PBS, was applied overnight at 4 °C, rinsed with PBS, rewetted, and replaced in the refrigerator until used.

3.2.8 Spiral capture experiments: Fixed MCF7-GFP cells labeled with HLA-ABC antibody prior to experiment were introduced to functionalized and non-functionalized spirals using a syringe pump (Harvard Apparatus, Holliston, MA) with a flow rate of 40 µL/min until 1 mL had been dispensed into the spiral. The spiral was exposed to a brief purging wash of PBS at the same flow rate until 1.5 mL had been dispensed, and then 4mM biotin was flown in at 40 µL/min and incubated for 10 min before completely eluting out the cells. All images were taken on 10 x

magnification Micromaster inverted microscope (Fisher Scientific, Pittsburg,PA). Cells were released via biotin flow at a rate of 40 µL/min.

3.2.9 qFlow cytometry. 25 µL aliquots of cells (1 x 10^5 cells) were added to 5 ml polystyrene round-bottom tubes (BD Biosciences, New Jersey) and labeled with phycoerythrin (PE)-conjugated monoclonal antibodies at the optimal concentrations: 14 µg/mL for VEGFR1, VEGFR2. Tubes were protected from light and incubated for 40 minutes on ice. Cells were washed, centrifuged at 500 ×g twice with 4 mL stain buffer, and resuspended in 300 µL stain buffer. The precision and accuracy of qFlow cytometry profiling has been rigorously tested (Bergers, Song, Meyer-Morse, Bergsland, & Hanahan, 2003; Casanovas, Hicklin, Bergers, & Hanahan, 2005; S. Chen et al., 2017, 2015; Erber et al., 2004; Willett et al., 2004). A LSR Fortessa (BD) was used for cell data acquisition; BD FACSDIVA software was used for data processing; and FlowJo (TreeStar) software was used for data analysis. Tubes were vortexed immediately prior to placement in the flow cytometer. 5,000–10,000 live single cells were collected from each tube. 5 µg/mL Sytox Blue (Invitrogen) was added to all samples to distinguish between live and dead cells.

3.2.10 Statistical Analysis- receptor concentrations: Quantibrite PE beads (BD) were collected and analyzed under the same compensation and voltage settings as cell fluorescence data. Quantibrite PE beads comprise a combination of polystyrene beads conjugated with different density of PE molecules: low (474 PE molecules/bead), medium–low (5,359 PE molecules/ bead), medium–high (23,843 PE molecules/bead), and high (62,336 PE molecules/bead). As described in our previously published work (S. Chen et al., 2015), a calibration curve that translated PE geometric mean to the number of bound molecules was determined using a linear

regression. In order to accurately quantify cell-by-cell receptor levels, the background signal from cell auto fluorescence must be subtracted from the fluorescence signal, as demonstrated in our previous work (S. Chen et al., 2015).

3.2.11 Cell size, osmolarity, and live percentage statistics: Significance was tested via the one way analysis of variance (ANOVA) Fisher test. Unless otherwise noted, $p<0.05$ was considered statistically significant and is indicated with *, $0.001<p<0.01$ is indicated with **, and $p<0.001$ is indicated with ***.

3.3 Results:

3.3.1 Computational simulations show wall shear stress within physiological levels: We computationally simulated the spiral design and quantified wall shear stresses (Fig. 3.2) to identify whether the spiral design was causing non-physiological stresses on the cells. In our simulation we found wall shear stresses to be between 0.1 to 0.3 Pa which is within an order of magnitude of arterial wall shear stresses (dela Paz, Walshe, Leach, Saint-Geniez, & D'Amore, 2012; Kornet, Hoeks, Lambregts, & Reneman, 1999, 2000; Samijo et al., 1998) which can range from 6-40 dynes/cm^2 (0.6-4 Pa). These physiological wall shear forces should not be high enough to trigger apoptosis or cell death, and thus should not cause rapid alteration of receptor levels.

3.3.2 Coiled Tube has a Higher Mixing Efficiency than Straight Tube

To determine the optimal microfluidic shape, we compare mixing efficacy. In the straight tube design, the blue and yellow fluids remained distinct throughout the 100 mm length (Fig.

3.2A). Conversely, a coiled 100 mm tube resulted in a uniform green mixture after traversing ~20% of the tube length (Fig. 3.3B). As expected, this indicates more efficient mixing in the coil rather than the straight tube. We show the color histogram distributions at different locations in the straight and coiled tube (Fig. 3.3D) for red, blue, and green color values. As previously stated, the homogeny of the coiled tube in comparison to the wide distributions of the straight tube show much more extensive mixing in the coiled tubing. The final spiral design (Fig. 3.3) is a planarized version of the coiled tube, which we use for microfluidic mixing.

These advantages can be understood through fluid dynamics fundamentals. In straight channels, the Reynolds number (Re): $\mathrm{Re} = \frac{\mathrm{Q*D}}{\mathrm{v*A}}$ (7)

characterizes flow as laminar (Re < 2500), transition (2500 < Re < 5000) (Capretto, Cheng, Hill, & Zhang, 2011), or turbulent (Re > 5000) (G. K. Batchelor, 1967), and Re is defined by flow rate (Q), hydrodynamic diameter (D), kinematic viscosity (ν), and cross sectional area (A), see Equation 9. In each case flow regime mixing is a function of both diffusion and advection with turbulent advection resulting in chaotic changes in fluid profile and greater mixing in comparison to transition flow advection, and laminar flow offers the lowest advection component, resulting in lesser mixing. In contrast, curved channels are influenced both by the Reynolds number as well as by secondary flow contributions, or vorticity, represented by the Dean number (De), see Equation 10. The Dean number is dependent on the Reynolds number, as well as the tubing's diameter and radius of curvature

(r_c): $De = Re * \sqrt{\frac{diameter}{2r_c}}$ (8)

Exploiting the secondary flow generated by a spiral allows for increased mixing without invoking turbulent flow (Gelber, Kole, Kim, Aluru, & Bhargava, n.d.) that damages and influences live cell signaling due to high shear stress (dela Paz et al., 2012; Fukuda & Schmid-Schönbein, 2002; Ludwig, Kretzmer, & Schügerl, 1992; Olesen, Clapham, & Davies, 1988; Tanzeglock, Soos, Stephanopoulos, & Morbidelli, 2009). Thus, optimizing the effects of secondary flow is crucial for allowing better mixing without altering or lysing the cells.

3.3.3 The biotin release solution maintains cell viability: A key goal of the SATCR-spiral system is to maintain cell viability; therefore, we sought to examine the limits of our device—specifically identifying whether biotin may affect cells. We observed that biotin does not affect cell viability through our device. There was no change in cell viability relative to control (HBSS without biotin) when a super-saturated biotin solution was applied to cells (20 mM, Fig. 3.4). Moreover, sub-saturating to super-saturating biotin concentrations (20 nm-20 mM) also do not affect cell viability, assayed via trypan blue staining (Fig. 3.4). These findings imply neither the control nor the biotin cause cell death, even when using a super saturated biotin solution beyond the 4 mM release saturation concentration.

3.3.4 The functionalized spiral allows targeted cell capture and release: MCF7-GFP cells were introduced to both the SATCR functionalized and a non-functionalized spiral mixer to compare cell capture and release. Eluents were collected after every wash for release quantification (Supplementary Fig.3. 3). Imaging shows the spiral before cell introduction with no cells adhered to the surface (Fig. 3.5A). Cells are then flown into the device, allowed to attach, and non-adherent cells are washed out with HBSS. The post-HBSS wash surface (Fig.3.4B) should primarily include cells captured via the SATCR system. Cells are captured in the SATCR

functionalized device via the interaction between the biotinylated antibodies and the cells of interest. Once captured, the cells are released via biotin competition with the secondary anchor-desthiobiotin. This competition results in the subsequent release of the cells of interest from the surface allowing for downstream recollection of the cells. After a 4 mM biotin wash (Fig. 3.5C), we see 1.4 fold larger cell release from the functionalized spiral as compared to the non-functionalized spiral. We conclude that although cells can attach non-specifically, as seen in the non-functionalized spirals, these cells were not released via biotin introduction and as such are not necessarily the intended cells of interest. Thus, the functionalized surface confers cell-specificity when compared to a non-functionalized surface.

3.3.5 Spiral design promotes better release from SATCR capture surface: We verified cell capture and release in both spiral and straight tube designs to quantify the improvements on the SATCR system's capture and release with the secondary forces associated with the spiral device,. Using the SATCR capture surface, 24% of MCF7-GFP cells were captured and 29% were released using a 4 mM biotin solution integrated with the spiral mixer. Conversely, a functionalized straight tube control allows for the 21% cell capture using the streptavidin capture surface, but only a 17% release from the surface. This 12% decrease in cells released shows the spiral allows for increased mixing and a better functionalized surface release (data not shown). Both spiral and straight tube were washed with 0.5 mg/mL PLL in PBS as well as released using 4 mM biotin solution with 0.5 mg/mL PLL. Thus, a spiral device allowing for better distribution of the biotin via the secondary flow would further optimize release from the SATCR surface.

3.3.6 Cell crowding should not occur in the spiral: To determine whether the surface area within the functionalized spiral was sufficient for capturing cells, we analyzed the total surface area of

the channel, cell capture efficiency, and total number of cells introduced (Equation 7). The properties defining the channel included a spiral length of 2.18 x 10^5 μm and a channel width 1000 μm, giving a total surface area of 2.18 x 10^8 μm^2. As a standard, we flow 1.0 x 10^6 cells/mL into the device, and we have previously calculated a minimum capture efficiency of 30% (Ansari et al., 2015). Together, this indicates that each cell would be allotted much more than 60-200 μm^2. Data on cells are described in Table 1. Even with a capture efficiency increased to 100%, the total available area per cell would be 10% more than space necessary for the largest cell size.

$$Area\ per\ Cell = \frac{Total\ Surface\ Area}{Capture\ \%* Total\ number\ of\ Cells} \quad (9)$$

This lack of crowding is beneficial for maintaining physiological expression of cells captured in the spiral SATCR device, as cells that are forced too close to each other would risk altering expression levels through signaling as well as through processes related to cell over-confluency such as selection stresses or even morphological changes (Ishibe, Haydu, Togawa, Marlier, & Cantley, 2006). Altering these receptors levels from physiological expression would bias downstream analysis, and give information that could be non-indicative of the patient's expression profile. Thus, to ensure physiological expression, cells captured on the SATCR surface must not be over-crowded.

3.3.7 Poly-L-Lysine stabilizes cell diameter: We examined whether the spiral (1) applies acceptable wall shear stress on captured cell surfaces and (2) alters cell sizes to examine the biological faithfulness of the device. First we estimate wall shear stress applied across captured cell surfaces to be < 0.3 Pa (Fig. 3.2), which we deem acceptably low wall shear stress as it falls

within physiological ranges (i.e. femoral artery wall shear stress is 0.32-0.38 Pa (Kornet et al., 1999, 2000)). We observed that cells isolated by our device experienced a decrease in cell diameter of >25% (Fig. 3.4 & Supplemental Fig. 3.1A). This change was not due to solution osmolarity. With increasing biotin concentration, DMEM, PBS, and HBSS are all within the range of what is considered isotonic osmolarity (Alexander, Corrigan, & Infusion Nurses Society., 2010; Kimura, Matsui, & Sato, 1974; McGurk, 2010) (Fig. 3.4 & Supplementary Fig. 3.1B). We hypothesized that the acidity of the streptavidin-coated surface (pI=5.0 (Kobayashi et al., 1995)) could lead to negative charge sequestration, a hypertonic microenvironment. An environment with high ionic character would result in cell shrinkage as cells aim to reach an osmotic balance. Towards stabilizing the cells, we further hypothesized that buffering via positively charged PLL could preserve cell diameter. To test this, we titrated PLL at concentrations up to 5 mg/mL and observed that 0.5 mg/mL PLL led to a significant stabilization of cell diameter (Supplementary Fig.3. 1C). The highest PLL concentrations (5 mg/mL) seemingly reversed this effect, decreasing cell diameter due to increased local osmolarity. This effect of the addition of PLL on total solution osmolarity can be easily calculated using the equation (Purssell, Pudek, Brubacher, & Abu-Laban, 2001):

$$Osmolarity\ (in\ Os) =$$

$$[Molar\ concentration\ of\ Constituent\ added] + Solvent\ Osmolarity \quad \text{..... (10)}$$

Using Equation 8 we can see that the 5 mg/ mL addition of PLL (assuming a molar mass of 2,000 g/mol) contributes to an addition of roughly 2.5 mOs, which doesn't really change the 260 mOs PBS solution. Thus, we can assume that the total osmolarity of the solution is not significantly affected, preventing cell lysis or death.

3.4 Discussion:

In this study, we optimized and implemented the secondary anchor tethered cell release (SATCR) system onto a spiral microfluidic device and achieved the following: we (1) increased spiral mixing efficacy compared to a straight channel; (2) computationally identified that a flow rate of 300 µl/min facilitates low wall shear stress (10^{-3} to 10^{1} Pa) within the spirals; (3) we determined that PLL supplementation in buffers preserves cell morphology; (4) determined that the device gently captures cells without changing VEGFR1 concentrations on endothelial plasma membranes; and (5) we successfully captured 60% of primary human endothelial cells (HUVEC-GFP) and 70% of a human breast cancer cell line (MCF7-GFP), using the device. These optimizations will enable the rapid and biologically faithful cell isolation needed for personalized cancer medicine, which we contextualize, herein.

3.4.1 *Spiral microfluidics can improve passive mixing:* Spiral microfluidics have been previously used for micromixing (Scherr et al., 2012; Sudarsan & Ugaz, 2006; Vanka et al., 2003; Vanka, Luo, & Winkler, 2004). The advantage lies in the curved walls, which allow for more physiological passive mixing without introducing active mixing elements through the use of secondary flow. Numerical simulations of spirals show that spirals with 1 mm diameter and device radius of 2.5 mm offer mixing efficiencies of 87% while maintaining laminar flow (Re= 67) (Scherr et al., 2012). It is important to note that a straight tube with a Re=67 would represent a diffusion based mixing regime.

Passive mixers also reduce the amount of stress that cells would experience, as there would not be any elements introducing heating, or rotating pieces for mixing. Thus, for our

microfluidic adaption, passive mixers are more optimized for receptor preserving capture and release.

3.4.2 *Particle and cell separations have used spiral microfluidics extensively:* In addition to mixing, spirals have been used to facilitate inertial-based cell separations (Kim et al., 2014; S. Kuntaegowdanahalli & Bhagat, 2009; Shields et al., 2015; Lidan Wu, Guan, Hou, Bhagat, & Han, 2012) . Inertial approaches refer to the centering of particles in non-turbulent flow profiles without the need for either outside electrical or physical assistance (Hahn, Hong, Kang, & Choi, 2016).Notable examples include the work of Hahn et al who demonstrated separation of particles between 15 -25 μm; here, they used flexible configurable tubing, which can customize the flow profiles without the complexities of conventional microfabrication techniques (Hahn et al., 2016). The Papautsky Lab has developed a size based spiral separation modality(S. Kuntaegowdanahalli & Bhagat, 2009) by harnessing the drag forces associated with spiral dean forces. Using a 5 loop Archimedes spiral which is 500 μm x 130 μm high, they center the particles and utilize a 1 mm wide chamber to size separate the output stream into 8 different outlets. By altering the Dean number, they increased the separation and migration of the different particles at 80% separation efficiency (S. S. Kuntaegowdanahalli, Bhagat, & Papautsky, 2009). With regards to cell separation the Han Lab, which demonstrated leukocyte separation from blood using inertial focusing (Lidan Wu et al., 2012). Additionally, the Kasagi Lab has separated a dual cell mixture of endothelial cells (HUVECs) and leukocytes (HL60) using an adhesion based spiral device which allows them to mix their biotinylated CD31 and CD86 antibody capturing components with their respective cellular targets (Miwa, Suzuki, & Kasagi, 2008). They harness the interaction with streptavidin to slow the velocity of positively labeled cells. They then separate their cells based on the time when they exit the channel. The development of

our spiral integrated cell isolation platform builds upon this existing literature, and represents the first application of a reversible affinity-based tethering to a spiral microfluidic design.

3.4.3 Spiral Wall Shear Stress should not alter physiological expression of cells via mechanotransduction: As we are optimizing the SATCR spiral device for physiological capture and release of cells, it is imperative that wall shear stress and flow rates are optimized to ensure a physiological cell isolation that does not alter angiogenic receptor expression levels such as VEGFR1 for the cells. Flow rates of 8 mL/ min are sensed by the glycocalyx (Ramiro-Diaz et al., n.d.), particularly by ion channels (Olesen et al., 1988) and integrins. These integrins further transduce forces to the cytoskeleton via adapter proteins (Barry, Wang, & Leckband, 2015), altering cell physiology and protein expression (T & Papaioannou T, 2005). Shear stress also activates the vascular endothelial growth factor receptors (VEGFR)-PI3K-Akt pathway (Coon et al., 2015), triggering a proliferative or migratory endothelial phenotype (Karar & Maity, 2011) and upregulating VEGFR expression on endothelial cells (dela Paz et al., 2012). This is particularly troublesome for biomarker detection, because VEGFRs on cancer-associated endothelial cells can serve as predictive biomarkers for anti-angiogenic drug efficacy (S. Chen et al., 2015; Weddell & Imoukhuede, 2014). Likewise, shear stress has been shown to modulate the expression of other key cancer biomarkers (Chang et al., 2008; Rizvi et al., 2013), which would similarly alter the ability of researchers to identify effective therapies (Rizvi et al., 2013). In order to test whether our spiral design would apply non-physiological forces onto the cells, we computationally identified that a 300 μL/min flow rate would present a peak Wall Shear Stress of 0.2 Pa (Fig. 3.2B). This value is comparable to the physiological Wall Shear Stress in large arteries, such as the common femoral artery (0.32 – 0.38 Pa (Kornet et al., 1999, 2000)). Moreover, the results indicated a linear trend between applied flow rate and peak Wall Shear

Stress, so flow rates up to 3,000 µL/min would be comparable to the wall shear stress experienced by small arteries, such as the common carotid artery (2.6 – 4.3 Pa (Samijo et al., 1998)). These simulations offer a range of physiological flow rates that can be used in our spiral microfluidic device. As such, these forces should not result in alteration of cellular expression from physiological expression. This preservation of cell expression is paramount for the construction of a "physiologically faithful" isolation modality. Therefore, our application of spiral mixing offers increased mixing while maintaining wall shear stress within physiologically accurate ranges.

3.4.4 Spiral capture does not alter VEGFR1 plasma membrane concentrations: We observed that the isolation of endothelial cells with our device did not significantly alter VEGFR1 concentrations on these cells (Fig. 3.7). Cell-by-cell analysis (Fig. 3.7A) show that the general frequency curve for VEGFR1 in all cell suspensions are similar and correspond to similar quantitative receptor values (Fig. 3.7B). Quantitative profiling of VEGFRs has identified that these receptors can provide insight into tissue heterogeneity, drug efficacy, and such data can enable computational model development. These computational models could allow for more accurate representation of patients for drug testing and further personalized medicine, but require more enriched samples of single cell types in order to quantify these different receptors. Previous quantification of VEGFRs from dissociated tissues used a magnetic bead isolation protocol (P I Imoukhuede, Dokun, Annex, & Popel, 2013b; Princess. I. Imoukhuede & Popel, 2014; Princess I Imoukhuede & Popel, 2012; Roxworthy et al., 2014) to enrich cell populations, which can take upwards of 7 hours. Indeed, cell isolation via magnetic bead isolation (Nagrath et al., 2007), laser capture microdissection (De Spiegelaere et al., 2011), and fluorescence activated cell-sorting (Wynick & Bloom, 1990) are all known to be time, labor, and at times reagent-intensive (De

Spiegelaere et al., 2011; Plouffe, Murthy, & Lewis, 2014). The development of this microfluidic device that can rapidly isolate cells while preserving biomarkers, like plasma membrane receptors, can enable the high-throughput screening needed for both precision medicine and systems biology applications.

3.4.5 Poly-L-Lysine preserves physiology by stabilizing cell diameter: PLL has previously been used for cell patterning (Almodóvar et al., 2013; Dertinger, Jiang, Li, Murthy, & Whitesides, 2002; Khademhosseini et al., 2004), microfluidics (Almodóvar et al., 2013; Dertinger et al., 2002; Khademhosseini et al., 2004; Millet, Stewart, Nuzzo, & Gillette, 2010; Togo, Takamura, Asai, Kaji, & Nishizawa, 2007). PLL is positively charged, which is useful to several applications, including: anode/cathode creation (Togo et al., 2007), and DNA protein adsorption (Vasdekis, O 'neil, Hubbell, & Psaltis, n.d.). Our microfluidic device uses the positively charged PLL in order to preserve cell physiology by mitigating the local osmolarity differences and restore the local osmolarity of the cell environment. Osmolarity is a well-established regulator of cell size in the body, and diseases that alter the osmotic balance affect cell size (Kiehl, Shen, Khattak, Jian Li, & Sharfstein, 2011; Lang et al., 1998) even resulting in cell lysis (Lang et al., 1998). Measuring the changes in cell diameter would correspond with how close the SATCR capture environment mimics the cell's native environment. Our results show that cell size is stabilized through the introduction of PLL (Fig. 3.6), indicating that it enables a more physiological device.

3.4.6 Functionalization of surface may also functionalize PDMS, increasing capture surface area: There is the possibility that our capture surface area includes both the glass surface and the PDMS channel walls, as both surfaces are silicon based. Several papers have shown the

attachment of self-assembled layers of silanes to alter the surface chemistry of the native PDMS (Chuah, Kuddannaya, Lee, Zhang, & Kang, 2015; Ibarlucea, Fernández-Sánchez, Demming, Büttgenbach, & Llobera, 2011; Kuddannaya & Chuah, 2013), so APTES may bind to both indiscriminately, forming a self-assembled monolayer. This functionalization displays the amine group necessary for 1-Ethyl- 3- (3-dimethylaminopropyl) carbodiimide (EDC) activation and all subsequent SATCR functionalization (Fig. 3.1). Thus, it can be hypothesized that the PDMS spiral also exhibits the same SATCR functionalization as the glass layer, which would increase the cell isolation surface area to three dimensions.

3.4.7 Conclusions and recommendations for optimized system: In conclusion, our spiral integrated SATCR system successfully isolates dissociated cells. We have optimized the system for maintaining physiological wall shear stress, cell diameter, and plasma membrane receptor concentrations. Our optimized surface is the 3D printed Stereolithographic apparatus mold which allows the greatest uniformity and reproducibility in creating the PDMS mold.

This design can be further optimized to separate multiple cell types of interest. With inputs and outputs at each spiral, antibodies and cells could be mixed in one non-functionalized spiral and sent into a functionalized spiral for cell capture. Non-captured cells plus an antibody to another cell-type could be introduced into a third, non-functionalized, spiral and sent to another functionalized spiral for cell capture. A serial spiral design such as this could isolate any number of cells of interest from dissociated tissue, plasma, serum, or whole blood.

The microfluidic implementation of the SATCR surface enables higher fidelity biomarker quantification by enriching and purifying samples prior to use in diagnostics. Quantifying

biomarkers on physiologically expressing cells gives information that can be used for both therapeutic and diagnostic advancement (S. Chen et al., 2017, 2015; P I Imoukhuede et al., 2013a; Princess. I. Imoukhuede & Popel, 2014; Princess I Imoukhuede & Popel, 2012). By exploring the expression levels of individual cell types of interest, it becomes possible to tailor individual drugs and regimens to cancers based on patient sample and drug resistances. Quantifying biomarker concentration on physiologically expressive cells also allows for diagnostics for disease progression. Thus, more accurate quantification of patient cell and biomarker expression is crucial for personalized medicine.

More accurate quantification of biomarkers from physiological expressive cells also advances computational modeling. Isolating physiologically expressing cells allows more accurate parameter building for computational modeling (S. Chen et al., 2017; Weddell & Imoukhuede, 2014). This can then be used to create individualized patient models that can then be used to design therapeutic regimens by using patient expression parameters.

Moreover, this technology is completely customizable: our use of antibodies, allows cells that can be distinguished by plasma membrane-specific proteins [e.g., cluster of differentiation (CD) markers] to be easily separated. Therefore, this approach can be extended to several disciplines, including neuroscience, where separating neurons and glia enables the structure-function studies necessary to map the human brain (Graf, Ralston, Ko, & Boppart, 2009; Mir et al., 2014; Motl et al., 2015). Similarly, this device can be extended to regenerative biology, where isolating adult progenitor cells can be challenging, due to the sensitivity of these cells to environmental changes (Erdbruegger, Haubitz, & Woywodt, 2006). However, tools like this are necessary to enable development of scaffolds for chrondrocytic and osteogenic differentiation of

human mesenchymal stem cells (Ren et al., 2016) or even customizable matrices for differentiation of liver progenitor cells (Kourouklis, Kaylan, & Underhill, 2016). Ultimately, this device can be commercialized and distributed as a customizable, rapid, low-cost, research and diagnostic tool.

3.5 Figures:

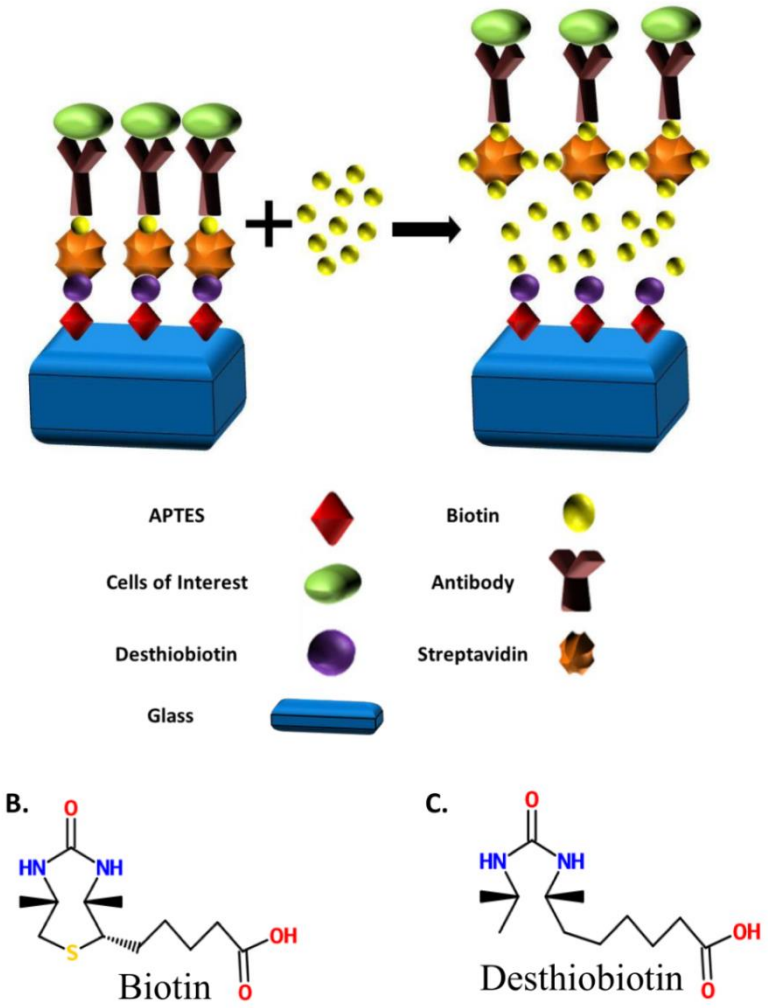

Figure 3.1: Secondary anchor targeted cell release (SATCR) surface (Ansari et al., 2015, 2016). (A).Target cells are first labeled with biotinylated antibodies, specific to the cells. The biotinylated antibodies are then attracted to and captured by the streptavidin molecules, functionalized on the surface. Cells are then released through the introduction of excess biotin (B), which out-competes the desthiobiotin (C), releasing the cells. Chemical formulas were made in emolecules software (Del Mar, CA).

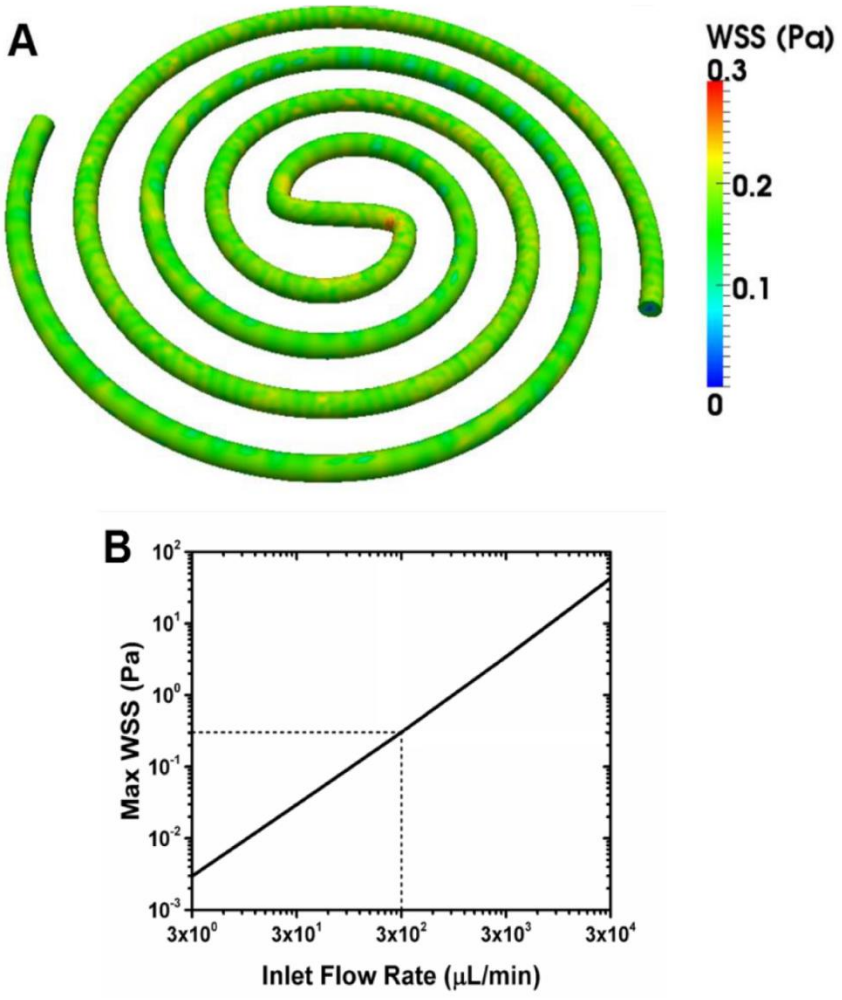

Figure 3.2 Wall Shear Stress Simulations. Fluid velocity and pressure profiles were solved using computational fluid dynamic simulations within the microfluidic device, as described in the Materials and Methods. (A) Wall Shear Stress distribution across the spiral use the standard 300 µL/min inlet flow rate. (B) Peak Wall Shear Stresses across the spiral are represented with inlet flow rates ranging between 3 – 30,000 µL/min. The dashed lines represent the maximum Wall Shear Stress obtained when using the standard 300 µL/min inlet flow rate.

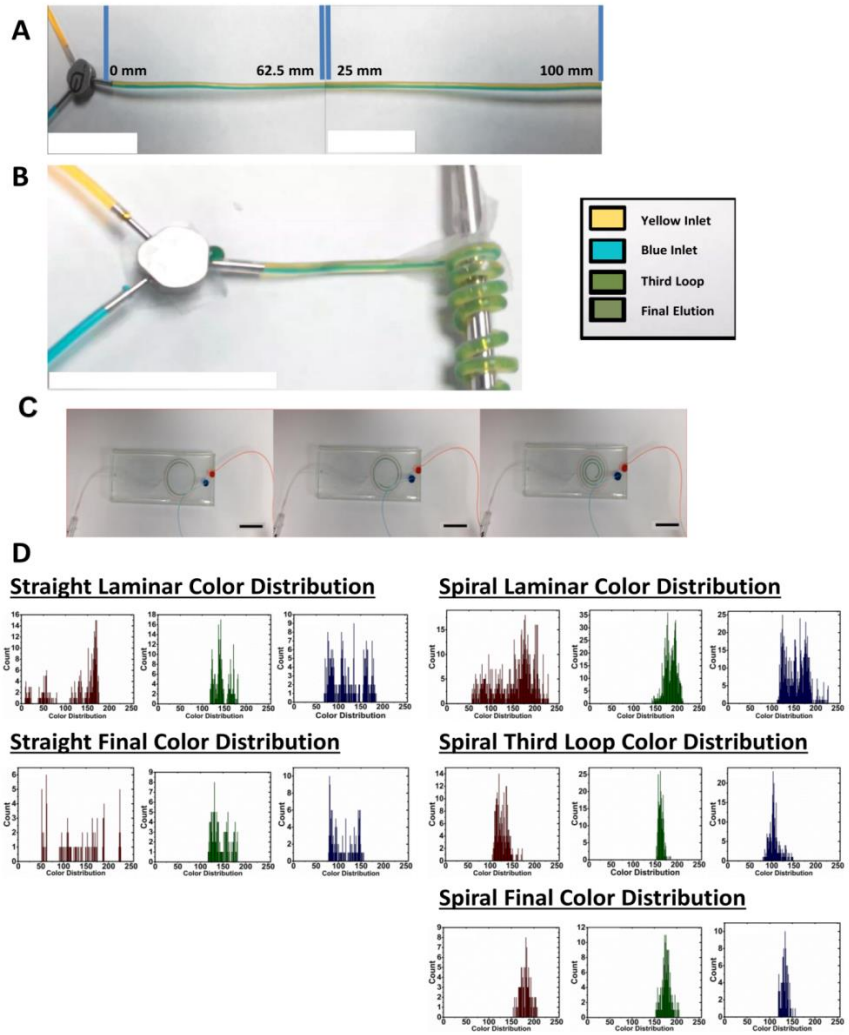

Figure 3.3: Fluid Mixing Comparison between Straight and Curved Tubing. Two colored fluids are introduced in a (A) straight tube and a (B) spiral of identical tubing. The planarized spiral design (C) also allows for more effective mixing of two inputs. As red and blue dyes are introduced, mixing is evident. When color histograms are analyzed of the red, green, and blue intensities (D) the final eluent of the straight tube (top row) shows wider distributions of colors in the red, blue and green colors histogram, owing to the less mixing and higher heterogeneity. In the curved tubing (bottom row), the secondary flow allows a more homogenous mixing for the spiral eluent. As expected, the spiral model allows for a more even distribution of colors, owing to its more complete mixing. Scale bars in (A) and (B) = 25 mm and (C) are 20 mm.

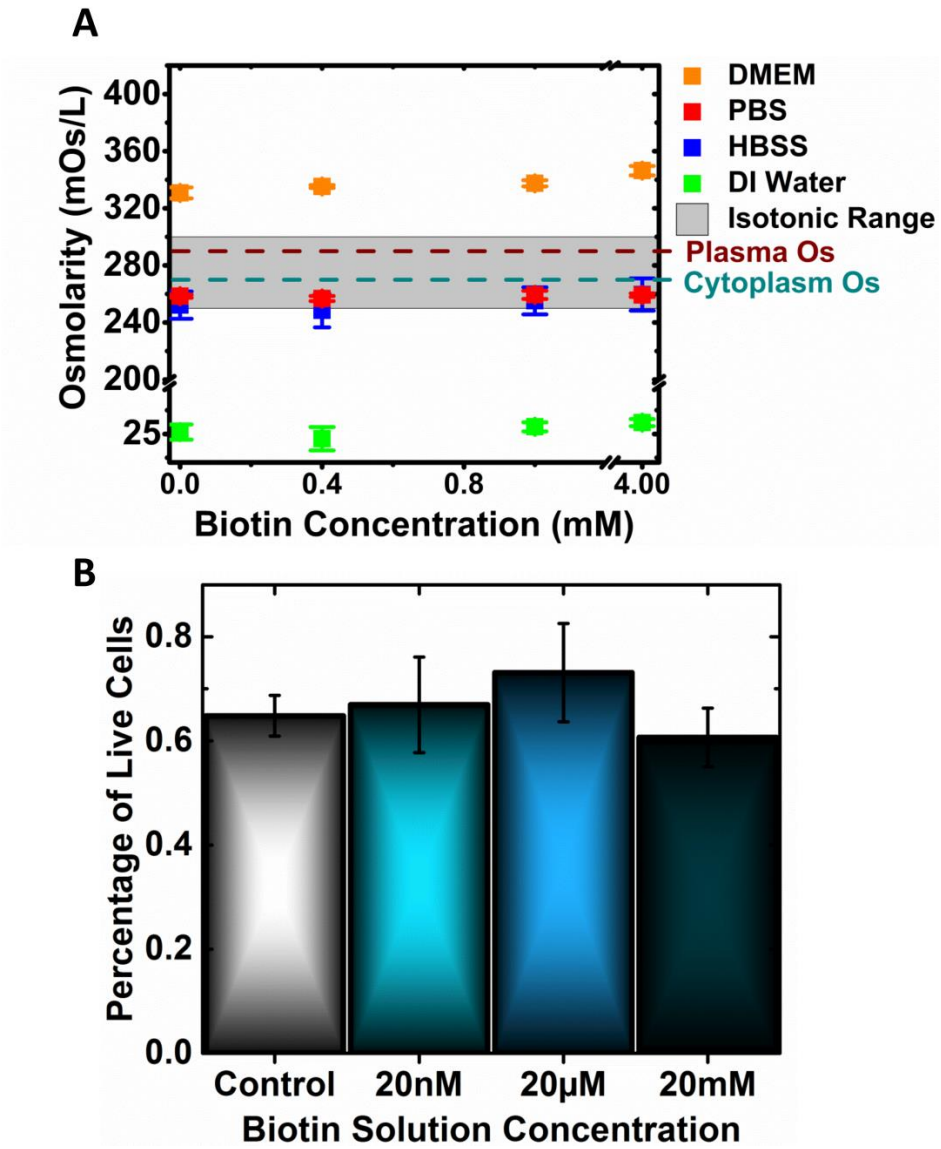

Figure 3.4: Biotin release solution osmolarity and cell viability (A) Osmolarity of biotin solutions were measured by Wescor Vapor Pressure Osmometer Vapro 5520 and were found to be in the physiological range of 260-300 mOs, greyed area(Kimura et al., 1974; McGurk, 2010) . (B) Trypan Blue-based cell viability was measured via a hemacytometer for a HBSS (control) and 20 nm - 20 mM Biotin in each solution. Biotin saturation in both PBS and HBSS solvent is 4 mM, so our data shows that a super-saturated biotin solution does not cause significant cell death relative to control.

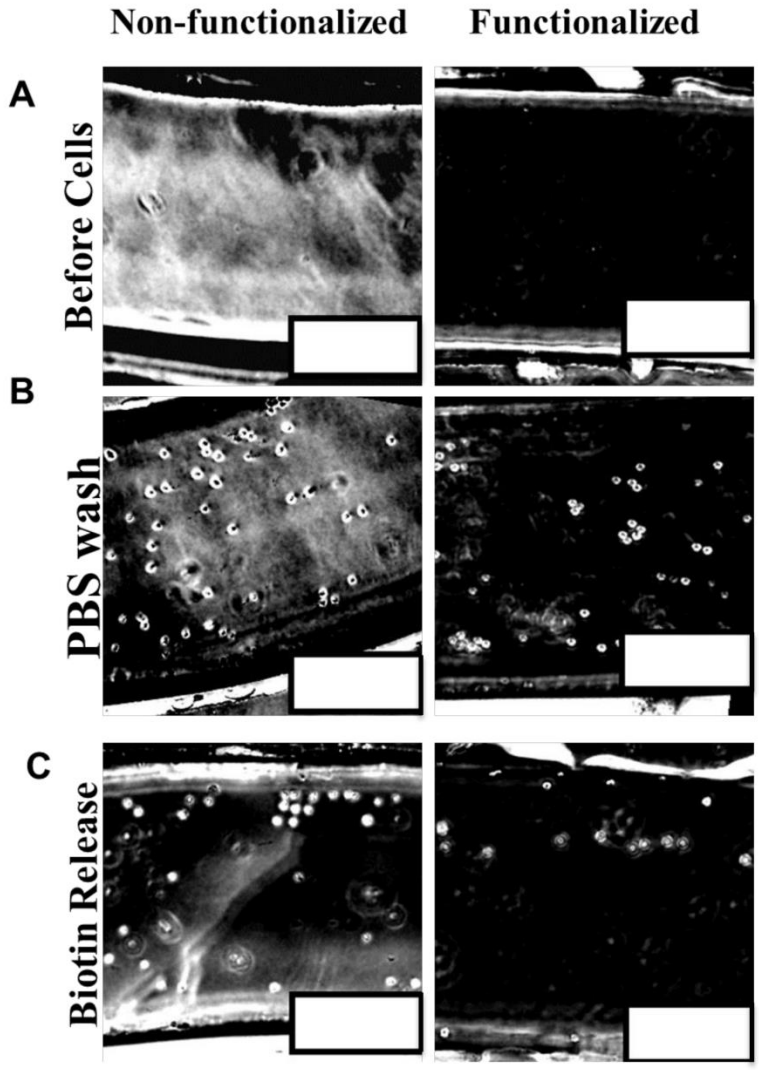

Figure 3.5: Brightfield imaging of MCF7-GFP cells isolated by hHLA-ABC antibody (A) Image represents non-functionalized and functionalized spiral before cells are introduced. (B) Non-functionalized spiral exhibits some nonspecific cell adhesion to glass after PBS wash and a functionalized spiral shows cell adhesion after PBS wash. (C) Biotin treatment releases 1.4-fold more cells from functionalized spiral. Flow-rate through spiral is 300 μL/ min. Magnification taken at 4X Objective with an Olympus UPlanFl with a numerical aperture of 0.13. The image is grayscaled and contrasted to show cells more clearly. Scale bars are 400 μm.

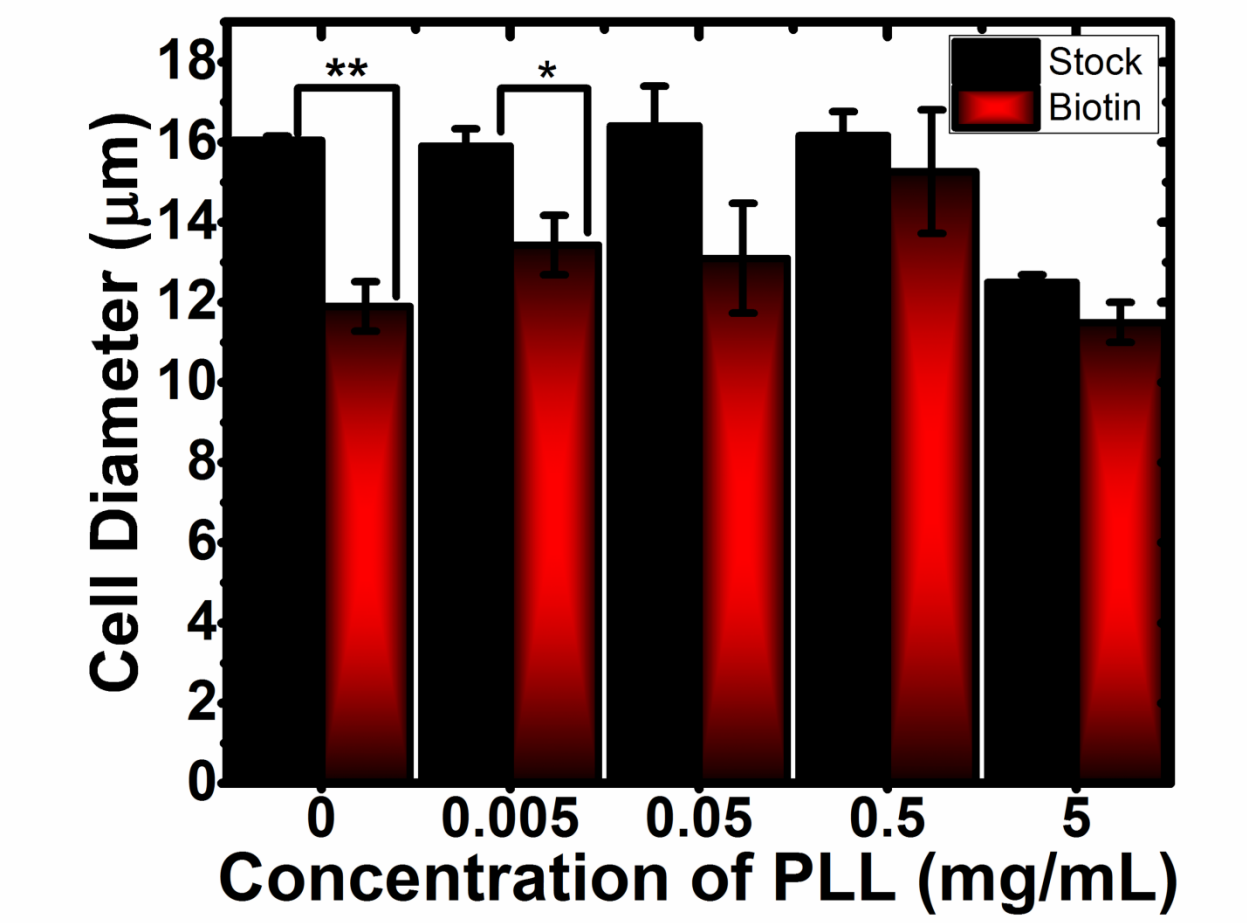

Figure 3.6: PLL supplementation and cell diameter. Captured cells eluted through the spiral exhibit a ~4 μm decrease in cell diameter. Supplementation of buffers with 0.05-5 mg/mL PLL stabilized cell diameter through the spiral.

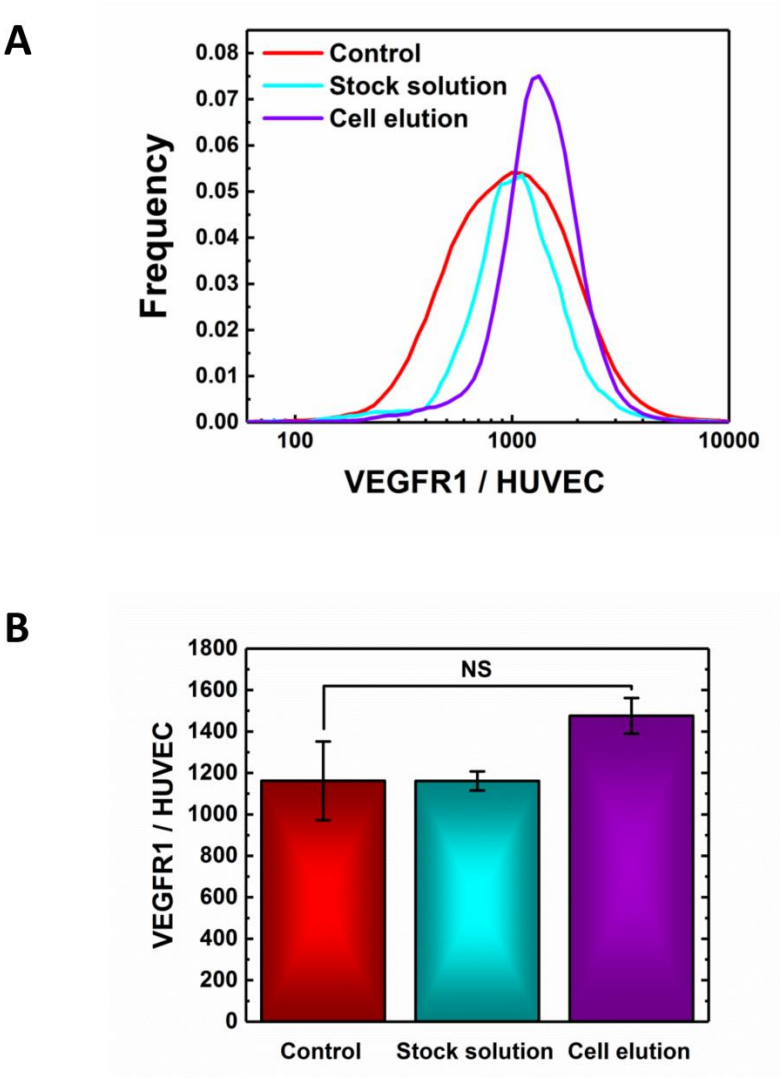

Figure 3.7: Cell-by-cell distribution of VEGFR1 on HUVECs captured and released from the device. qFlow cytometry was used to measure the cell by cell receptor distribution (A) of VEGFR1 and the average receptor numbers (B) on: (1) control HUVECs that were not exposed to CD31 antibody and not flown through the device, (2) HUVECs in stock solution that were exposed to the biotinylated CD31 antibody but were not flown through the device, and (3) HUVECs from cell elution that were flown through the device. The distributions show non-significant changes in VEGFR1 expression throughout the different cases, showing preservation of expression within the device.

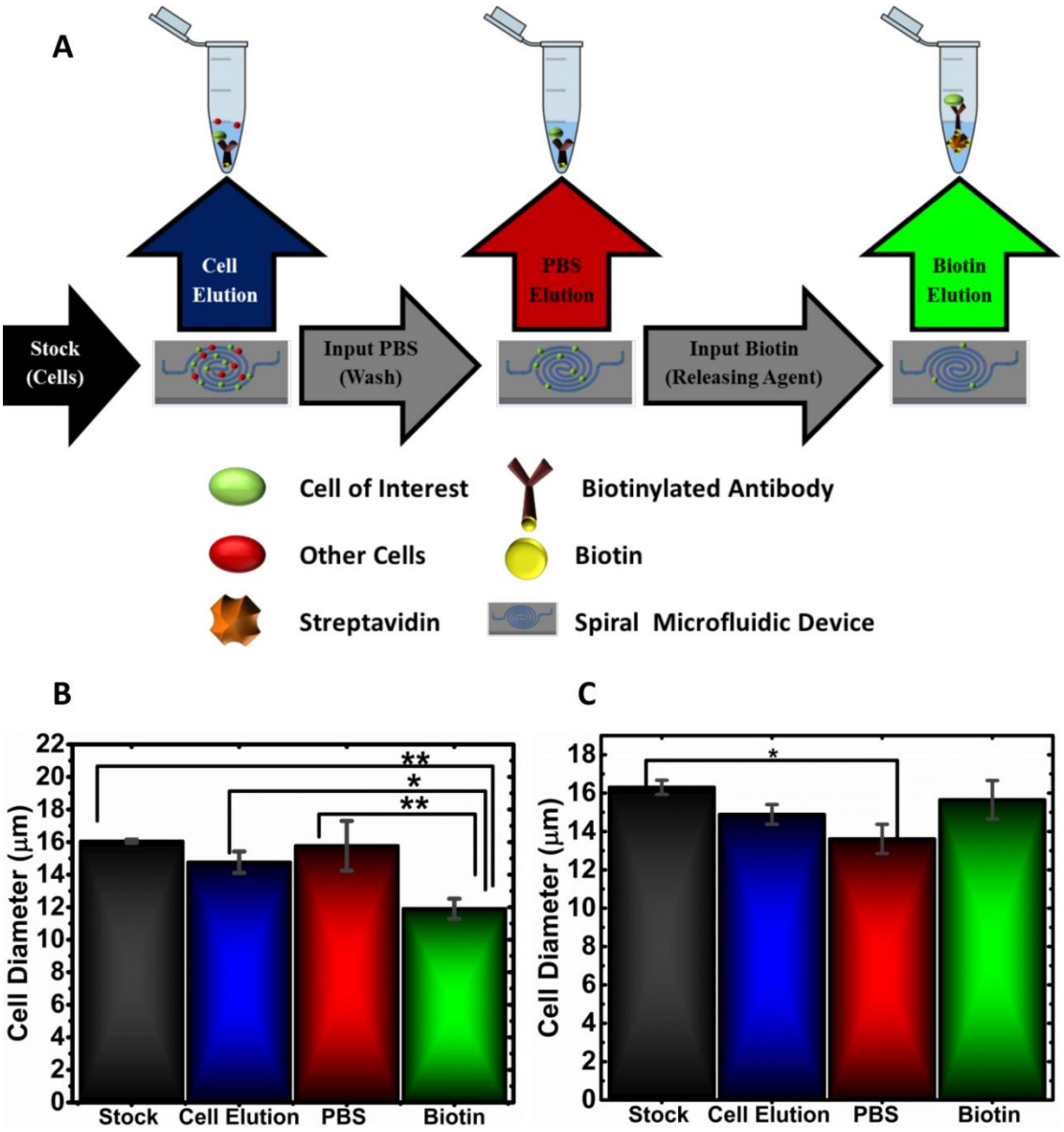

Supplementary Figure 3.1: Spiral effect on cell diameter. (A) Eluents taken from spiral and (B) cell diameter are measured via Countess II Automatic Cell Counter. A 26% decrease in cell diameter is seen when the stock solution of cells introduced to the spiral is compared to the cells released via 4mM biotin. (C) Supplementation of all solutions (cell stock, PBS wash, and biotin release) with 0.5 mg/mL PLL stabilized the cell diameter. Significance is tested via ANOVA Fisher Test where $p < 0.05$ is indicated with *, $0.001<p<0.01$ is indicated with **, and $p<0.001$ is indicated with ***.

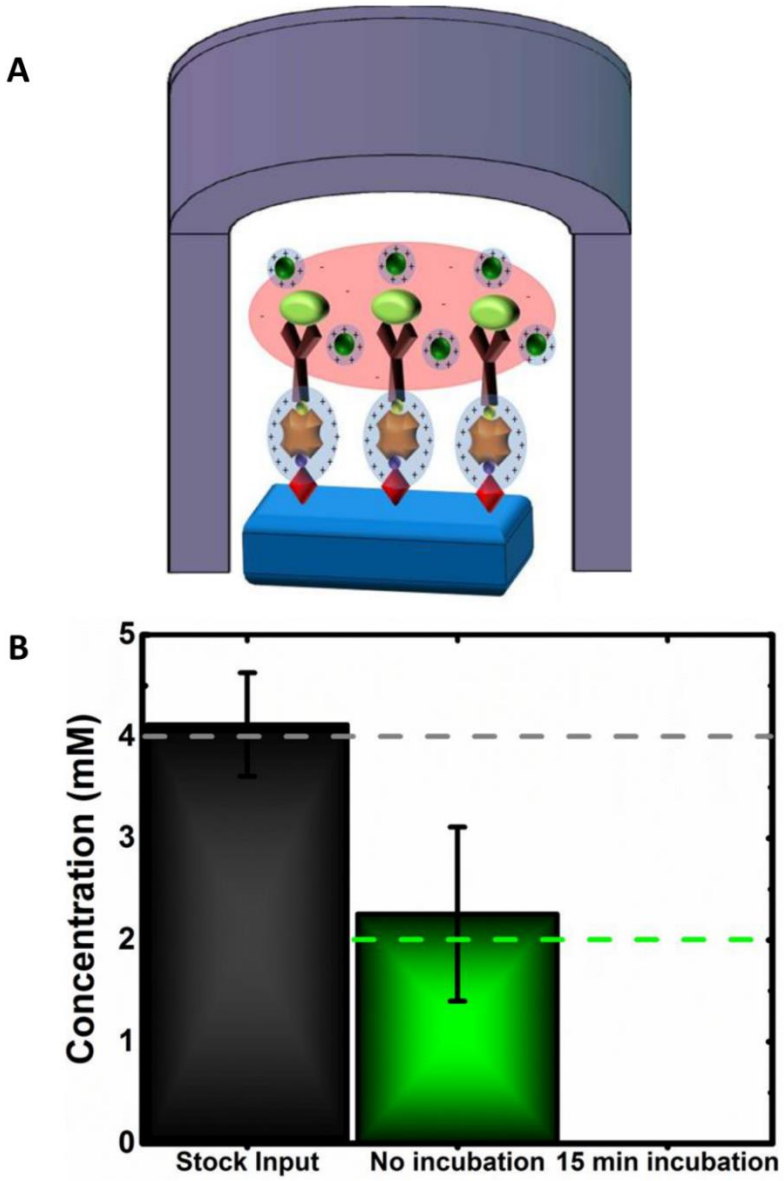

Supplementary Figure 3.2: Schematic of osmolaric effects in spiral and biotin Loss into PDMS. Schematic of spiral channel (A) shows charge around streptavidin (in blue) due to its isoelectric point, which pulls down charged ions (in red) towards the streptavidin, which surrounds the cells in a locally high osmolaric environment. The PLL cations (in green) serve to mitigate this charge and reduce the stress the cells experience. The purple PDMS encases the entire SATCR surface. However, the PDMS acts like a sponge for biotin, resulting in the complete loss of detectable biotin after 15 min incubation (B).

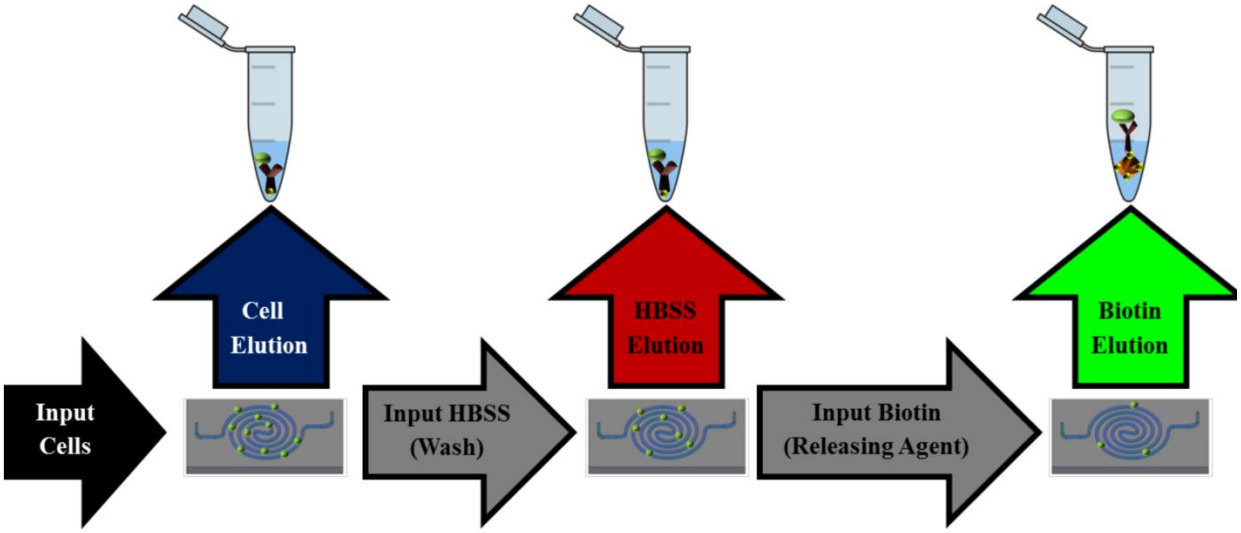

Supplementary Figure 3.3: Schematic for Non-functionalized vs Functionalized Spiral Experiments. Both functionalized and non-functionalized spirals were first exposed to an input cell solution after which the elution was collected via Eppendorf. The spiral was then exposed to an input solution to wash away non-specific adhered cells and collected via Eppendorf. In the non-functionalized spirals, the cells were adherent to the glass bottom of the spiral, while in the functionalized spiral the cells adhered to the SATCR surface. After the HBSS wash, the cells are exposed to a biotin solution for 15 minutes and then collected via Eppendorf.

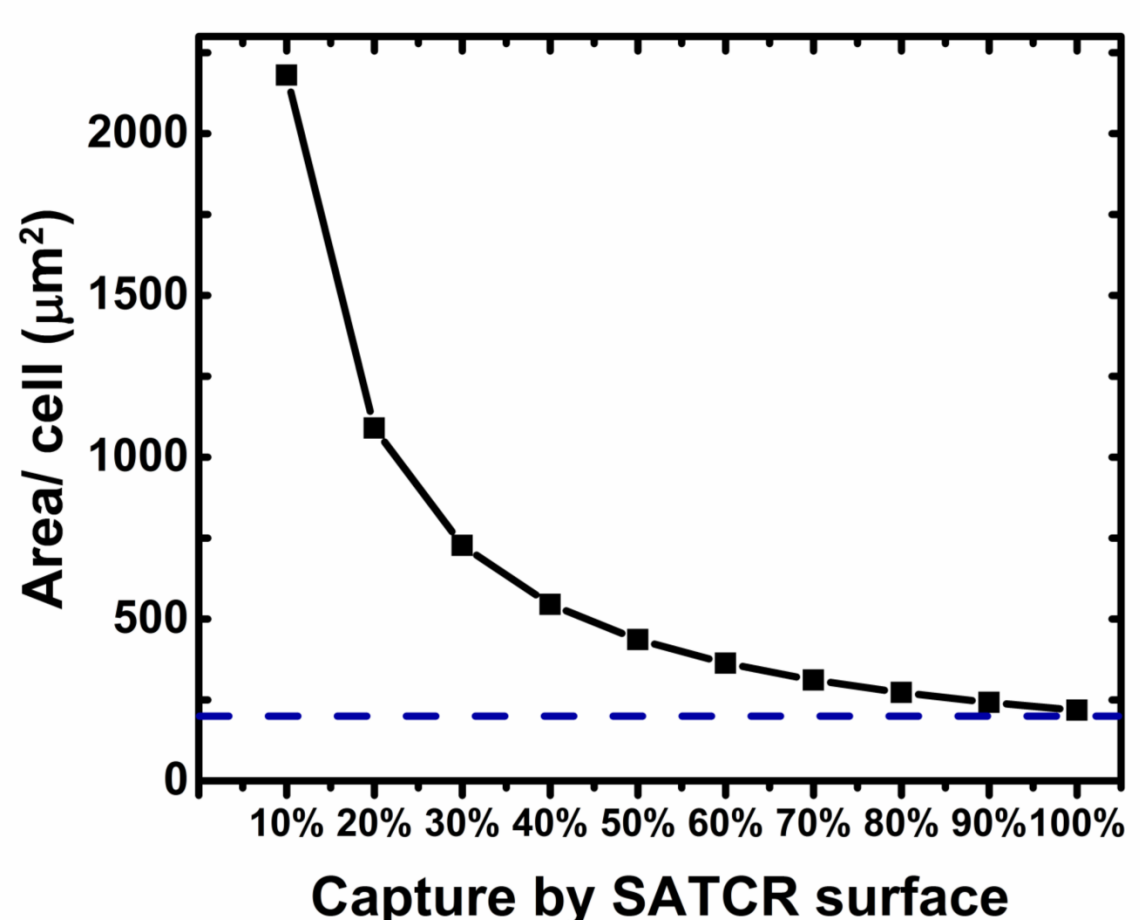

Supplementary Figure 3.4: Crowding Analysis of SATCR surface. Cell crowding was calculated by using size values from Table 1, and using total area of the glass surface to ascertain total area allotted per cell. The blue line represents the total area of the largest cell size used, the MCF7GFP cell line.

CHAPTER 4

RELEASE OPTIMIZATION AND ADAPTION OF THE SATCR SURFACE TO ALTERNATE MODALITIES

4.1 Introduction:

Cancers can be very difficult to treat in large part, due to the fact that therapeutic responsiveness can vary from patient to patient. These variations in responsiveness can be attributed to tumor heterogeneity on several levels, including: cell, gene, and protein. Indeed, we recently showed that tumor xenografts of the same cancer subtype present heterogeneity in morphology and receptor levels---beyond the normal variability observed in clonal cell populations (Princess. I. Imoukhuede & Popel, 2014). Tumor heterogeneity is particularly challenging to anti-angiogenic drug treatment, as tumors are either intrinsically resistant to these drugs (Sharma et al., 2010) or resistance can be acquired during treatment (Bergers & Hanahan, 2008). Such intrinsic and acquired resistances are likely linked to the hallmarks of cancer, including, the overexpression of receptors, second messaging signaling molecules, and other deregulated biomarkers (Hanahan & Weinberg, 2011, 2000). Therefore, developing an understanding of these biomarkers and how they map to intrinsic and acquired anti-angiogenic drug resistance remains a pressing need.

Plasma membrane receptors often serve as biomarkers that correlate with drug efficacy and patient survival (T. T. Batchelor et al., 2007; Papadopoulos, Kinzler, & Vogelstein, 2006; Ziegler, Koch, Krockenberger, & Großhennig, 2012). A well-known biomarker for breast cancer is the plasma membrane receptor: HER2. Companion diagnostics (Diagnostics, Companion,

Devices, & Tools, 2014; FDA, 2014; FDA, AACR, ASC, & Mansfield, 2015) like the SPoT-Light HER2 CISH test and HerceptTest guide safe and effective breast cancer treatment by screening patients to see if their tumor cells carry the HER2 biomarker. HER2-positive patients are then treated with HER2-targeting drugs like Herceptin/trastuzumab, Tykerb/lapatinib, and Perjeta/pertuzumab (Bussolati et al., 2005; Jørgensen, 2013). In addition to examining the presence of biomarkers, knowing their abundance is also important for patient treatment (Weddell & Imoukhuede, 2014; Weickhardt et al., 2015). The emerging approach, quantitative flow (qFlow) cytometry, provides absolute quantification of many plasma membrane receptors on cells (S. Chen et al., 2017, 2015; P.I. Imoukhuede & Popel, 2011; P I Imoukhuede et al., 2013b; Princess. I. Imoukhuede & Popel, 2014; Weddell & Imoukhuede, 2014). Indeed, receptor quantification and computational modeling have enabled accurate prediction of patient response to chemotherapeutics (S. Chen et al., 2017; Weddell & Imoukhuede, 2014), and one such model predicted VEGFR1 as a biomarker of anti-angiogenic drug efficacy (Weddell & Imoukhuede, 2014). Therefore, developing diagnostic tools that enable accurate measurement of plasma membrane receptors, or "biomarker preserving diagnostics" is a necessary step towards precision medicine (Alunni-Fabbroni & Sandri, 2010; S. Chen et al., 2017, 2015).

Towards the goal of biomarker-preserving diagnostics, physiological cell isolation is needed. Current methodologies pose challenges of time-intensiveness or protein disruption (Ansari et al., 2015; De Spiegelaere et al., 2011; Nagrath et al., 2007). We recently applied magnetic beads to isolate endothelial cells from mouse skeletal muscle (Princess I Imoukhuede & Popel, 2012), endothelial cells from ischemic mouse tissue (P I Imoukhuede et al., 2013a), and both endothelial cells and tumor cells from mouse breast cancer xenografts (Princess. I. Imoukhuede & Popel, 2014). We found that magnetic bead isolation of 1-2 cell types could take

upwards of five hours, which limits the clinical translation of these approaches (Nagrath et al., 2007; Naranbhai et al., 2011). Many lab-on-a-chip approaches offer faster cell isolation (Dittrich & Manz, 2006; Nagrath et al., 2007). However, these approaches often involve physical (De Spiegelaere et al., 2011; Nagrath et al., 2007; Privorotskaya et al., 2010; Wynick & Bloom, 1990) or chemical methods (Adams et al., 2008; Shields et al., 2015) of manipulating cells, which may cause irreversible cell damage. In particular, enzymatic degradation (Adams et al., 2008) can degrade plasma membrane proteins, affecting accurately quantifying biomarkers and altering downstream signaling pathways (Alunni-Fabbroni & Sandri, 2010; Blann et al., 2005; De Spiegelaere et al., 2011; Mizuarai et al., 2005; van Beijnum et al., 2008; Wynick & Bloom, 1990). Therefore, there is a need for physiological and rapid cell isolation techniques that reduce non-physiological changes (Alunni-Fabbroni & Sandri, 2010) to protein and genes.

To address that need, we recently developed the Secondary Anchor Targeted Cell Release System (SATCR) (Ansari et al., 2015, 2016) (Ansari et al 2018 in submission) . Briefly, this system isolates cells by harnessing the reversible interaction between streptavidin and desthiobiotin (a modified version of biotin). The captured cells are then released through high-affinity biotin competition. In order to develop the system to release cells from a device efficiently, we integrated the SATCR system into a spiral PDMS design and optimized shape and printing modalities. We also moved beyond the PDMS modality and attempted to adapt the SATCR functionalization to polyvinyl chloride tubing to address fundamental limitations of the PDMS elastomeric system (Toepke & Beebe, 2006).

Here we achieve the second goal of the system: rapid cell isolation via implementation of SATCR onto a spiral microfluidic device and non-glass modalities. We analyze shrink dink

molding versus stereolithography, “3D printing” mold fabrication. We also show future adaptions and optimizations of the SATCR system to freeform PVC tubing in order to address critical problems with the PDMS modality absorbing small molecules such as the releasing agent biotin.

4.2 Materials and Methods:

4.2.1 *Shrinky dink fabrication and curing:* Printing - The shrinky dink plastic (Graphix, Maple Heights, OH) was printed via previously established methods (Grimes et al., 2008). Briefly, a spiral design, composed of two, 4 cm spirals, developed in AutoCAD software (Autodesk, San Rafael, CA) was printed on the shrinking din, plastic using an ink jet printer (2270DW Brother, Bridgewater, NJ). The design was trimmed and carefully cleaned with 100% ethanol and DI water.

Baking - The oven (Thermo Fisher, Waltham, Massachusetts) was preheated to 150° C, and a 12 x 9 x 0.5--inch glass surface was prepared and washed with 100% ethanol and water. Once cleaned, the surface of the glass was fully spray-coated for 2-3 s with a silicone spray (Liquid Wrench, Indian Trail, NC) to reduce irreversible sticking of the plastic to the glass. The shrink dink was introduced to the oven. After 2 min the oven temperature was lowered to 120° C to minimize shrinky dink warping. The design was then placed in the oven with the design face-up. The shrinky design was baked in the oven for 6-7 min, periodically checked to ensure no design folding was occurring. Curved and regular forceps were used to carefully correct the orientation if warping occurred. After 7 min, the glass was removed using heat gloves and cooled for 10 min at room temperature. Once cool, the shrink dink on the glass was baked again for 15 min at 120°

C to verify that the shrink dink is fully set. The shrinky dink was removed and cooled at room temperature for 5 min.

Frying - Canola Oil was heated on an Isotemp hot plate (Fisher Scientific, Waltham, MA) to 160°C. The shrinky dinks were submerged for ~10 seconds when size was stabilized. The fried shrinky dinks were flattened and planarized using 75 x 38 mm glass slides (Corning, Corning, NY), and cooled for 5-10 min. The shrinky dinks washed thoroughly in 100% ethanol and then DI water to remove excess oil.

4.2.2 *Atomic force microscopy measurements:* All AFM measurements were performed in tapping mode on an Asylum Research MFP-3D AFM (Asylum Research, Santa Barbara, CA). The scan rate was 1Hz, and 256 line resolution. The scan size was 30 µm x 30 µm for most images, although a few were 30 µm x 25 µm due to tip destruction and wear. We used Tap300-G silicon tips from Budget Sensors (USA) with force constants of 20 N/m to 75 N/m. The software program Igor was used for data analysis from the raw AFM data.

4.2.3 *Spiral versus straight microchannel comparison:* Functionalized spiral microfluidic molds were suffused with fixed MCF7-GFP cells at 40 µL/min for 30 minutes until 1 mL of cell solution had exited the spiral. The cells had been incubated with HLA-ABC antibody prior to experiment. Cells were washed with a PBS-based solution supplemented with 0.5 mg/mL Poly-L-Lysine. Following this Poly-L-Lysine wash step, cells were released with 4 mM biotin. Cell capture and release was analyzed at distances of 2 cm and 3 cm in the spiral and compared to a functionalized straight microchannel at the same distances via an Olympus IX51 microscope with a 4x UPlanFl objective. Cells were counted via Image J using the ITCN plugin. .

In order to retain physiological time frames, flow rate was increased to 300 µL/min for 1.5 min until 750 µL had exited the spiral for cell diameter and Poly-L-Lysine experiments. Cells eluted from both the spiral and the straight microchannels were collected and cell concentration and diameter were analyzed on a Countess II (ThermoFisher, Waltham, MA).

4.2.4 *Polyvinyl chloride ethylenediamine functionalization:* Polyvinyl chloride (PVC) tubing is cut into 1.5 meter strands and placed inside a 1000 mL beaker with one end attached to a syringe pump held needle filled with 10 mL of 80% ethylenediamine solution in DI water and is emptied into a 2 L Erlenmeyer flask filled with 1 M Sodium Carbonate which is placed in an ice bucket. The 500 mL of DI water is heated and maintained at 80 °C within the 1000 mL beaker with the tubing submerged in the water; PVC is flowed with 10 mL of ethylenediamine solution at 200 mL/min and kept inside the tube for 1 hour to produce primary amine groups on the surface of the tube. This method for PVC functionalization produces hydrochloric acid as a byproduct, thus the PVC tubes will be treated with excess sodium carbonate solution in the Erlenmeyer flask on ice to neutralize the acid. After the ethylenediamine is flowed in, ethanol and DI water are introduced at 200 mL/min in order to remove any lingering ethylenediamine and hydrochloric acid. After the washes, 1.5 mg/mL Desthiobiotin (DSB) and 7.5 mg/mL 1-Ethyl-3-(3-dimethylaminopropyl) carbodiimide (EDC) dissolved in 2-(N-morpholino) ethanesulfonic acid (MES buffer) for 15 min and quenched using 1 µL mercaptoethanol and then applied to the tube are added with 10 µL of dimethyl sulfoxide per mg of DSB. Following overnight incubation at 4° C in a refrigerator, excess DSB is washed with phosphate buffered saline (PBS). 0.4 mg/ml streptavidin in PBS, and stored 18-24 hr at 4 °C in a refrigerator, rinsed with PBS, rewetted, and replaced in the refrigerator until used.

4.2.5 *Polyvinyl chloride MPTMS functionalization:* Polyvinyl chloride (PVC) tubing is cut into 1.5 meter strands connected to a syringe needle with a 5% MPTMS solution in Acetone. The tube is suffused with the solution for 30 minutes, and the waste solution is emptied into a 2 L Erlenmeyer flask filled with 1 M Sodium Carbonate in an ice bath. This method for PVC functionalization produces hydrochloric acid as a byproduct, thus the PVC tubes will be treated with excess sodium carbonate solution in the Erlenmeyer flask on ice to neutralize the acid. After the MPTMS is flowed in, the tube is rinsed with ethanol in order to remove any lingering excess MTPMS and hydrochloric acid. The tubing is then placed in a 50 mL conical and submerged in a 3.76 mM APTES solution for 18 hours on an end over end mixer. After the incubation the tube is rinsed in ethanol and then of the washes 1.5 mg/mL Desthiobiotin (DSB) and 7.5 mg/mL 1-Ethyl-3-(3-dimethylaminopropyl) carbodiimide (EDC) dissolved in 2-(N-morpholino) ethanesulfonic acid (MES buffer) for 15 min and quenched using 1 µL mercaptoethanol and then applied to the tube are added with 10 µL of dimethyl sulfoxide per mg of DSB. Following overnight incubation at 4° C in a refrigerator, excess DSB is washed with phosphate buffered saline (PBS). 0.4 mg/ml streptavidin in PBS, and stored 18-24 hr at 4 °C in a refrigerator, rinsed with PBS, rewetted, and replaced in the refrigerator until used.

4.2.6 *Functionalized polyvinyl chloride comparison experiment:* Both functionalized (ethylenediamine and MPTMS) and unfunctionalized PVC tubing is cut into lengths of 220 mm to match the length of the PDMS spiral. Fixed HUVECGFP cells are incubated with hCD31 for 35 minutes and then DAPI for 10 minutes. Tubing is then rinsed prior to experiment with PBS to remove any remaining excess functionalization reagents, and then cells are run through the tubing either in a straight or spiral configuration. A non-specific wash is applied to the cells, and then the cells are fluorescently imaged for both GFP and DAPI stains. Release of the cells is

done through the introduction of 4 mM biotin. Tubings are again fluorescently imaged for GFP and DAPI stains. Once all pieces of PVC tubing have been imaged, a functionalized PDMS spiral and PDMS straight tube are used as controls to quantify capture and release efficiency in comparison to our existing technology.

4.3 Results:

4.3.1 Stereo Lithography provides more uniform channel fabrication than shrinky dinks:

Towards the goal of optimizing the spiral microfluidic fabrication, we compared the uniformity across three fabrication methods: (1) "baking" shrinky dinks (2) "frying" shrinky dinks, and (3) "3D-printing" (stereolithography). Firstly, surface uniformity of the molds was tested by imaging the shrink dink mold surface with atomic force microscopy (AFM). The baked shrinky dinks were more uniform than the fried shrinky dinks with a 2.6 fold smaller standard deviation in height across the surface (Fig. 4.1). Despite this, the shrinking percentage among them was inconsistent, varying between 39%-42% of original size as compared to literature values ranging from 50%(C.-S. Chen et al., 2008) to 60% (D. Nguyen, McLane, Lew, Pegan, & Khine, 2011). This variability did not allow for reproducible molds. The baked shrink dinks took considerably longer to cure, about 12 min versus ~6 s curation of the fried shrinky dinks had the advantage of rapid curation (6 s), and fried shrinky dinks had a maximal standard deviation of 237 nm (Fig. 4.2). They also suffered from the pervasive issue of excess oil, resisting 70% ethanol, 100% ethanol, and soap and deionized water washes. It was determined that the oil would consequently contaminate all PDMS casts, rendering them unusable.

The 3D Stereo Lithographic Apparatus yielded the most consistent molds. AFM quantification of the surface found a range-range 15 nm standard deviation, a value almost 16

times smaller than the largest standard deviation of the fried shrinky dinks (Fig. 4.3). The Stereo Lithographic Apparatus mold was also relatively easy to alter and inexpensive to produce, costing only a few dollars per set of identical molds. We utilized this modality as the basis for our spiral capture device.

4.3.2 Functionalized PVC shows successful capture and release of cells from solution: We imaged HUVECGFP cells within the MPTMS functionalized PVC tubing and were able to verify preliminary cell capture (Fig. 4.5G) as well as release (Fig. 4.5H), however, this release percentage is much lower than the glass and PDMS based SATCR system with a release percentage of 13%. As a preliminary adaption of the SATCR modality to a completely different polymer modality, this was a successful test, but there remain large optimizations in order to make this a viable alternate to the glass and PDMS microfluidics. Future experiments would allow for the optimizations necessary in functionalization, flow rate, and reagent concentrations that may allow for greater capture and release percentages.

4.4 Discussion:

4.4.1 *Polystyrene Thermoplastics (Shrinky Dinks): Fast, but how reliable?*: In order to develop the masters for our spiral microfluidic device, our lab investigated low cost design modalities to find the ideal fabrication technique. Shrinky dinks offer rapid prototyping, ease, and low cost and have been used to create low-cost microfluidic channels and molds for PDMS devices (Grimes et al., 2008), including: micro lenses (Dyer et al., 2011), electrodes (Pegan, Ho, Bachman, & Khine, 2013), as well as microfluidics (C.-S. Chen et al., 2008; Grimes et al., 2008; D. Nguyen et al., 2011; Pegan et al., 2013). Previous literature have also described methodologies for curation of the shrinky dinks that involves “baking” the thermoplastics inside a preheated lab oven

(Grimes et al., 2008), which takes several minutes. We also developed a new methodology for curation of the thermoplastic-the immersion of the thermoplastic into an oil bath for rapid curation. The time scale for the "frying" of the thermoplastic is on the scale of several seconds. The oil bath, although much more rapid, results in an oily residue that is not easily removed from the master, and the mold itself is non-planar unless cooled between two glass panes. For those interested in applying a frying methodology, we would recommend additional exploration into solvents that more effectively remove the non-polar oil from the plastic. We sequentially used ethanol, detergent, and deionized water to "wash" the plastic; however, additional options could include: (i) Acetone (due to its carbonyl group) is a more effective solvent than ethanol, as it is a less polar a molecule and thus can dissolve non-polar contaminants much more effectively. However this risks dissolving the non-polar polystyrene (Fox & Flory, 1950) plastic shrinky dinks as well. (ii)Hexane (Ferreira-Dias, Valente, & Abreu, 2003; Haijie et al., 2016), another non-polar solvent, which has been used to dissolve coffee oils from filters and plastics as it is specific in what contaminants (oils) it can remove, but which is 4-12 times less efficient at removing oils than ethanol (Ferreira-Dias et al., 2003). (iii) Commercial oil removal and lubrication products such as WD 40 can displace both oil residue and water, replacing it with another type of lubricating oil; however, the lubricating oil contaminant may limit the downstream biological applications, as it may result in cell death, non-physiological signaling, and potential dissolution of the lipid bilayer.

Despite these shrink dink advantages, we observed only ~40% shrinkage with either the baked or fried approach, while others report variations in shrinking from 50 (C.-S. Chen et al., 2008)- 60% (D. Nguyen et al., 2011). In addition to lower shrinking, we observed significant variations in mold surface with baking or frying. These variations would lead to inconsistent

devices, while possibly altering flow profile and wall shear stress(Vukasinovic, Cullen, LaPlaca, & Glezer, 2009). Indeed, reproducible microfluidic devices are an important need. Glezer et al stated this well, describing how consistent devices enabled the generation 'high fidelity [data into] *in vivo* function' in their work (Vukasinovic et al., 2009). It is also becoming critical workflow parameter when developing microfluidic devices (Cooksey, Elliott, & Plant, 2011; Mueller et al., 2000; Strehle et al., 2007; Valencia, Farokhzad, Karnik, & Langer, 2012; Lei Wu, Wang, Zong, & Cui, 2014). Thus reproducibility is paramount to the development of physiological and consistent modalities for our microfluidic device, and the lack of consistency we found in the shrink dinks prevented their use as the master mold for our device.

4.4.2 3D Printing, "Additive Manufacturing is Advantageous": To overcome the challenge in shrink dink variability, we use 3D printing, which is also described as "additive manufacturing(Au, Lee, & Folch, 2014)." Many researchers have discussed the advantages of 3D printing for microfluidics (Adamski, Kubicki, & Walczak, 2016; Anciaux, Geiger, & Bowser, 2016; J. M. Lee, Zhang, & Yeong, 2016; Macdonald et al., 2016; Raman et al., 2016; Yi-Qiang, Mei, & ZHANG, 2016), chief among these advantages is the precise modeling of the master in AutoCAD before printing (Au et al., 2014; Waheed et al., 2016).The speed and low cost of 3D printing holds the added advantage of "on the fly" changes to the mold. This allowed us to create several molds in parallel (Au, Bhattacharjee, Horowitz, Chang, & Folch, 2015). Additionally, 3D printed masters are extremely reproducible. Indeed, the 3D printed mold had a much more consistent surface, resulting in ~16 times lower variation in surface height compared to the best Shrinky Dink.

*4.4.*3 *Resin Biocompatibility is crucial for physiological application :* There are limitations to 3D printing: resin biocompatibility may pose a challenge to translation for biomedical applications (Au et al., 2014; Waheed et al., 2016). Un-polymerized resin can leach out of the mold, which may affect the cells in the microfluidic devices (Macdonald et al., 2016). Currently, our device does not pose biocompatibility issues; since we use PDMS and glass, only the negative master mold used a Proteogen 18420 resin. However, biocompatibility should be considered for point of care translation, which may involve a 3D printed device. Indeed, resins, such as Fototec 7150, Fullcare 720, ABSplus-p430, and PEG-da are known to have varying degrees of biocompatibility. Fototec 7150 biocompatibility was measured by checking for zebrafish embryonic toxicity in the presence of 15 mm x 1 mm disks of the Fototec resin after an ethanol wash. Embryo viability was observed to be ~ 90% and no teratogenic effects were observed (Fraysse, Mons, & Garric, 2006; Lammer, Carr, et al., 2009; Lammer, Kamp, et al., 2009; Macdonald et al., 2016). The biocompatibility of Fullcure 720 was observed by examining live vs. dead staining of C2C12 myocytes. Cells incubated on UV sterilized Fullcure resin disks of 400 mm^2 x 2 mm, resulted in ~80% C2C12 myocytes viability. The 20% cell death was attributed to potential leaching of free radicals from the 3D printed pieces after being photo-polymerized(J. M. Lee et al., 2016). Additional biocompatible resins include UV or ethanol sterilized ABSplus-p430 and PEG-da, which result in ~95% viability of C2C12 myocytes on the 400 mm^2 x 2 mm ABSplus-p430 disks (J. M. Lee et al., 2016) and ~90% viability of NIH/3T3 fibroblasts, C166 Endothelial cells, C2C12 myocytes, and D1 bone marrow stromal cells embedded within a 740 um x 530 um and 360 um thick hydrogel block of 3400 g/mol PEG-da, via both the (3-(4,5-dimethylthiazol-2-yl)-5-(3-carboxymethoxyphenyl)-2-(4-sulfophenyl)-2H-tetrazolium) (MTS) colorimetric assay and chick chorioallantoic membrane assay (Raman et al.,

2016). Our spiral master is 3D printed with the Protogen 18420, which has cleared ISO 10993 biocompatibility testing. Thus, Protogen 18420 may be a good resin for non-PDMS device development.

4.4.4 High Resolution 3D printing can be used to print devices on and below the cellular scale: Another consideration in using 3D printing is fabrication resolution. In 3D printing, the resolution is a function of two primary factors: the beam width (Abbe's diffraction limit) and the material properties, the latter of which is the primary limitation. Some resins such as hydrogels exhibit a large amount of swelling, further limiting their ability to resolve sub-micron fabrications. Additionally, impurities in the resin can scatter and reduce resolution further. The Viper SI Stereolithographic Apparatus that we used in our studies has a vertical resolution of 2.5 μm and a beam width of 250 μm, and depending on the resin this may limit channel width to around 0.5 - 1 mm (J. M. Lee et al., 2016; Zhu, Macdonald, Skommer, & Wlodkowic, 2015). New research into high-resolution printing suggests that resolution limits may go down to less than 5 μm (Raman et al., 2016), and the field may even attain submicron resolution. Some novel approaches include optimizing the beam with the use of two-photon laser-based stereolithography (Raman & Bashir, 2015). New research at the materials-beam interface uses demagnification lenses to focus projected light and reduce the beam width, by creating grayscale digital masks- allowing single exposure design (Raman et al., 2016). Using this approach, Raman et al encapsulated 7.5×10^6 cells into a hydrogel resin, and were able to resolve features below 10 μm (Raman et al., 2016). Continued work in this area may enable direct micro-fluidic or nano-fluidic device manufacturing via stereolithography (Au, Huynh, Horowitz, & Folch, 2016).

4.4.5 Weaknesses of PDMS require inventive solutions to point of care design: PDMS has been used extensively as a prototyping material for microfluidics for several years. However, researchers have found that small molecules are absorbed into the elastomeric matrix (Toepke & Beebe, 2006). Our lab has shown data where biotin was undetectable in eluents that were measured form the output of a PDMS spiral. These solutions were initially at the saturation concentration of biotin, so their complete depletion is worrying as the amount of loss is staggering. If the cells release biomarkers or chemical signals within the PDMS device, these signals and markers would be lost inside the PDMS matrix and would not be able to be quantified reliably, unless we only quantified cell surface receptors or internalized biomarkers. In order to mitigate this problem, our lab has attempted to functionalize polymer tubing which would be less permissive to small molecules as they are not elastomeric matrices, as well as being well established in the field as microfluidic modalities. In order to decide which material to begin functionalizing, we made a comparison of existing polymers that are commonly used in microfluidics (Tsao, 2016; Tsao & DeVoe, 2009), and compared them to find the optimal system for our capture surface (Table 2). Through functionalizing these flexible PVC tubing, we can manually customize the overall device to any shape, which allows another degree of freedom for microfluidic design. Thus, this functionalization can be done without the need of any expensive devices or machines and can be done at any labs. This is critical for the design and maintenance of a point of care design- inability to afford or create the necessary device would mean lower implementation of our cell isolation modality and ultimately our methodology for cell isolation.

4.4.6 PVC opacity shows new challenges in fluorescence imaging: PVC has been previously functionalized in existing literature (Balakrishnan et al., 2005; Stachelek et al., 2011)in order to allow it to more physiologically interface with cellular. Our research into functionalizing PVC

tubing has used two different types of mechanisms (Fig. 4.4A & B) in order append the necessary amines for our previously established functionalization protocols(Ansari et al., 2015, 2016). Through functionalization with ethylenediamine and MPTMS, we were able to couple the SATCR functionalized surface onto the PVC tubing (Fig. 4.4C & D). Upon further inspection of the functionalized tubing (Fig. 4.7) we observed a color change in the tubing from the optically clear unfunctionalized PVC Tubing (Fig. 4.5 A & D) to the ethylenediamine functionalized PVC tubing (Fig. 4.5 C & F). This color change was similarly present in the MPTMS functionalized tubing (Fig. 4.4D & 4.5B& E), but not to the same degree as the ethylenediamine functionalized tubing, which possessed a visible white ring within the tubing (Fig. 4.5C). This layer of opaque PVC prevented imaging of cells within the ethylenediamine functionalized tubing, however, the cells could be imaged when captured (Fig. 4.5G.) and released (Fig. 4.5H) from the MPTMS functionalized tubing.

4.5 Future Applications and Directions for the SATCR System:

The SATCR system allows for the selective and receptor preserving capture and release of cells of interest from single or multi-cell samples. As the technology isolates cells based on targeted antibodies, this system can be customized to target any cell of interest as long as an appropriate antibody tag has been selected. We have also shown that this technology can be adapted into microfluidic devices consisting of glass and PDMS, as well as polymer tubing consisting of polyvinyl chloride. This is due to the fact that the chemistry that is used to append the amine groups on the glass and PDMS surfaces (Ansari et al., 2015, 2016) (Fig. 4.6A) can be reduced down to a more simplistic (4.6B) in which the R represents any chemical that is able to expose an amine group to be further reacted with our SATCR chemistry. In this sense, as long as the material allows for chemical addition of that amine group, theoretically it could be integrated

with the capture surface. These translations allow for the SATCR surface to be implemented regardless of substrate, further increasing the customizability and flexibility of the SATCR capture modality.

In addition to the adaption of the surface to other substrates, there are a series of adaptions that could be done to further optimize it and other systems. One such optimization could be the adaption of the capture surface to using a neutravidin surface rather than a streptavidin one (Fig. 4.7). As previously discussed, streptavidin has an isoelectric point of 5, which results in a charge density around it at physiological pH. In order to mitigate this charge, substitution of the streptavidin with the neutral isoelectric point neutravidin would remedy that charge potential. Another such evolution of the system would involve the replacement of the biotinylated antibodies which allow for targeted capture of the cells of interest. If the system was to adopt aptamers, specifically folded sequences of nucleic acids which can mimic the precise folding of other proteins (Bunka & Stockley, 2006; Gotrik et al., 2016), then capture selectivity would go up to match the higher resolution of the aptamers in comparison to the antibody system. In addition, both thermo-stability and reproducibility of the antibody are fundamental limitations of the antibody system, which the aptamer modality does not have to deal with, as they can be shared via nucleic acid sequence rather than clone number (Gotrik et al., 2016). We also show preliminary data on using 6x larger volumes of biotin to increase residence time results in recapitulation of release percentages that we have previously established for the SATCR system (Supplementary Fig. 4.1). Another integratable optimization is the addition of a thermal gradient in order to move particles from the solution to the wall or from the walls to the center of the solution using thermophoresis. As particles tend to move towards the colder region, the thermal gradient can be tuned to send biotin in the solution to the wall, or to use

thermophoretic force to help biotin pull cells from the capture surface. We show preliminary data that using a 4° C PDMS microfluidic chip with the 40° C solution had a larger release of nearly 60% which recapitulates previous release percentages reported by the SATCR system (Supplementary Fig. 4.2). This implies that the movement of biotin from the warm fluid to the colder capture surface results in more cells being released from the surface through thermophoretic force.

Lastly, this technology to capture and physiologically release cells could even be appended to existing technologies to provide another level of innovation to them. One such technology could be something similar to whole cell ELISA, in which the existing system of primary and secondary antibody could be appended to the top of the existing SATCR system. In this way, once the ELISA is completed, the cells could be released from the capture surface through the introduction of excess biotin. This recollection would allow researchers to recollect the cells that they had already analyzed and do any number of downstream analyses or culturing for further experimentation.

4.6 Conclusions*:*

We have shown implementation of the SATCR capture surface from a static glass well plate into a more dynamic microfluidic modality. We have also shown optimizations in different conditions to improve and retain the physiological expression and environment of the cells. Lastly, we have created a methodology for adoption of the SATCR capture surface on modalities beyond glass and PDMS, opening the doors to functionalizing numerous polymers and non-standard materials, requiring only the functionalization of an amine group on the surface prior to the SATCR functionalization. However, despite all of these innovations and implementations,

there still remains a great deal of optimizations and adaptions that can be done to the SATCR capture surface. These improvements and optimizations would better allow this technology to transition closer to a diagnostic tool enabling downstream analyses for personalized medicine. Furthermore, this technology can be appended to extant diagnostic tools, providing greater flexibility and dimensionality to the data gleaned from these tools by allowing recollection of sample after other analyses. It is our hope that this technology can be used in this way to build the basis for more effective biomarker screening for more personalized medicine.

4.7 Figures and Tables:

TABLE 4.1 COMPARISON OF SPIRAL MOLD MODALITIES

Mold Curing Process		Curing Time	Surface Uniformity (Height Min-Max Range)	Other Concerns
Shrinky Dink	Fried	6 seconds	1.3 μm	Oil residue
	Baked	12 minutes	200 nm	inconsistent
Stereo Lithographic Apparatus		60 minutes	60 nm	N/A

TABLE 4.2 COMPARISON OF NON-GLASS POLYMER MODALITIES

	Polydimethyl siloxane (PDMS)	**Polycarbonate (PC)**	**Poly (Methyl Methacrylate) (PMMA)**	**Polystyrene (PS)**	**Polyvinyl chloride (PVC)**
Mechanics of System	Elastomer	Rigid	Rigid	Rigid	Rigid
Thermal (Tg)	80 °C	140-150 °C	100-125 °C	90-100 °C	80 °C
Solvent Resistance	Poor	Poor	Good	Poor	Good
Acid/Base Resistance	Poor	Good	Good	Good	Good
Overhead Cost	Oxygen Plasma Treatment and Casting $400-10,000	Thermal Bonding $10,000-30,000	Laser Machining $15,000-40,000	Hot Embossing/ Injection Molding $20,000-40,000	Hot embossing $200-20,000

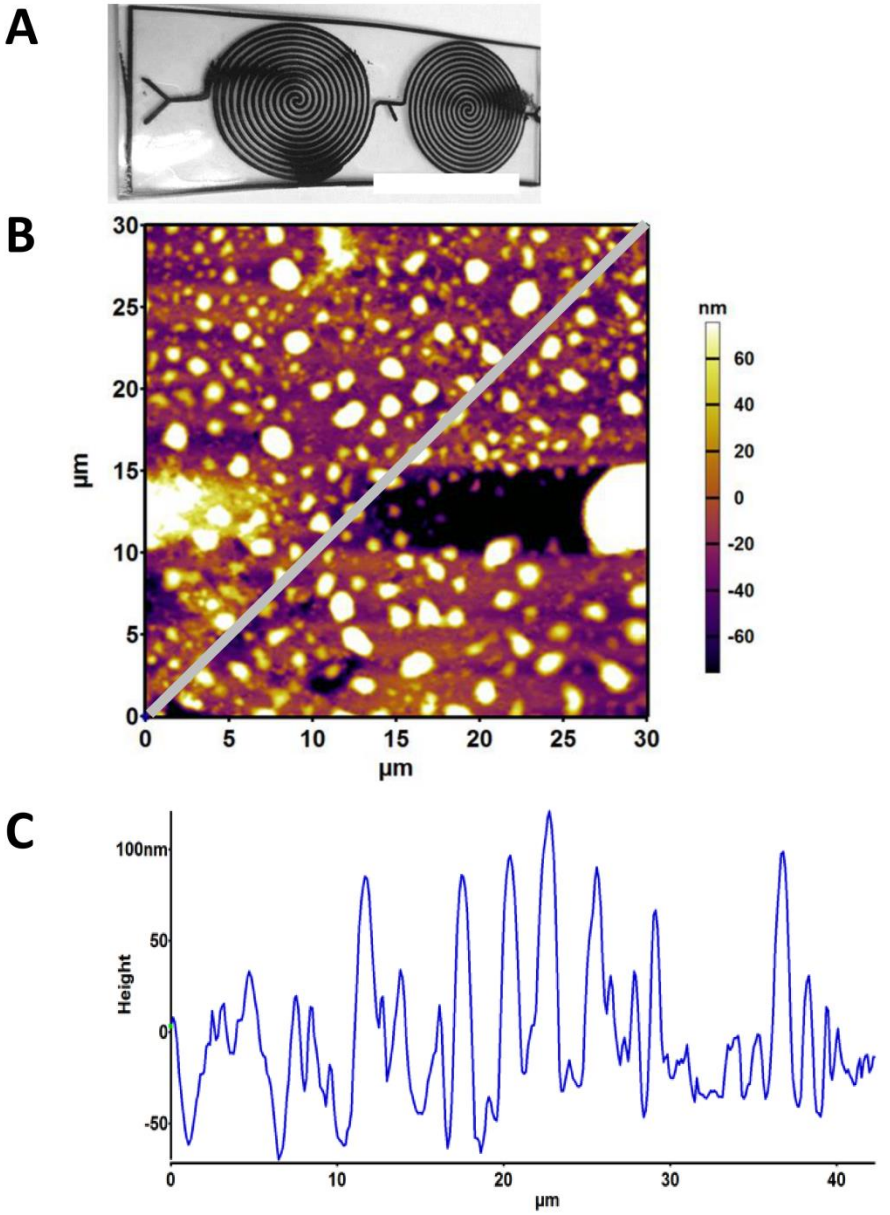

Figure 4.1: Baked Shrinky Dink Curing shows large variations across surface. (A) Visualization of the resulting shrink dink mold following baking at 120 °C. (B) Atomic force microscopy shows height variations of up to 160 nm. (C) Height variability across the grey line in (B) is shown. Scale bar in (A) is 20 mm.

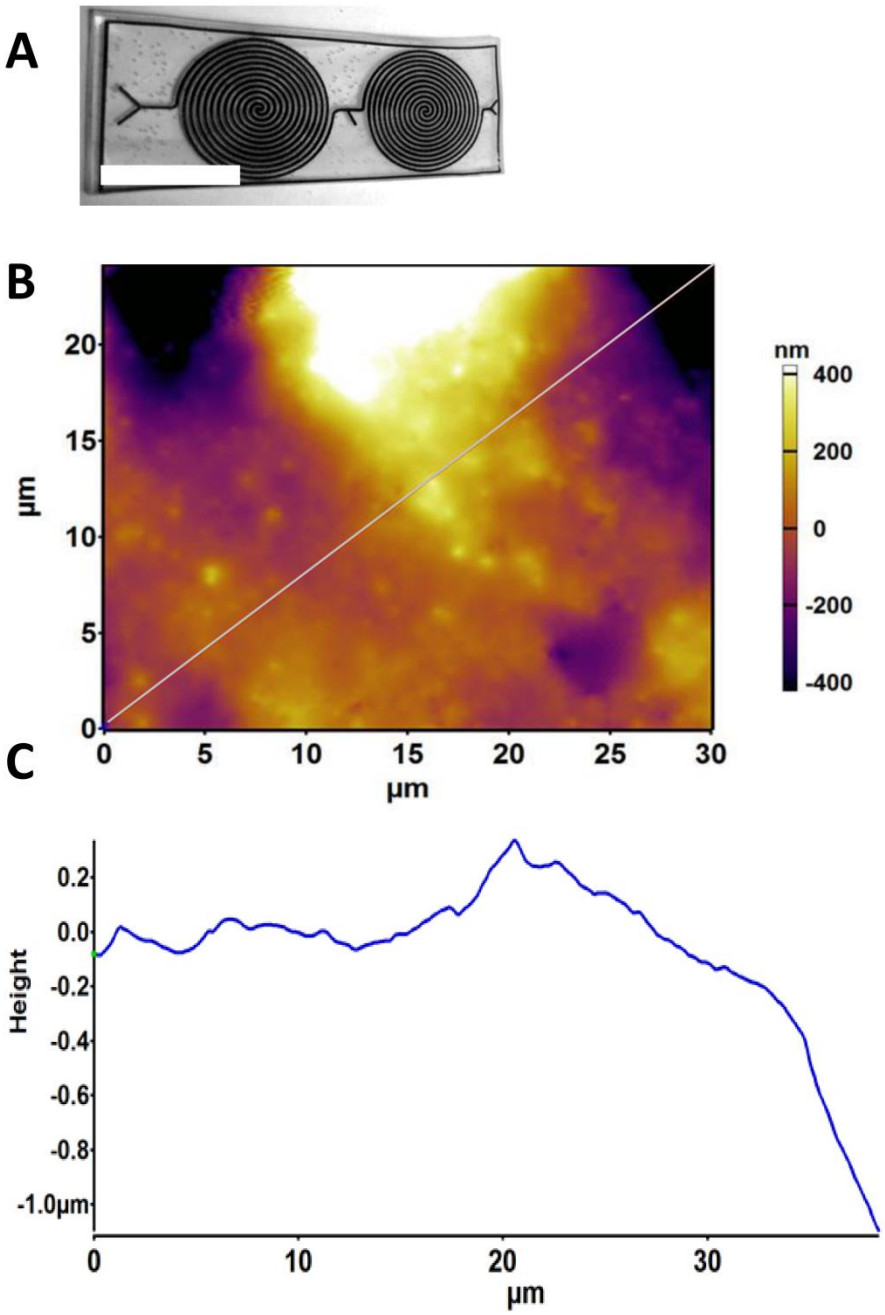

Figure 4.2: Frying Shrinky Dink Curing shows near micron level variations in height. (A) Visualization of the resulting shrink dink mold following frying at 160 °C. (B) Atomic force microscopy shows height variations of up to 800 nm. (C) Height variability across the grey line in (B) is shown. Scale bar in (A) is 20 mm.

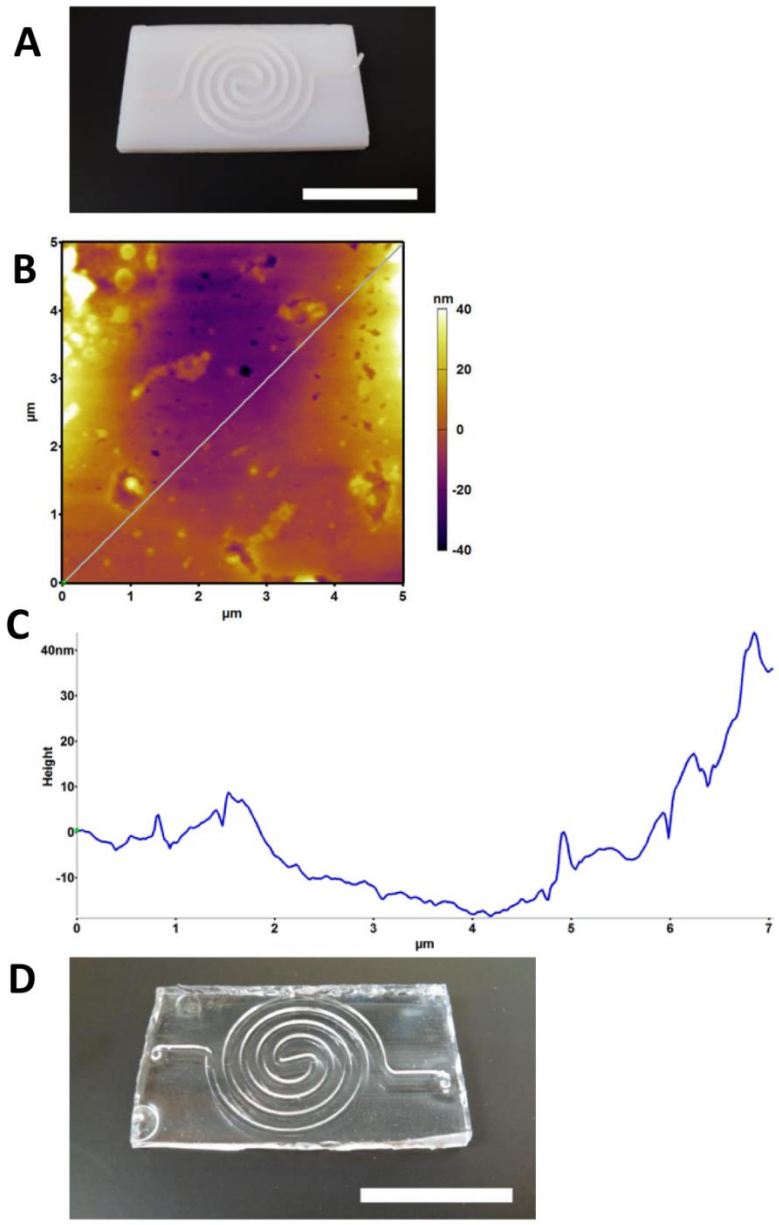

Figure 4.3: 3D Stereolithographic Mold shows much more consistent and reproducible molding. . (A) Molds are created using AutoCAD 2015 and printed on a stereo lithographic apparatus. (B) Atomic force microscopy shows height variations of up to 80 nm. C) Height variability across the grey line in (B) is shown. (D) The molds are then immersed in PDMS such that the pillars are left exposed above the PDMS level. Scale bars in (A) and (D) are 20 mm.

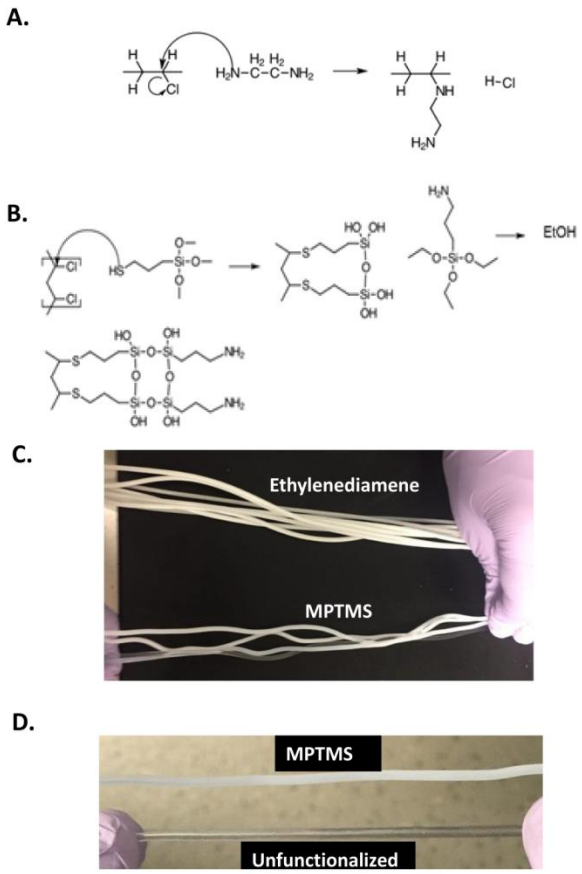

Figure 4.4: Functionalization Mechanism of Poly-Vinyl Chloride (PVC). Functional amine groups are added to PVC tubing using Ethylenediamine (A) or (3-Mercaptopropyl) trimethoxysilane (MPTMS) and (3-Aminopropyl) triethoxysilane (APTES) (B). Once amine groups have been added to PVC tubing, existing protocols can be used to functionalize the tubing with the Secondary Anchor Targeted Cell Release (SATCR) system. Figure 2: Opacity comparison of functionalization schema of PVC tubing. Functionalization of PVC via ethylenediamine (ED) functionalization protocol at 80°C and functionalization via MPTMS and APTES treatment both results in tube discoloration and increases in opacity (A). PVC treated with ED results in greater homogeny and higher degree of opacity (B). MPTMS still has a large degree of discoloration compared to a non-functionalized PVC control (C), showing that the discoloration is most likely due to a chemical change in the PVC itself.

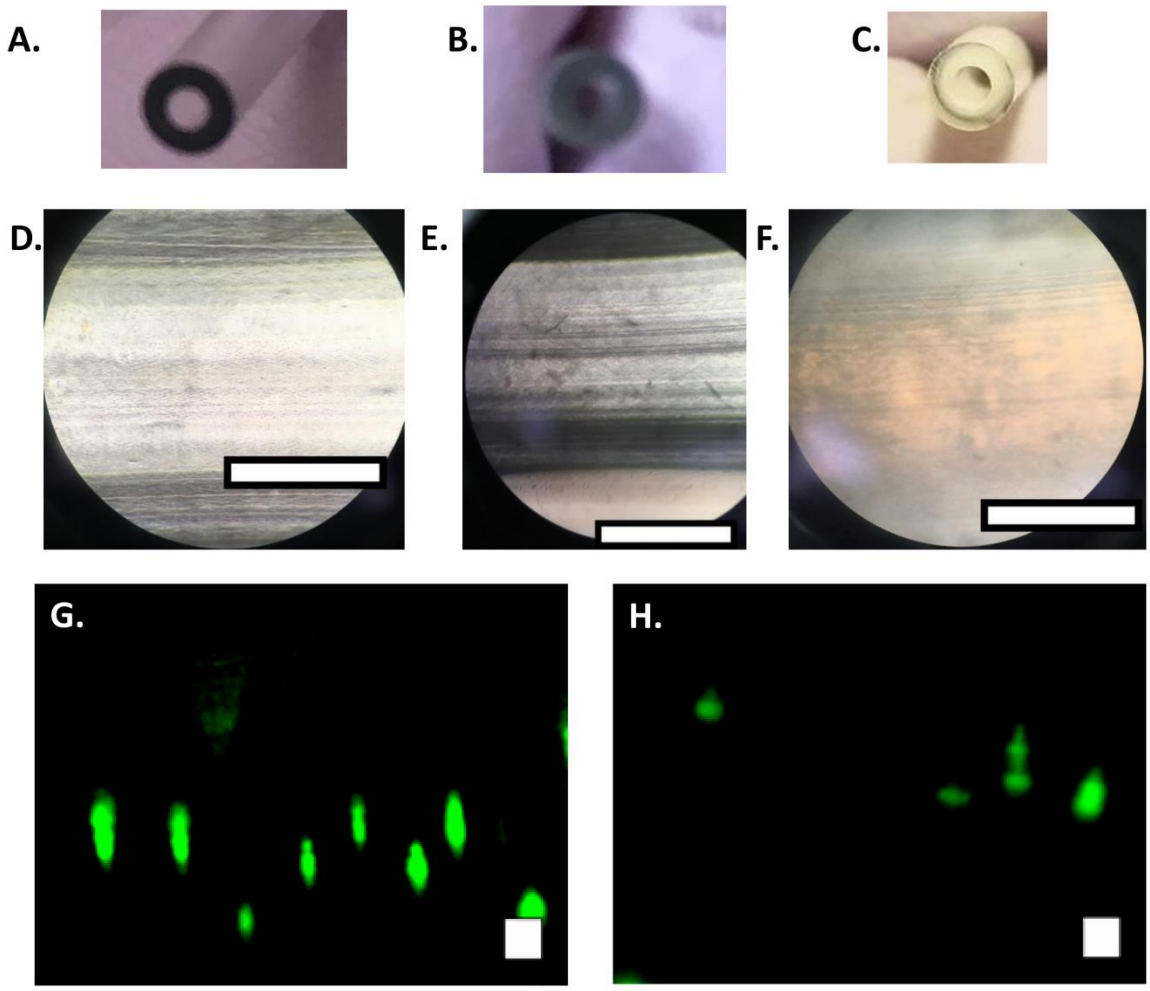

Figure 4.5: Imaging Comparison through both unfunctionalized and functionalized PVC tubing. Unfunctionalized PVC (A.) and MPTMS functionalized tubing (B.) both show slight attenuation of light throughout tubing (D. & E.), while ethylenediamine functionalized tubing (C.) shows white inner ring which creates a more opaque layering, severely limiting imaging of tubing (F.) Scale bars are 1 mm. Imaging of HUVECGFP cells within the (3-Mercaptopropyl) trimethoxysilane (MPTMS) and (3-Aminopropyl)triethoxysilane (APTES) functionalized Poly-Vinyl Chloride (PVC) tubing shows that HUVECGFP cells are pulled down via biotinylated antibodies and are pulled to MPTMS functionalized PVC tubing (G) and then released through the addition of 4 mM biotin solution (H). Scale bars are 100 μm.

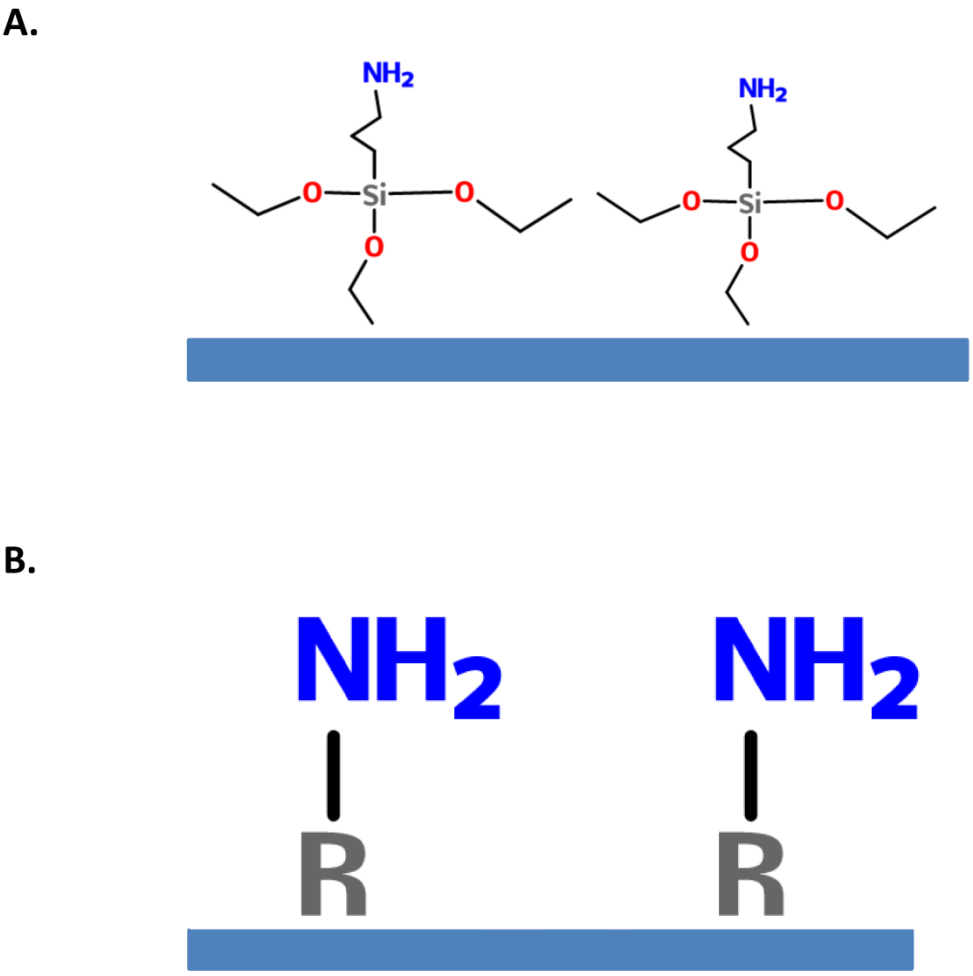

Figure 4.6: Simplified Schematic of Amine Functionalization of Substrates. Glass and PDMS surfaces are functionalized through the aminosilane (3-Aminopropyl) triethoxysilane (APTES) which self-assemble to the surface (A.). This chemistry can be generalized independent of substrate by substituting a generic R group to the amine (B.). Thus, any material that is functionaliz-able such that it can display amine groups is a possible substrate to be integrated with the SATCR surface. The R group, then, will be whatever chemical that can react with the substrate in order to expose the amine needed.

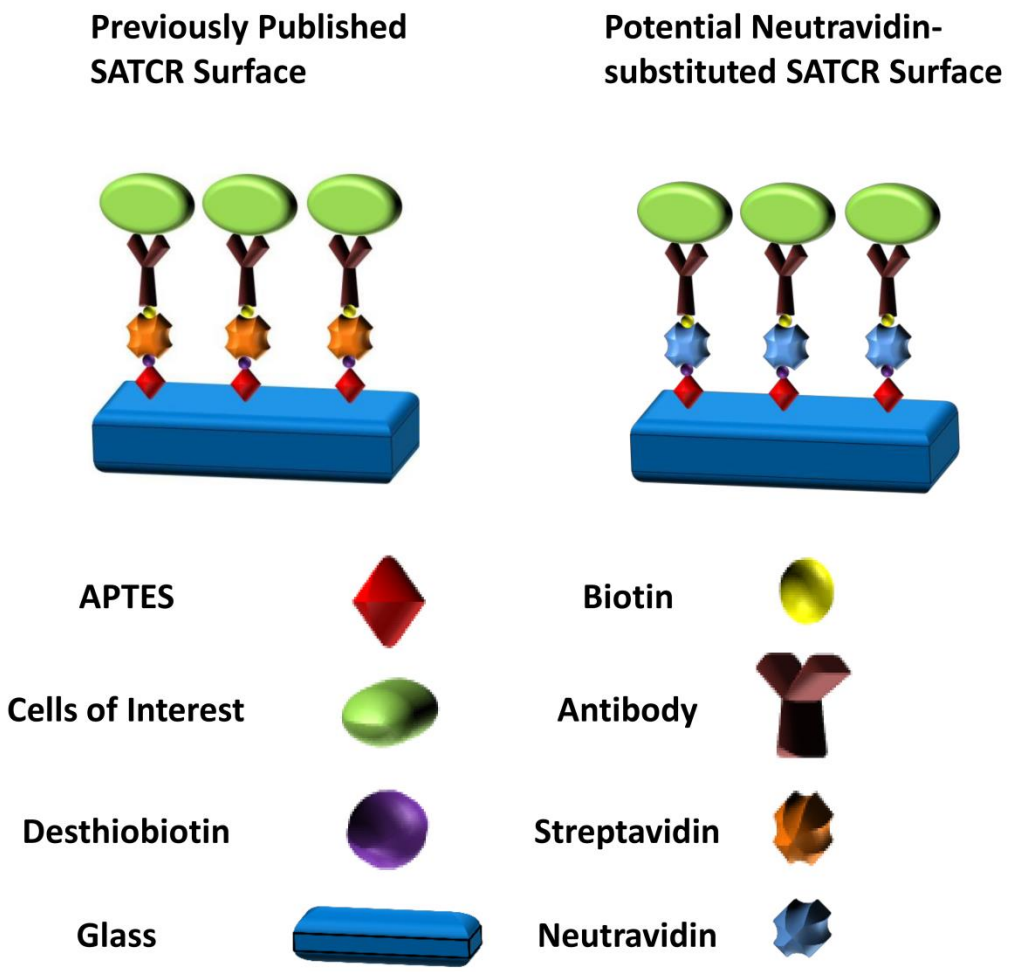

Figure 4.7: Neutravidin Integration within SATCR surface. The replacement of the streptavidin in the SATCR surface with neutravidin would be very easily implemented. As neutravidin has an isoelectric point of 7, it would be more conducive to cell based experiments that would be done with physiological environments.

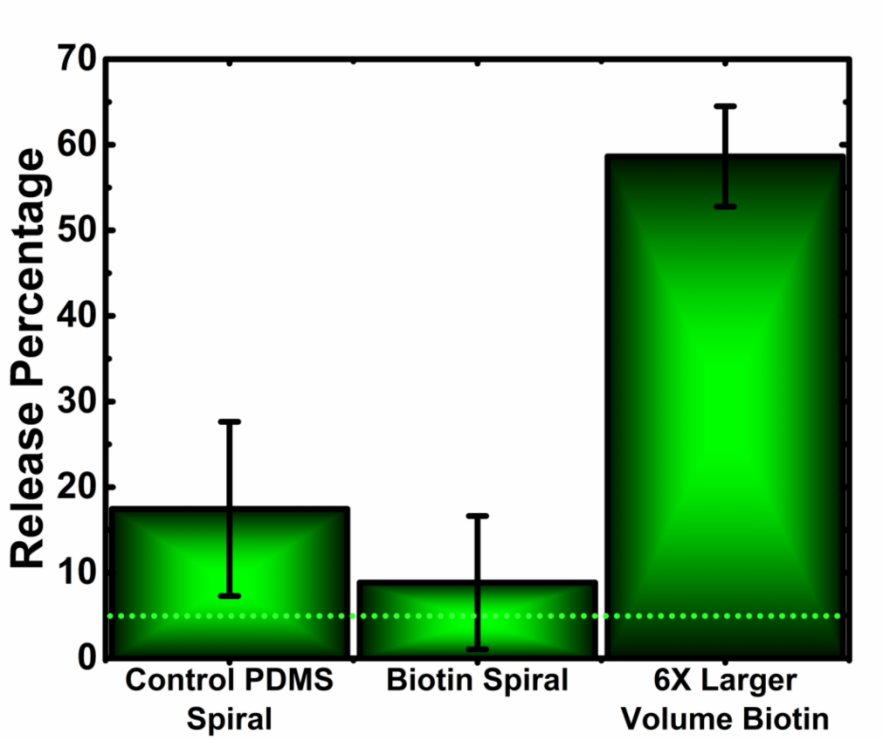

Supplementary Figure 4.1: Increased residence time preliminary experiment shows restoration of previously established release percentages. Release percentages compared across SATCR functionalized PDMS and glass microfluidic devices, PDMS and glass microfluidic devices with biotin crosslinked within the PDMS, and spirals with a 6x longer biotin wash to increase residence time of the biotin inside the spiral. The green dotted line corresponds with a consolidated average for previous release experiments using the same cells. The biotin spiral shows lower release percentage than both other spirals, which could be due to the leeching of uncrosslinked biotin into the SATCR release system prior to capture of the cells. This leeching would result in reduction of available capturing streptavidin units, as the biotin would occupy them rather than the biotinylated antibody laden cells. The larger volume of biotin resulted in recapitulation of previously established release percentages, as the increase in residence time allowed for larger release of cells from the capture surface.

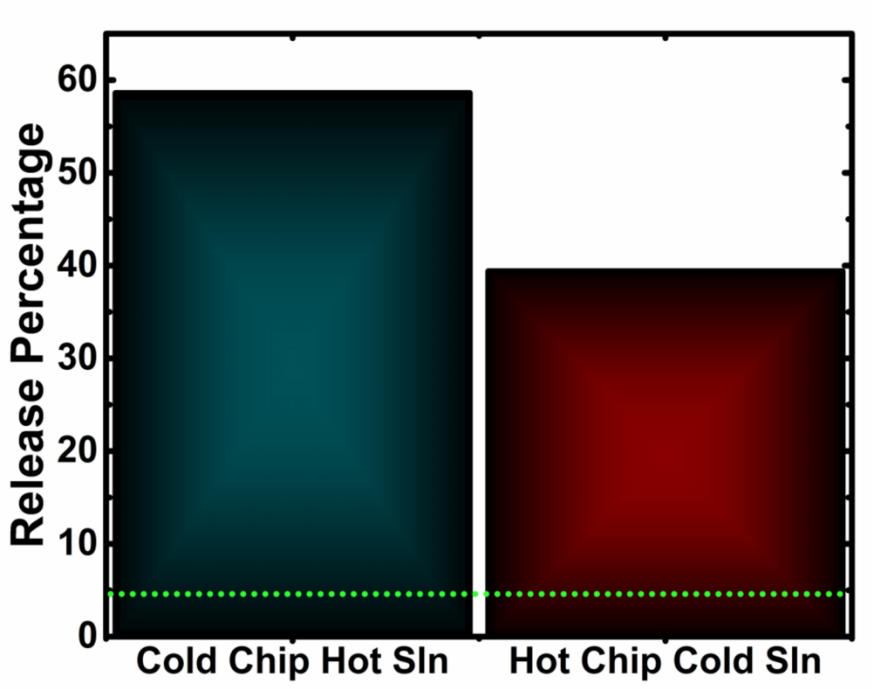

Supplementary Figure 4.2: Implementation of the thermophoresis gradient in capture experiments results in larger release percentages. Changing the thermal gradient that the microfluidic chip and the release solution have allows for either the movement of fluid from the walls of the channel to the center of the channel, or the movement of particles from the center of the fluid to the walls of the channel. The 4° C microfluidic chip with the 40° C solution had a larger release of nearly 60% which recapitulates previous release percentages reported by the SATCR system. This implies that the movement of biotin from the warm fluid to the colder capture surface results in more release than the reverse gradient of force assisting the biotin release of cells from the surface through thermophoretic force. The green dotted line is the consolidated release of similar cells using a non-thermophoretic system.

CHAPTER 5

REFERENCES

Adams, A. a., Okagbare, P. I., Feng, J., Hupert, M. L., Patterson, D., Götten, J., … Soper, S. a. (2008). Highly efficient circulating tumor cell isolation from whole blood and label-free enumeration using polymer-based microfluidics with an integrated conductivity sensor. *Journal of the American Chemical Society*, *130*(27), 8633–8641. http://doi.org/10.1021/ja8015022

Adamski, K., Kubicki, W., & Walczak, R. (2016). 3D Printed Electrophoretic Lab-on-chip for DNA Separation. *Procedia Engineering*, *168*, 1454–1457. http://doi.org/10.1016/j.proeng.2016.11.416

Alexander, M., Corrigan, A., & Infusion Nurses Society. (2010). *Infusion nursing : an evidence-based approach*. Saunders/Elsevier. Retrieved from https://books.google.com/books?id=GjY2NKEYhC8C&pg=PA233&lpg=PA233&dq=isotonic+solution+osmolarity&source=bl&ots=CdL1CRwn-6&sig=-VrfXW0wq7vbXVcwdiGXO5eD8eE&hl=en&sa=X&ved=0ahUKEwj-lPP3nZ3TAhUnllQKHdU4D4Y4ChDoAQgkMAI#v=onepage&q=isotonic solution osmolarity&f=false

Almodóvar, J., Crouzier, T., eila Selimovi, Š., Thomas Boudou, bc, Khademhosseini bcd, A., & Picart, C. (2013). Gradients of physical and biochemical cues on polyelectrolyte multilayer films generated via microfluidics, *13*. http://doi.org/10.1039/c3lc41407h

Alunni-Fabbroni, M., & Sandri, M. T. (2010). Circulating tumour cells in clinical practice: Methods of detection and possible characterization. *Methods (San Diego, Calif.)*, *50*(4), 289–97. http://doi.org/10.1016/j.ymeth.2010.01.027

Anciaux, S. K., Geiger, M., & Bowser, M. T. (2016). 3D Printed Micro Free-Flow Electrophoresis Device. *Analytical Chemistry*, *88*(15), 7675–7682. http://doi.org/10.1021/acs.analchem.6b01573

Andree, K. C., Barradas, A. M. C., Nguyen, A. T., Mentink, A., Stojanovic, I., Baggerman, J., … Terstappen, L. W. M. M. (2016). Capture of Tumor Cells on Anti-EpCAM-Functionalized Poly(acrylic acid)-Coated Surfaces. *ACS Applied Materials and Interfaces*, *8*(23), 14349–14356. http://doi.org/10.1021/acsami.6b01241

Ansari, A., Lee-Montiel, F. T., Amos, J. R., & Imoukhuede, P. I. (2015). Secondary anchor targeted cell release. *Biotechnology and Bioengineering*, *112*(11), 2214–2227. http://doi.org/10.1002/bit.25648

Ansari, A., Patel, R., Schultheis, K., Naumovski, V., & Imoukhuede, P. I. (2016). A Method of Targeted Cell Isolation via Glass Surface Functionalization. *Journal of Visualized Experiments*, (115), 1–9. http://doi.org/10.3791/54315

Ariyasu, S., Hanaya, K., Watanabe, E., Suzuki, T., Horie, K., Hayase, M., … Aoki, S. (2012). Selective capture and collection of live target cells using a photoreactive silicon wafer device modified with antibodies via a photocleavable linker. *Langmuir*, *28*(36), 13118–13126. http://doi.org/10.1021/la302393p

Aswal, D. K., Lenfant, S., Guerin, D., Yakhmi, J. V., & Vuillaume, D. (2006). Self assembled monolayers on silicon for molecular electronics. *Analytica Chimica Acta*. http://doi.org/10.1016/j.aca.2005.10.027

Au, A. K., Bhattacharjee, N., Horowitz, L. F., Chang, T. C., & Folch, A. (2015). 3D-printed microfluidic automation. *Lab on a Chip*, *15*(8), 1934–41. http://doi.org/10.1039/c5lc00126a

Au, A. K., Huynh, W., Horowitz, L. F., & Folch, A. (2016). 3D-Printed Microfluidics. *Angewandte Chemie International Edition*, *55*(12), 3862–3881. http://doi.org/10.1002/anie.201504382

Au, A. K., Lee, W., & Folch, A. (2014). Lab on a Chip Mail-order microfluidics: evaluation of stereolithography for the production of microfluidic devices, *14*. http://doi.org/10.1039/c3lc51360b

Bacakova, L., Filova, E., Parizek, M., Ruml, T., & Svorcik, V. (2011). Modulation of cell adhesion, proliferation and differentiation on materials designed for body implants. *Biotechnology Advances*, *29*(6), 739–767. http://doi.org/10.1016/j.biotechadv.2011.06.004

Bain, C. D., Troughton, E. B., Tao, Y. T., Evall, J., Whitesides, G. M., & Nuzzo, R. G. (1989). Formation of Monolayer Films by the Spontaneous Assembly of Organic Thiols from Solution onto Gold. *Journal of the American Chemical Society*, *111*(1), 321–335. http://doi.org/10.1021/ja00183a049

Bain, C. D., & Whitesides, G. M. (1988). Molecular-Level Control over Surface Order in Self-Assembled Monolayer Films of Thiols on Gold. *Science*, *240*(4848), 62–63. http://doi.org/10.1126/science.240.4848.62

Balakrishnan, B., Kumar, D. S., Yoshida, Y., & Jayakrishnan, A. (2005). Chemical modification of poly(vinyl chloride) resin using poly(ethylene glycol) to improve blood compatibility. *Biomaterials*, *26*(17), 3495–3502. http://doi.org/10.1016/j.biomaterials.2004.09.032

Barry, A. K., Wang, N., & Leckband, D. E. (2015). Local VE-cadherin mechanotransduction triggers long-ranged remodeling of endothelial monolayers. *Journal of Cell Science*, *128*(7), 1341–51. http://doi.org/10.1242/jcs.159954

Bashir, R., Gomez, R., Sarikaya, a, Ladisch, M. R., Sturgis, J., & Robinson, J. P. (2001). Adsorption of avidin on microfabricated surfaces for protein biochip applications. *Biotechnology and Bioengineering*, *73*(4), 324–8. Retrieved from http://www.ncbi.nlm.nih.gov/pubmed/11283915

Batchelor, G. K. (1967). *An Introduction to Fluid Dynamics.) Batchelor, G. K.: An Introduction to Fluid Dynamics. Cambridge University Press, 1967, ISBN 0-521-66396-2.* http://doi.org/10.1063/1.3060769

Batchelor, T. T., Sorensen, a. G., di Tomaso, E., Zhang, W. T., Duda, D. G., Cohen, K. S., … Jain, R. K. (2007). AZD2171, a Pan-VEGF Receptor Tyrosine Kinase Inhibitor, Normalizes Tumor Vasculature and Alleviates Edema in Glioblastoma Patients. *Cancer Cell*, *11*(1), 83–95. http://doi.org/10.1016/j.ccr.2006.11.021

Bergers, G., & Hanahan, D. (2008). Modes of resistance to anti-angiogenic therapy. *Nat Rev Cancer*, *8*(8), 592–603.

Bergers, G., Song, S., Meyer-Morse, N., Bergsland, E., & Hanahan, D. (2003). Benefits of targeting both pericytes and endothelial cells in the tumor vasculature with kinase inhibitors. *The Journal of Clinical Investigation*, *111*(9), 1287–1295. http://doi.org/10.1172/jci17929

Berthier, E., Young, E. W. K., & Beebe, D. (2012). Engineers are from PDMS-land, Biologists are from Polystyrenia. *Lab on a Chip*, *12*(7), 1224. http://doi.org/10.1039/c2lc20982a

Bhattacharya, S., Datta, a., Berg, J. M., & Gangopadhyay, S. (2005). Studies on surface wettability of poly(dimethyl) siloxane (PDMS) and glass under oxygen-plasma treatment and correlation with bond strength. *Journal of Microelectromechanical Systems*, *14*(3), 590–597. http://doi.org/10.1109/JMEMS.2005.844746

Biebuyck, H. A., Bain, C. D., & Whitesides, G. M. (1994). Comparison of Organic Monolayers on Polycrystalline Gold Spontaneously Assembled from Solutions Containing Dialkyl Disulfides or Alkanethiols. *Langmuir*, *10*(6), 1825–1831. http://doi.org/10.1021/la00018a034

Blann, A. D., Woywodt, A., Bertolini, F., Bull, T. M., Buyon, J. P., Clancy, R. M., … Dignat-george, F. (2005). Circulating endothelial cells Biomarker of vascular disease, (3), 228–235. http://doi.org/10.1160/TH04

Bunka, D. H. J., & Stockley, P. G. (2006). Aptamers come of age - At last. *Nature Reviews Microbiology*, *4*(8), 588–596. http://doi.org/10.1038/nrmicro1458

Burdick, J. A., & Prestwich, G. D. (2011). Hyaluronic acid hydrogels for biomedical applications. *Advanced Materials (Deerfield Beach, Fla.)*, *23*(12), H41-56. http://doi.org/10.1002/adma.201003963

Bussolati, G., Montemurro, F., Righi, L., Donadio, M., Aglietta, M., & Sapino, a. (2005). A modified Trastuzumab antibody for the immunohistochemical detection of HER-2 overexpression in breast cancer. *British Journal of Cancer*, *92*(7), 1261–7. http://doi.org/10.1038/sj.bjc.6602507

Camci-Unal, G., Nichol, J. W., Bae, H., Tekin, H., Bischoff, J., & Khademhosseini, A. (2013). Hydrogel surfaces to promote attachment and spreading of endothelial progenitor cells. *Journal of Tissue Engineering and Regenerative Medicine*, *7*(5), 337–347. http://doi.org/10.1002/term.517

Capretto, L., Cheng, W., Hill, M., & Zhang, X. (2011). Micromixing within microfluidic devices. *Microfluidics*, (April), 27–68. http://doi.org/10.1007/128

Carvalho, A., Geissler, M., Schmid, H., Michel, B., & Delamarche, E. (2002). Self-assembled monolayers of eicosanethiol on palladium and their use in microcontact printing. *Langmuir*, *18*(6), 2406–2412. http://doi.org/10.1021/la015596y

Casanovas, O., Hicklin, D. J., Bergers, G., & Hanahan, D. (2005). Drug resistance by evasion of antiangiogenic targeting of VEGF signaling in late-stage pancreatic islet tumors. *Cancer Cell*, *8*(4), 299–309. http://doi.org/10.1016/j.ccr.2005.09.005

Chang, S.-F., Chang, C. A., Lee, D.-Y., Lee, P.-L., Yeh, Y.-M., Yeh, C.-R., … Chiu, J.-J. (2008). Tumor cell cycle arrest induced by shear stress: Roles of integrins and Smad. *Proceedings of the National Academy of Sciences* , *105*(10), 3927–3932. JOUR.

Chen, C.-S., Breslauer, D. N., Luna, J. I., Grimes, A., Chin, W., Lee, L. P., & Khine, M. (2008). Shrinky-Dink microfluidics: 3D polystyrene chips. *Lab on a Chip*, *8*(4), 622. http://doi.org/10.1039/b719029h

Chen, H. W., Medley, C. D., Sefah, K., Shangguan, D., Tang, Z., Meng, L., … Tan, W. (2008). Molecular recognition of small-cell lung cancer cells using aptamers. *ChemMedChem*, *3*(6), 991–1001. http://doi.org/10.1002/cmdc.200800030

Chen, L., Liu, X., Su, B., Li, J., Jiang, L., Han, D., & Wang, S. (2011). Aptamer-mediated efficient capture and release of T lymphocytes on nanostructured surfaces. *Advanced Materials*, *23*(38), 4376–4380. http://doi.org/10.1002/adma.201102435

Chen, S., Guo, X., Imarenezor, O., & Imoukhuede, P. I. (2015). Quantification of VEGFRs, NRP1, and PDGFRs on Endothelial Cells and Fibroblasts Reveals Serum, Intra-Family Ligand, and Cross-Family Ligand Regulation. *Cellular and Molecular Bioengineering*, *8*(3), 383–403. http://doi.org/10.1007/s12195-015-0411-x

Chen, S., Weddell, J., Gupta, P., Conard, G., Parkin, J., & Imoukhuede, P. I. (2017). Qflow cytometry-based receptoromic screening: A high-throughput quantification approach informing biomarker selection and nanosensor development. *Methods in Molecular Biology*, *1570*(In Press), 117–138. http://doi.org/10.1007/978-1-4939-6840-4_8

Chuah, Y. J., Kuddannaya, S., Lee, M. H. A., Zhang, Y., & Kang, Y. (2015). The effects of poly(dimethylsiloxane) surface silanization on the mesenchymal stem cell fate. *Biomaterial Science*, *3*(2), 383–390. http://doi.org/10.1039/C4BM00268G

Coad, B. R., Vasilev, K., Diener, K. R., Hayball, J. D., Short, R. D., & Griesser, H. J. (2012). Immobilized Streptavidin Gradients as Bioconjugation Platforms. *Langmuir*, *28*(5), 2710–2717. http://doi.org/10.1021/la204714p

Cohen, S. J., Punt, C. J. a, Iannotti, N., Saidman, B. H., Sabbath, K. D., Gabrail, N. Y., … Meropol, N. J. (2008). Relationship of circulating tumor cells to tumor response, progression-free survival, and overall survival in patients with metastatic colorectal cancer. *Journal of Clinical Oncology : Official Journal of the American Society of Clinical Oncology*, *26*(19), 3213–21. http://doi.org/10.1200/JCO.2007.15.8923

Compton, J. L., Luo, J. C., Ma, H., Botvinick, E., & Venugopalan, V. (2014). High-throughput

optical screening of cellular mechanotransduction. *Nat Photonics*, *8*(9), 710–715. http://doi.org/10.1038/nphoton.2014.165

Cooksey, G. A., Elliott, J. T., & Plant, A. L. (2011). Reproducibility and Robustness of a Real-Time Microfluidic Cell Toxicity Assay. | *Anal. Chem*, *83*, 3890–3896. http://doi.org/10.1021/ac200273f

Coon, B. G., Baeyens, N., Han, J., Budatha, M., Ross, T. D., Fang, J. S., … Schwartz, M. A. (2015). Intramembrane binding of VE-cadherin to VEGFR2 and VEGFR3 assembles the endothelial mechanosensory complex. *The Journal of Cell Biology , 208*(7), 975–986. JOUR.

Corominas-Faja, B., Cufí, S., Oliveras-Ferraros, C., Cuyàs, E., López-Bonet, E., Lupu, R., … Menendez, J. a. (2013). Nuclear reprogramming of luminal-like breast cancer cells generates Sox2-overexpressing cancer stem-like cellular states harboring transcriptional activation of the mTOR pathway. *Cell Cycle (Georgetown, Tex.)*, *12*(18), 3109–24. http://doi.org/10.4161/cc.26173

Custódio, C. A., Frias, A. M., del Campo, A., Reis, R. L., & Mano, J. F. (2012). Selective cell recruitment and spatially controlled cell attachment on instructive chitosan surfaces functionalized with antibodies. *Biointerphases*, *7*(1–4), 1–9. http://doi.org/10.1007/s13758-012-0065-3

De Castro, D. G., Clarke, P. A., Al-Lazikani, B., & Workman, P. (2013). Personalized Cancer Medicine: Molecular Diagnostics, Predictive biomarkers, and Drug Resistance. *Clinical Pharmacology and Therapeutics*, *93*(3), 252–259. http://doi.org/10.1038/clpt.2012.237

De Spiegelaere, W., Cornillie, P., Van Poucke, M., Peelman, L., Burvenich, C., & Van den Broeck, W. (2011). Quantitative mRNA expression analysis in kidney glomeruli using microdissection techniques. *Histology and Histopathology*, *26*(2), 267–75. Retrieved from http://www.ncbi.nlm.nih.gov/pubmed/21154239

dela Paz, N. G., Walshe, T. E., Leach, L. L., Saint-Geniez, M., & D'Amore, P. A. (2012). Role of shear-stress-induced VEGF expression in endothelial cell survival. *Journal of Cell Science*, *125*(Pt 4), 831–843. http://doi.org/10.1242/jcs.084301

den Toonder, J. (2011). Circulating tumor cells: the Grand Challenge. *Lab on a Chip*, *11*(3), 375. http://doi.org/10.1039/c0lc90100h

Dertinger, S. K. W., Jiang, X., Li, Z., Murthy, V. N., & Whitesides, G. M. (2002). Gradients of substrate-bound laminin orient axonal specification of neurons.

Diagnostics, V., Companion, A., Devices, D., & Tools, I. (2014). List of Cleared or Approved Companion Diagnostic Devices (In Vitro and Imaging Tools), 1–5.

Diéguez, L., Winter, M. A., Pocock, K. J., Bremmell, K. E., & Thierry, B. (2015). Efficient microfluidic negative enrichment of circulating tumor cells in blood using roughened PDMS. *The Analyst*, *140*(10), 3565–3572. http://doi.org/10.1039/C4AN01768D

Dillmore, W. S., Yousaf, M. N., & Mrksich, M. (2004). A photochemical method for patterning

the immobilization of ligands and cells to self-assembled monolayers. *Langmuir*, *20*(17), 7223–7231. http://doi.org/10.1021/la049826v

Dittrich, P. S., & Manz, A. (2006). Lab-on-a-chip: microfluidics in drug discovery. *Nat Rev Drug Discov*, *5*(3), 210–218. http://doi.org/10.1038/nrd1985

Doroshow, J. H. (2009). NCI's Roadmap to Personalized Medicine in Cancer Treatment. In *NCAB 150th Meeting*.

Dubois, L. H., Zegarski, B. R., & Nuzzo, R. G. (1993). Molecular ordering of organosulfur compounds on Au(111) and Au(100): Adsorption from solution and in ultrahigh vacuum. *The Journal of Chemical Physics*, *98*(1), 678–688. http://doi.org/10.1063/1.464613

Dyer, D., Shreim, S., Jayadev, S., Lew, V., Botvinick, E., & Khine, M. (2011). Sequential shrink photolithography for plastic microlens arrays. *Applied Physics Letters*, *99*(3), 19–22. http://doi.org/10.1063/1.3609322

Erber, R., Thurnher, A., Katsen, A. D., Groth, G., Kerger, H., Hammes, H.-P., … Vajkoczy, P. (2004). Combined inhibition of VEGF and PDGF signaling enforces tumor vessel regression by interfering with pericyte-mediated endothelial cell survival mechanisms. *FASEB Journal : Official Publication of the Federation of American Societies for Experimental Biology*, *18*(2), 338–40. http://doi.org/10.1096/fj.03-0271fje

Erdbruegger, U., Haubitz, M., & Woywodt, A. (2006). Circulating endothelial cells: a novel marker of endothelial damage. *Clinica Chimica Acta; International Journal of Clinical Chemistry*, *373*(1–2), 17–26. http://doi.org/10.1016/j.cca.2006.05.016

FDA. (2014). In Vitro Companion Diagnostic Devices: Guidance for Industry and Food and Drug Administration Staff. *Federal Register*, 12.

FDA, AACR, ASC, & Mansfield, E. (2015). Complexities in Personalized Medicine: Harmonizing Companion Diagnostics Across a Class of Targeted Therapies.

Fenter, P., Eisenberger, P., Li, J., Camillone, N., Bernasek, S., Scoles, G., … Liang, K. S. (1991). Structure of octadecyl thiol self-assembled on the silver(111) surface: an incommensurate monolayer. *Langmuir*, *7*(10), 2013–2016. http://doi.org/10.1021/la00058a008

Ferreira-Dias, S., Valente, D. G., & Abreu, J. M. F. (2003). Comparison between ethanol and hexane for oil extraction from Quercus suber L. fruits. *Grasas Y Aceites*, *54*(4), 378–383. http://doi.org/10.3989/gya.2003.v54.i4.225

Feynman, R. P. (2011). There's plenty of room at the bottom. *Resonance*, *16*(9), 890–905. http://doi.org/10.1007/s12045-011-0109-x

Fox, T. G., & Flory, P. J. (1950). Second-order transition temperatures and related properties of polystyrene. I. Influence of molecular weight. *Journal of Applied Physics*, *21*(6), 581–591. http://doi.org/10.1063/1.1699711

Fraysse, B., Mons, R., & Garric, J. (2006). Development of a zebrafish 4-day embryo-larval bioassay to assess toxicity of chemicals. *Ecotoxicology and Environmental Safety*, *63*(2),

253–267. http://doi.org/10.1016/j.ecoenv.2004.10.015

Fukuda, S., & Schmid-Schönbein, G. W. (2002). Centrifugation attenuates the fluid shear response of circulating leukocytes. *Journal of Leukocyte Biology*, *72*(July), 133–139.

Gao, Y., Li, W., & Pappas, D. (2013). Recent advances in microfluidic cell separations. *The Analyst*, *138*(17), 4714. http://doi.org/10.1039/c3an00315a

Gelber, M. K., Kole, M. R., Kim, N., Aluru, N. R., & Bhargava, R. (n.d.). Quantitative Chemical Imaging of Nonplanar Microfluidics. http://doi.org/10.1021/acs.analchem.6b03943

Gervais, T., El-Ali, J., Günther, A., & Jensen, K. F. (2006). Flow-induced deformation of shallow microfluidic channels. *Lab on a Chip*, *6*(4), 500–7. http://doi.org/10.1039/b513524a

Gonzá, M., Bagatolli, L. A., Echabe, I., Arrondo, J. L. R., Argarañ, C. E., Cantor, C. R., & Fidelio, G. D. (n.d.). Interaction of Biotin with Streptavidin THERMOSTABILITY AND CONFORMATIONAL CHANGES UPON BINDING*. Retrieved from http://www.jbc.org/content/272/17/11288.full.pdf

González, M., Bagatolli, L. A., Echabe, I., Arrondo, J. L. R., Argaraña, C. E., Cantor, C. R., & Fidelio, G. D. (1997). Interaction of biotin with streptavidin. Thermostability and conformational changes upon binding. *Journal of Biological Chemistry*, *272*, 11288–11294. http://doi.org/10.1074/jbc.272.17.11288

Gotrik, M. R., Feagin, T. A., Csordas, A. T., Nakamoto, M. A., & Soh, H. T. (2016). Advancements in Aptamer Discovery Technologies. *Accounts of Chemical Research*, *49*(9), 1903–1910. http://doi.org/10.1021/acs.accounts.6b00283

Graf, B. W., Ralston, T. S., Ko, H.-J., & Boppart, S. A. (2009). Detecting intrinsic scattering changes correlated to neuron action potentials using optical coherence imaging. *Optics Express*, *17*(16), 13447–57. http://doi.org/10.1364/OE.17.013447

Grimes, A., Breslauer, D. N., Long, M., Pegan, J., Lee, L. P., & Khine, M. (2008). Shrinky-Dink microfluidics: rapid generation of deep and rounded patterns. *Lab on a Chip*, *8*(1), 170–2. http://doi.org/10.1039/b711622e

Hahn, Y. K., Hong, D., Kang, J. H., & Choi, S. (2016). A reconfigurable microfluidics platform for microparticle separation and fluid mixing. *Micromachines*, *7*(8), 139. http://doi.org/10.3390/mi7080139

Haijie, W., Wei, H., Yunyun, Z., Langhuan, H., Jingxian, Z., Shaozao, T., … and Xiaoyan, L. (2016). Effect of oil extraction on properties of spent coffee ground–plastic composites. *J Mater Sci*, *51*, 10205–10214. http://doi.org/0.1007/s10853-016-0248-2

Hanahan, D., & Weinberg, R. a. (2011). Hallmarks of cancer: the next generation. *Cell*, *144*(5), 646–74. http://doi.org/10.1016/j.cell.2011.02.013

Hanahan, D., & Weinberg, R. A. (2000). The Hallmarks of Cancer. *Cell*, *100*(1), 57–70. http://doi.org/10.1016/S0092-8674(00)81683-9

Hansen, C. (2015). Personalized Medicine: The Future of Cancer Care. Retrieved from http://www.acscan.org/content/cancer-candor/personalized-medicine-the-future-of-cancer-care/

Harris, L. G., Tosatti, S., Wieland, M., Textor, M., & Richards, R. G. (2004). Staphylococcus aureus adhesion to titanium oxide surfaces coated with non-functionalized and peptide-functionalized poly(L-lysine)-grafted- poly(ethylene glycol) copolymers. *Biomaterials*, *25*(18), 4135–4148. http://doi.org/10.1016/j.biomaterials.2003.11.033

Hassan, U., Ghonge, T., Reddy Jr., B., Patel, M., Rappleye, M., Taneja, I., … Bashir, R. (2017). A point-of-care microfluidic biochip for quantification of CD64 expression from whole blood for sepsis stratification. *Nature Communications*, *8*, 15949. http://doi.org/10.1038/ncomms15949

Holmberg, A., Blomstergren, A., Nord, O., Lukacs, M., Lundeberg, J., & Uhlén, M. (2005). The biotin-streptavidin interaction can be reversibly broken using water at elevated temperatures. *ELECTROPHORESIS*, *26*(3), 501–510. http://doi.org/10.1002/elps.200410070

Ibarlucea, B., Fernández-Sánchez, C., Demming, S., Büttgenbach, S., & Llobera, A. (2011). Selective functionalisation of PDMS-based photonic lab on a chip for biosensing. *The Analyst*, *136*(17), 3496–502. http://doi.org/10.1039/c0an00941e

Imoukhuede, P. I., Dokun, A. O., Annex, B. H., & Popel, A. S. (2013a). Endothelial cell-by-cell profiling reveals temporal dynamics of VEGFR1 and VEGFR2 membrane-localization following murine hindlimb ischemia. *Am J Physiol Heart Circ Physiol*, *4*(8), H1085-93. http://doi.org/10.1152/ajpheart.00514.2012

Imoukhuede, P. I., Dokun, A. O., Annex, B. H., & Popel, A. S. (2013b). Endothelial cell-by-cell profiling reveals the temporal dynamics of VEGFR1 and VEGFR2 membrane localization after murine hindlimb ischemia. *American Journal of Physiology. Heart and Circulatory Physiology*, *304*(8), H1085-93. http://doi.org/10.1152/ajpheart.00514.2012

Imoukhuede, P. I., & Popel, A. S. (2011). Quantification and cell-to-cell variation of vascular endothelial growth factor receptors. *Experimental Cell Research*, *317*(7), 955–965. http://doi.org/10.1016/j.yexcr.2010.12.014

Imoukhuede, P. I., & Popel, A. S. (2011). Quantification and cell-to-cell variation of vascular endothelial growth factor receptors. *Experimental Cell Research*, *317*(7), 955–965. http://doi.org/10.1016/j.yexcr.2010.12.014

Imoukhuede, P. I., & Popel, A. S. (2012). Expression of VEGF receptors on endothelial cells in mouse skeletal muscle. *PloS One*, *7*(9), e44791. http://doi.org/10.1371/journal.pone.0044791

Imoukhuede, P. I., & Popel, A. S. (2014). Quantitative fluorescent profiling of VEGFRs reveals tumor cell and endothelial cell heterogeneity in breast cancer xenografts. *Cancer Medicine*, *3*(2), 225–44. http://doi.org/10.1002/cam4.188

Inaba, R., Khademhosseini, A., Suzuki, H., & Fukuda, J. (2009). Electrochemical desorption of self-assembled monolayers for engineering cellular tissues. *Biomaterials*, *30*(21), 3573–3579. http://doi.org/10.1016/j.biomaterials.2009.03.045

Ingber, D. E. (2016). Reverse Engineering Human Pathophysiology with Organs-on-Chips. *Cell*, *164*(6), 1105–1109. http://doi.org/10.1016/j.cell.2016.02.049

Ishibe, S., Haydu, J. E., Togawa, A., Marlier, A., & Cantley, L. G. (2006). Cell Confluence Regulates Hepatocyte Growth Factor-Stimulated Cell Morphogenesis in a ᴺᴸ-Catenin-Dependent Manner □. *MOLECULAR AND CELLULAR BIOLOGY*, *26*(24), 9232–9243. http://doi.org/10.1128/MCB.01312-06

Jiang, X., Ferrigno, R., Mrksich, M., & Whitesides, G. M. (2003). Electrochemical desorption of self-assembled monolayers noninvasively releases patterned cells from geometrical confinements. *Journal of the American Chemical Society*, *125*(9), 2366–2367. http://doi.org/10.1021/ja029485c

Jørgensen, J. T. (2013). Companion diagnostics in oncology - Current status and future aspects. *Oncology (Switzerland)*. http://doi.org/10.1159/000353454

Karabacak, N. M., Spuhler, P. S., Fachin, F., Lim, E. J., Pai, V., Ozkumur, E., … Toner, M. (2014). Microfluidic, marker-free isolation of circulating tumor cells from blood samples. *Nat Protoc*, *9*(3), 694–710. http://doi.org/Doi 10.1038/Nprot.2014.044

Karar, J., & Maity, A. (2011). PI3K/AKT/mTOR pathway in Angiogenesis . *Frontiers in Molecular Neuroscience* . JOUR .

Kato, K., Sato, H., & Iwata, H. (2007). Ultrastructural study on the specific binding of genetically engineered epidermal growth factor to type I collagen fibrils. *Bioconjugate Chemistry*, *18*(6), 2137–2143. http://doi.org/10.1021/bc700259g

Khademhosseini, A., Suh, K. Y., Yang, J. M., Eng, G., Yeh, J., Levenberg, S., & Langer, R. (2004). Layer-by-layer deposition of hyaluronic acid and poly-L-lysine for patterned cell co-cultures. *Biomaterials*, *25*(17), 3583–3592. http://doi.org/10.1016/j.biomaterials.2003.10.033

Kiehl, T. R., Shen, D., Khattak, S. F., Jian Li, Z., & Sharfstein, S. T. (2011). Observations of cell size dynamics under osmotic stress. *Cytometry Part A*, *79A*(7), 560–569. http://doi.org/10.1002/cyto.a.21076

Kim, T. H., Yoon, H. J., Stella, P., & Nagrath, S. (2014). Cascaded spiral microfluidic device for deterministic and high purity continuous separation of circulating tumor cells. *Biomicrofluidics*, *8*(6). http://doi.org/10.1063/1.4903501

Kimura, T., Matsui, K., & Sato, T. (1974). Relationship between plasma osmolality and plasma concentration of antidiuretic hormone in normal subjects, patients with chronic renal diseases, and patients with central diabetes insipidus. *Tohoku Journal of Experimental Medicine*, *113*(1), 77–88. Retrieved from http://ovidsp.ovid.com/ovidweb.cgi?T=JS&CSC=Y&NEWS=N&PAGE=fulltext&D=emcl

2&AN=0975073139%5Cnhttp://sfx.ucl.ac.uk/sfx_local?sid=OVID:embase&id=pmid:&id=doi:&issn=0040-8727&isbn=&volume=113&issue=1&spage=77&pages=77-88&date=1974&title=Tohoku+Journal+of+Expe

Kobayashi, H., Sakahara, H., Endo, K., Hosono, M., Yao, Z. S., Toyama, S., & Konishi, J. (1995). Comparison of the chase effects of avidin, streptavidin, neutravidin, and avidin-ferritin on a radiolabeled biotinylated anti-tumor monoclonal antibody. *Japanese Journal of Cancer Research : Gann*, *86*(3), 310–314. http://doi.org/091050509599413L [pii]

Kornet, L., Hoeks, A. P. G., Lambregts, J., & Reneman, R. S. (1999). In the Femoral Artery Bifurcation, Differences in Mean Wall Shear Stress Within Subjects Are Associated With Different Intima-Media Thicknesses. *Arteriosclerosis, Thrombosis, and Vascular Biology*, *19*(12), 2933–2939. http://doi.org/10.1161/01.ATV.19.12.2933

Kornet, L., Hoeks, A. P., Lambregts, J., & Reneman, R. S. (2000). Mean wall shear stress in the femoral arterial bifurcation is low and independent of age at rest. *Journal of Vascular Research*, *37*(0), 112–122. http://doi.org/10.1159/000025722

Kourouklis, A. P., Kaylan, K. B., & Underhill, G. H. (2016). Substrate stiffness and matrix composition coordinately control the differentiation of liver progenitor cells. *Biomaterials*, *99*, 82–94. http://doi.org/10.1016/j.biomaterials.2016.05.016

Kuddannaya, S., & Chuah, Y. (2013). Surface chemical modification of poly (dimethylsiloxane) for the enhanced adhesion and proliferation of mesenchymal stem cells. *ACS: Applied Materials & Interfaces*, *5*, 9777–9784. http://doi.org/10.1021/am402903e

Kuntaegowdanahalli, S., & Bhagat, A. (2009). Inertial microfluidics for continuous particle separation in spiral microchannels. *Lab on a Chip*, *9*(20), 2973–80. http://doi.org/10.1039/b908271a

Kuntaegowdanahalli, S. S., Bhagat, A. A. S., & Papautsky, I. (2009). Continuous multi-particle separation using deterministic focusing in spiral microchannels. In *TRANSDUCERS 2009 - 15th International Conference on Solid-State Sensors, Actuators and Microsystems* (pp. 2139–2142). http://doi.org/10.1109/SENSOR.2009.5285629

Kurkuri, M. D., Al-Ejeh, F., Shi, J. Y., Palms, D., Prestidge, C., Griesser, H. J., … Thierry, B. (2011). Plasma functionalized PDMS microfluidic chips: towards point-of-care capture of circulating tumor cells. *Journal of Materials Chemistry*, *21*(24), 8841. http://doi.org/10.1039/c1jm10317b

Kusnezow, W., & Hoheisel, J. D. (2003). Solid supports for microarray immunoassays. *Journal of Molecular Recognition*, *16*(4), 165–176. http://doi.org/10.1002/jmr.625

Kutsenko, V. Y., Lopatina, Y. Y., Bossard-Giannesini, L., Marchenko, O. A., Pluchery, O., & Snegir, S. V. (2017). Alkylthiol self-assembled monolayers on Au(111) with tailored tail groups for attaching gold nanoparticles. *Nanotechnology*, *28*(23). http://doi.org/10.1088/1361-6528/aa6e3d

Kwak, B., Lee, J., Lee, J., Kim, H. S., Kang, S., & Lee, Y. (2018). Spiral shape microfluidic

channel for selective isolating of heterogenic circulating tumor cells. *Biosensors and Bioelectronics*, *101*, 311–316. http://doi.org/10.1016/j.bios.2017.10.036

Lai, Y.-K., & Fan, R. F. T. (1996). Effect of heparin-surf ace-modified poly(methyl methacrylate) intraocular lenses on the postoperative inflammation in an Asian population. http://doi.org/10.1016/S0886-3350(96)80170-2

Laibinis, P. E., Whitesides, G. M., Allara, D. L., Tao, Y.-T., Parikh, A., & Nuzzo, R. (1991). Comparison of the Structures and Wetting Properties of Self-Assembled Monolayers of n-Alkanethiols on the Coinage Metal Surfaces, Cu, Ag, Au. *Journal of the American Chemical Society*, *113*(19), 7152–7167. http://doi.org/10.1021/ja00019a011

Lammer, E., Carr, G. J., Wendler, K., Rawlings, J. M., Belanger, S. E., & Braunbeck, T. (2009). Is the fish embryo toxicity test (FET) with the zebrafish (Danio rerio) a potential alternative for the fish acute toxicity test? *Comparative Biochemistry and Physiology Part C: Toxicology & Pharmacology*, *149*(2), 196–209. http://doi.org/10.1016/j.cbpc.2008.11.006

Lammer, E., Kamp, H. G., Hisgen, V., Koch, M., Reinhard, D., Salinas, E. R., … Braunbeck, T. (2009). Development of a flow-through system for the fish embryo toxicity test (FET) with the zebrafish (Danio rerio). *Toxicology in Vitro*, *23*(7), 1436–1442. http://doi.org/10.1016/j.tiv.2009.05.014

Lang, F., Busch, G. L., Ritter, M., Lkl, H. V, Waldegger, S., Gulbins, E., & Ussinger, D. H. (1998). Functional Significance of Cell Volume Regulatory Mechanisms. *PHYSIOLOGICAL REVIEWS*, *78*(1).

Lee-Montiel, F. T., & Imoukhuede, P. I. (2013). Engineering quantum dot calibration standards for quantitative fluorescent profiling. *Journal of Materials Chemistry B*, *1*, 6434. http://doi.org/10.1039/c3tb20904k

Lee-Montiel, F. T., Li, P., & Imoukhuede, P. I. (2015a). Quantum dot multiplexing for the profiling of cellular receptors. *Nanoscale*, *7*(44), 18504–18514. http://doi.org/10.1039/C5NR01455G

Lee-Montiel, F. T., Li, P., & Imoukhuede, P. I. (2015b). Quantum dot multiplexing for the profiling of cellular receptors. *Nanoscale*, *7*(44), 18504–14. http://doi.org/10.1039/c5nr01455g

Lee, G. U., Kidwell, D. a, & Colton, R. J. (1994). Sensing Discrete Streptavidin-Biotin Interactions with Atomic Force Microscopy. *Langmuir*, *2*(9), 354–357. http://doi.org/10.1021/la00014a003

Lee, J. M., Zhang, M., & Yeong, W. Y. (2016). Characterization and evaluation of 3D printed microfluidic chip for cell processing. *Microfluidics and Nanofluidics*, *20*(1), 1–15. http://doi.org/10.1007/s10404-015-1688-8

Li, Y., Yuan, B., Ji, H., Han, D., Chen, S., Tian, F., & Jiang, X. (2007). A method for patterning multiple types of cells by using electrochemical desorption of self-assembled monolayers within microfluidic channels. *Angewandte Chemie - International Edition*, *46*(7), 1094–

1096. http://doi.org/10.1002/anie.200603844

Li, Z., Chang, S. C., & Williams, R. S. (2003). Self-assembly of alkanethiol molecules onto platinum and platinum oxide surfaces. *Langmuir*, *19*(17), 6744–6749. http://doi.org/10.1021/la034245b

Lin, M., Chen, J. F., Lu, Y. T., Zhang, Y., Song, J., Hou, S., … Tseng, H. R. (2014). Nanostructure embedded microchips for detection, isolation, and characterization of circulating tumor cells. *Accounts of Chemical Research*, *47*(10), 2941–2950. http://doi.org/10.1021/ar5001617

Lippert, L. G., Hallock, J. T., Dadosh, T., Diroll, B. T., Murray, C. B., & Goldman, Y. E. (2016). NeutrAvidin Functionalization of CdSe/CdS Quantum Nanorods and Quantification of Biotin Binding Sites using Biotin-4-Fluorescein Fluorescence Quenching. *Bioconjugate Chemistry*, *27*(3), 562–568. http://doi.org/10.1021/acs.bioconjchem.5b00577

Liu, H., Li, Y., Sun, K., Fan, J., Zhang, P., Meng, J., … Jiang, L. (2013). Dual-responsive surfaces modified with phenylboronic acid-containing polymer brush to reversibly capture and release cancer cells. *Journal of the American Chemical Society*, *135*(20), 7603–7609. http://doi.org/10.1021/ja401000m

Love, J. C., Estroff, L. A., Kriebel, J. K., Nuzzo, R. G., & Whitesides, G. M. (2005). Self-assembled monolayers of thiolates on metals as a form of nanotechnology. *Chemical Reviews*. http://doi.org/10.1021/cr0300789

Love, J. C., Wolfe, D. B., Haasch, R., L, M., Paul, K. E., Whitesides, G. M., … Chabinyc, M. L. (2003). Formation and Structure of Self-Assembled Monolayers of Alkanethiolates on Palladium Formation and Structure of Self-Assembled Monolayers of Alkanethiolates on Palladium, 2597–2609. http://doi.org/10.1021/ja028692

Ludwig, a, Kretzmer, G., & Schügerl, K. (1992). Determination of a "critical shear stress level" applied to adherent mammalian cells. *Enzyme and Microbial Technology*, *14*(3), 209–13. Retrieved from http://www.ncbi.nlm.nih.gov/pubmed/1367978

Macdonald, N. P., Zhu, F., Hall, C. J., Reboud, J., Crosier, P. S., Patton, E. E., … Cooper, J. M. (2016). Assessment of biocompatibility of 3D printed photopolymers using zebrafish embryo toxicity assays. *Lab Chip*, *16*(2), 291–297. http://doi.org/10.1039/C5LC01374G

Mahmood, M. A. I., Arafat, C. M. A., Kim, Y. tae, & Iqbal, S. M. (2013). Quantitative classification of tumor cell morphological changes on selectively functionalized biochips. *Conference Proceedings : ... Annual International Conference of the IEEE Engineering in Medicine and Biology Society. IEEE Engineering in Medicine and Biology Society. Annual Conference*, *2013*, 4164–4166. http://doi.org/10.1109/EMBC.2013.6610462

Mahmood, M. A. I., Wan, Y., Islam, M., Ali, W., Hanif, M., Kim, Y. T., & Iqbal, S. M. (2014). Micro plus nanotexturing of substrates to enhance ligand-assisted cancer cell isolation. *Nanotechnology*, *25*(47). http://doi.org/Artn 475102\r10.1088/0957-4484/25/47/475102

Mamer, S. B., Chen, S., Weddell, J. C., Palasz, A., Wittenkeller, A., Kumar, M., & Imoukhuede,

P. I. (2017). Discovery of High-Affinity PDGF-VEGFR Interactions: Redefining RTK Dynamics. *Scientific Reports*, *7*(1). http://doi.org/10.1038/s41598-017-16610-z

McGurk, S. (2010). Berne and Levy Physiology – Sixth edition. *Nursing Standard*, *24*(31), 31–31. http://doi.org/10.7748/ns2010.04.24.31.31.b1041

Mikolajczyk, S. D., Millar, L. S., Tsinberg, P., Coutts, S. M., Zomorrodi, M., Pham, T., … Pircher, T. J. (2011). Detection of EpCAM-negative and cytokeratin-negative circulating tumor cells in peripheral blood. *Journal of Oncology*, *2011*. http://doi.org/10.1155/2011/252361

Millet, L. J., Stewart, M. E., Nuzzo, R. G., & Gillette, M. U. (2010). Guiding neuron development with planar surface gradients of substrate cues deposited using microfluidic devices. http://doi.org/10.1039/c001552k

Mir, M., Kim, T., Majumder, A., Xiang, M., Wang, R., Liu, S. C., … Popescu, G. (2014). Label-free characterization of emerging human neuronal networks. *Scientific Reports*, *4*, 4434. http://doi.org/10.1038/srep04434

Miwa, J., Suzuki, Y., & Kasagi, N. (2008). Adhesion-based cell sorter with antibody-coated amino-functionalized-parylene surface. *Journal of Microelectromechanical Systems*, *17*(3), 611–622. http://doi.org/10.1109/JMEMS.2008.921706

Miyazaki, H., Kato, K., Teramura, Y., & Iwata, H. (2008). A collagen-binding mimetic of neural cell adhesion molecule. *Bioconjugate Chemistry*, *19*(6), 1119–1123. http://doi.org/10.1021/bc700470v

Mizuarai, S., Takahashi, K., Kobayashi, T., & Kotani, H. (2005). Advances in isolation and characterization of homogeneous cell populations using laser microdissection. *Histology and Histopathology*, *20*(1), 139–46. Retrieved from http://www.ncbi.nlm.nih.gov/pubmed/15578433

Motl, R. W., Pilutti, L. A., Hubbard, E. A., Wetter, N. C., Sosnoff, J. J., & Sutton, B. P. (2015). Cardiorespiratory fitness and its association with thalamic, hippocampal, and basal ganglia volumes in multiple sclerosis. *NeuroImage: Clinical*, *7*, 661–666. http://doi.org/10.1016/j.nicl.2015.02.017

Mrksich, M. (1998). Tailored substrates for studies of attached cell culture. *Cellular and Molecular Life Sciences*, *54*(7), 653–662. http://doi.org/10.1007/s000180050193

Mrksich, M., Chen, C. S., Xia, Y., Dike, L. E., Ingber, D. E., & Whitesides, G. M. (1996). Controlling cell attachment on contoured surfaces with self-assembled monolayers of alkanethiolates on gold. *Proceedings of the National Academy of Sciences of the United States of America*, *93*(20), 10775–8. http://doi.org/10.1073/pnas.93.20.10775

Mueller, O., Hahnenberger, K., Dittmann, M., Herman, Y., Dubrow, R., Nagle, R., & Ilsley, D. (2000). A microfluidic system for high-speed reproducible DNA sizing and quantitation. *Electrophoresis*, *21*(1), 128–134. http://doi.org/10.1002/(SICI)1522-2683(20000101)21:1<128::AID-ELPS128>3.0.CO;2-M

Muskal, N., Turyan, I., & Mandler, D. (1996). Self-assembled monolayers on mercury surfaces. *Journal of Electroanalytical Chemistry*, *409*(1–2), 131–136. http://doi.org/10.1016/0022-0728(96)04529-9

Myung, J. H., Launiere, C. A., Eddington, D. T., & Hong, S. (2010). Enhanced tumor cell isolation by a biomimetic combination of e-selectin and anti-epcam: Implications for the effective separation of circulating tumor cells (CTCs). *Langmuir*, *26*(11), 8589–8596. http://doi.org/10.1021/la904678p

Nagrath, S., Sequist, L. V., Maheswaran, S., Bell, D. W., Irimia, D., Ulkus, L., … Toner, M. (2007). Isolation of rare circulating tumour cells in cancer patients by microchip technology. *Nature*, *450*(7173), 1235–1239. http://doi.org/10.1038/nature06385

Naranbhai, V., Bartman, P., Ndlovu, D., Ramkalawon, P., Ndung'u, T., Wilson, D., … Carr, W. H. (2011). Impact of blood processing variations on natural killer cell frequency, activation, chemokine receptor expression and function. *Journal of Immunological Methods*, *366*(1–2), 28–35. http://doi.org/10.1016/j.jim.2011.01.001

Nguyen, D., McLane, J., Lew, V., Pegan, J., & Khine, M. (2011). Shrink-film microfluidic education modules: Complete devices within minutes. *Biomicrofluidics*, *5*(2), 22209. http://doi.org/10.1063/1.3576930

Nguyen, T. T., Sly, K. L., & Conboy, J. C. (2012). Comparison of the energetics of avidin, streptavidin, neutrAvidin, and anti-biotin antibody binding to biotinylated lipid bilayer examined by second-harmonic generation. *Analytical Chemistry*, *84*(1), 201–8. http://doi.org/10.1021/ac202375n

Nolan, J. P., Condello, D., Duggan, E., Naivar, M., & Novo, D. (2013). Visible and near infrared fluorescence spectral flow cytometry. *Cytometry. Part A : The Journal of the International Society for Analytical Cytology*, *83*(3), 253–64. http://doi.org/10.1002/cyto.a.22241

O'Flaherty, J. D., Gray, S., Richard, D., Fennell, D., O'Leary, J. J., Blackhall, F. H., & O'Byrne, K. J. (2012). Circulating tumour cells, their role in metastasis and their clinical utility in lung cancer. *Lung Cancer*, *76*(1), 19–25. http://doi.org/10.1016/j.lungcan.2011.10.018

Okano, T., Yamada, N., Sakai, H., & Sakurai, Y. (1993). A novel recovery system for cultured cells using plasma-treated polystyrene dishes grafted with poly(N-isopropylacrylamide). *Journal of Biomedical Materials Research*, *27*(10), 1243–1251. http://doi.org/10.1002/jbm.820271005

Olesen, S. P., Clapham, D. E., & Davies, P. F. (1988). Haemodynamic shear stress activates a K+ current in vascular endothelial cells. *Nature*, *331*(6152), 168–170. JOUR. http://doi.org/10.1038/331168a0

Papadopoulos, N., Kinzler, K. W., & Vogelstein, B. (2006). The role of companion diagnostics in the development and use of mutation-targeted cancer therapies. *Nature Biotechnology*, *24*(8), 985–995. http://doi.org/10.1038/nbt1234

Pecot, C. V., Bischoff, F. Z., Mayer, J. A., Wong, K. L., Pham, T., Bottsford-Miller, J., … Sood,

A. K. (2011). A novel platform for detection of CK + and CK - CTCs. *Cancer Discovery*, *1*(12), 580–586. http://doi.org/10.1158/2159-8290.CD-11-0215

Pegan, J. D., Ho, A. Y., Bachman, M., & Khine, M. (2013). Flexible shrink-induced high surface area electrodes for electrochemiluminescent sensing. *Lab on a Chip*, *13*(21), 4205. http://doi.org/10.1039/c3lc50588j

Peluso, P., Wilson, D. S., Do, D., Tran, H., Venkatasubbaiah, M., Quincy, D., … Nock, S. (2003). Optimizing antibody immobilization strategies for the construction of protein microarrays. *Analytical Biochemistry*, *312*(2), 113–124. http://doi.org/10.1016/S0003-2697(02)00442-6

Plouffe, B. D., Murthy, S. K., & Lewis, L. H. (2014). Fundamentals and application of magnetic particles in cell isolation and enrichment: a review. *Reports on Progress in Physics. Physical Society (Great Britain)*, *78*(1), 16601. http://doi.org/10.1088/0034-4885/78/1/016601

Privorotskaya, N., Liu, Y.-S., Lee, J., Zeng, H., Carlisle, J. a, Radadia, A., … King, W. P. (2010). Rapid thermal lysis of cells using silicon-diamond microcantilever heaters. *Lab on a Chip*, *10*(9), 1135–41. http://doi.org/10.1039/b923791g

Purssell, R. A., Pudek, M., Brubacher, J., & Abu-Laban, R. B. (2001). Derivation and validation of a formula to calculate the contribution of ethanol to the osmolal gap. *Annals of Emergency Medicine*, *38*(6), 653–659. http://doi.org/10.1067/mem.2001.119455

Raman, R., & Bashir, R. (2015). Stereolithographic 3D Bioprinting for Biomedical Applications. In *Essentials of 3D Biofabrication and Translation* (pp. 89–121). Elsevier. http://doi.org/10.1016/B978-0-12-800972-7.00006-2

Raman, R., & Bashir, R. (2017). Biomimicry, Biofabrication, and Biohybrid Systems: The Emergence and Evolution of Biological Design. *Advanced Healthcare Materials*, *6*(20), 1–20. http://doi.org/10.1002/adhm.201700496

Raman, R., Bhaduri, B., Mir, M., Shkumatov, A., Lee, M. K., Popescu, G., … Bashir, R. (2016). High-Resolution Projection Microstereolithography for Patterning of Neovasculature. *Advanced Healthcare Materials*, *5*(5), 610–619. http://doi.org/10.1002/adhm.201500721

Raman, R., Grant, L., Seo, Y., Cvetkovic, C., Gapinske, M., Palasz, A., … Bashir, R. (2017). Damage, Healing, and Remodeling in Optogenetic Skeletal Muscle Bioactuators. *Advanced Healthcare Materials*, *6*(12), 1–9. http://doi.org/10.1002/adhm.201700030

Ramiro-Diaz, J., Barajas-Espinosa, A., Chi-Ahumada, E., Perez-Aguilar, S., Torres-Tirado, D., Castillo-Hernandez, J., … Castillo-Hernandez, D. (n.d.). Luminal endothelial lectins with affinity for N-acetylglucosamine determine flow-induced cardiac and vascular paracrine-dependent responses. Retrieved from http://ajpheart.physiology.org/content/ajpheart/299/3/H743.full.pdf

Regehr, K. J., Domenech, M., Koepsel, J. T., Carver, K. C., Ellison-Zelski, S. J., Murphy, W. L., … Beebe, D. J. (2009). Biological implications of polydimethylsiloxane-based microfluidic

cell culture. *Lab on a Chip*, *9*(15), 2132. http://doi.org/10.1039/b903043c

Ren, X., Weisgerber, D. W., Bischoff, D., Lewis, M. S., Reid, R. R., He, T.-C., … Lee, J. C. (2016). Nanoparticulate Mineralized Collagen Scaffolds and BMP-9 Induce a Long-Term Bone Cartilage Construct in Human Mesenchymal Stem Cells. *Advanced Healthcare Materials*, *5*(14), 1821–1830. http://doi.org/10.1002/adhm.201600187

Rizvi, I., Gurkan, U. A., Tasoglu, S., Alagic, N., Celli, J. P., Mensah, L. B., … Hasan, T. (2013). Flow induces epithelial-mesenchymal transition, cellular heterogeneity and biomarker modulation in 3D ovarian cancer nodules. *Proceedings of the National Academy of Sciences of the United States of America*, *110*(22), E1974–E1983. JOUR. http://doi.org/10.1073/pnas.1216989110

Roxworthy, B. J., Johnston, M. T., Lee-Montiel, F. T., Ewoldt, R. H., Imoukhuede, P. I., & Toussaint, K. C. (2014). Plasmonic optical trapping in biologically relevant media. *PloS One*, *9*(4), e93929. http://doi.org/10.1371/journal.pone.0093929

Salwitz, J. C. (2012). The Future is Now: Personalized Medicine. Retrieved from http://blogs.cancer.org/expertvoices/2012/04/18/the-future-is-now-personalized-medicine/

Samijo, S. K., Willigers, J. M., Barkhuysen, R., Kitslaar, P. J., Reneman, R. S., Brands, P. J., … Hoeks, a P. (1998). Wall shear stress in the human common carotid artery as function of age and gender. *Cardiovascular Research*, *39*(2), 515–522. http://doi.org/10.1016/S0008-6363(98)00074-1

Saneinejad, S., & Shoichet, M. S. (1998). Patterned glass surfaces direct cell adhesion and process outgrowth of primary neurons of the central nervous system. *Journal of Biomedical Materials Research*, *42*(1), 13–19. http://doi.org/10.1002/(SICI)1097-4636(199810)42:1<13::AID-JBM3>3.0.CO;2-R

Saunders, N. A., Simpson, F., Thompson, E. W., Hill, M. M., Endo-Munoz, L., Leggatt, G., … Guminski, A. (2012). Role of intratumoural heterogeneity in cancer drug resistance: molecular and clinical perspectives. *EMBO Molecular Medicine*, *4*(8), 675–684. http://doi.org/10.1002/emmm.201101131

Scherr, T., Quitadamo, C., Tesvich, P., Park, D. S., Tiersch, T., Hayes, D., … Monroe, W. T. (2012). A Planar Microfluidic Mixer Based on Logarithmic Spirals. *J Micromech Microeng*, *22*(5), 55019. http://doi.org/10.1088/0960-1317/22/5/055019

Schneider, B. P., & Sledge, G. W. (2007). Drug insight: VEGF as a therapeutic target for breast cancer. *Nature Clinical Practice. Oncology*, *4*(3), 181–9. http://doi.org/10.1038/ncponc0740

Séguin, C., McLachlan, J. M., Norton, P. R., & Lagugné-Labarthet, F. (2010). Surface modification of poly(dimethylsiloxane) for microfluidic assay applications. *Applied Surface Science*, *256*(8), 2524–2531. http://doi.org/10.1016/j.apsusc.2009.10.099

Shaporenko, A., Cyganik, P., Buck, M., Terfort, A., & Zharnikov, M. (2005). Self-assembled monolayers of aromatic selenolates on noble metal substrates. *Journal of Physical Chemistry B*, *109*(28), 13630–13638. http://doi.org/10.1021/jp050731r

Sharma, S. V, Lee, D. Y., Li, B., Quinlan, M. P., Takahashi, F., Maheswaran, S., … Settleman, J. (2010). A chromatin-mediated reversible drug-tolerant state in cancer cell subpopulations. *Cell*, *141*(1), 69–80. http://doi.org/10.1016/j.cell.2010.02.027

Sheng, W., Chen, T., Kamath, R., Xiong, X., Tan, W., & Fan, Z. H. (2012). Aptamer-enabled efficient isolation of cancer cells from whole blood using a microfluidic device. *Analytical Chemistry*, *84*(9), 4199–4206. http://doi.org/10.1021/ac3005633

Shields, C. W., Reyes, C. D., López, G. P., Wyatt Shields IV, C., Reyes, C. D., & López, G. P. (2015). Microfluidic cell sorting: a review of the advances in the separation of cells from debulking to rare cell isolation. *Lab on a Chip*, *15*(5), 1230–49. http://doi.org/10.1039/c4lc01246a

Sigal, G. B., Mrksich, M., & Whitesides, G. M. (1998). Effect of surface wettability on the adsorption of proteins and detergents. *Journal Of The American Chemical Society*, *120*(14), 3464–3473. http://doi.org/10.1021/ja970819l

Silva, A. K. A., Richard, C., Ducouret, G., Bessodes, M., Scherman, D., & Merten, O. W. (2013). Xyloglucan-derivatized films for the culture of adherent cells and their thermocontrolled detachment: A promising alternative to cells sensitive to protease treatment. *Biomacromolecules*, *14*(2), 512–519. http://doi.org/10.1021/bm3017737

Song, Y., Tian, T., Shi, Y., Liu, W., Zou, Y., Khajvand, T., … Yang, C. (2017). Enrichment and single-cell analysis of circulating tumor cells. *Chem. Sci.*, *8*(3), 1736–1751. http://doi.org/10.1039/C6SC04671A

Stachelek, S. J., Finley, M. J., Alferiev, I. S., Wang, F., Tsai, R. K., Eckells, E. C., … Levy, R. J. (2011). The effect of CD47 modified polymer surfaces on inflammatory cell attachment and activation. *Biomaterials*, *32*(19), 4317–4326. http://doi.org/10.1016/j.biomaterials.2011.02.053

Strehle, K. R., Cialla, D., Rösch, P., Henkel, T., Köhler, M., & Popp, J. (2007). A reproducible surface-enhanced Raman spectroscopy approach. Online SERS measurements in a segmented microfluidic system. *Analytical Chemistry*, *79*(4), 1542–1547. http://doi.org/10.1021/ac0615246

Su, X., Wu, Y.-J., Robelek, R., & Knoll, W. (2005). Surface plasmon resonance spectroscopy and quartz crystal microbalance study of streptavidin film structure effects on biotinylated DNA assembly and target DNA hybridization. *Langmuir : The ACS Journal of Surfaces and Colloids*, *21*(1), 348–53. http://doi.org/10.1021/la047997u

Sudarsan, A. P., & Ugaz, V. M. (2006). Fluid mixing in planar spiral microchannels. *Lab Chip*, *6*(1), 74–82. http://doi.org/10.1039/B511524H

Swaminathan, V. V., Gannavaram, S., Li, S., Hu, H., Yeom, J., Wang, Y., & Zhu, L. (2013). Microfluidic platform with hierarchical micro/nanostructures and SELEX nucleic acid aptamer coating for isolation of circulating tumor cells. *Proceedings of the IEEE Conference on Nanotechnology*, (c), 370–373. http://doi.org/10.1109/NANO.2013.6720968

T, S. C. P., & Papaioannou T, S. C. (2005). Vascular wall shear stress: basic principles and methods. *Hellenic J Cardiol*, *46*, 9–15. JOUR.

Tanzeglock, T., Soos, M., Stephanopoulos, G., & Morbidelli, M. (2009). Induction of mammalian cell death by simple shear and extensional flows. *Biotechnology and Bioengineering*, *104*(2), 360–70. http://doi.org/10.1002/bit.22405

Toepke, M. W., & Beebe, D. J. (2006). PDMS absorption of small molecules and consequences in microfluidic applications. *Lab on a Chip*, *6*(12), 1484. http://doi.org/10.1039/b612140c

Togo, M., Takamura, A., Asai, T., Kaji, H., & Nishizawa, M. (2007). An enzyme-based microfluidic biofuel cell using vitamin K 3 -mediated glucose oxidation. *Electrochimica Acta*, *52*, 4669–4674. http://doi.org/10.1016/j.electacta.2007.01.067

Tsao, C. W. (2016). Polymer microfluidics: Simple, low-cost fabrication process bridging academic lab research to commercialized production. *Micromachines*, *7*(12), 225. http://doi.org/10.3390/mi7120225

Tsao, C. W., & DeVoe, D. L. (2009). Bonding of thermoplastic polymer microfluidics. *Microfluidics and Nanofluidics*, *6*(1), 1–16. http://doi.org/10.1007/s10404-008-0361-x

Valencia, P. M., Farokhzad, O. C., Karnik, R., & Langer, R. (2012). Microfluidic technologies for accelerating the clinical translation of nanoparticles. *Nature Nanotechnology*, *7*(10), 623–629. http://doi.org/10.1038/nnano.2012.168

van Beijnum, J. R., Rousch, M., Castermans, K., van der Linden, E., & Griffioen, A. W. (2008). Isolation of endothelial cells from fresh tissues. *Nature Protocols*, *3*(6), 1085–1091. http://doi.org/10.1038/nprot.2008.71

Vanka, S. P., Luo, G., & Winkler, C. M. (2004). Numerical study of scalar mixing in curved channels at low Reynolds numbers. *AIChE Journal*, *50*(10), 2359–2368. http://doi.org/10.1002/aic.10196

Vanka, S. P., Winkler, C. M., Coffman, J., Linderman, E., Mahjub, S., & Young, B. (2003). Novel Low Reynolds Number Mixers for Microfluidic Applications. *ASME Conference Proceedings*, *2003*(36975), 887–892. http://doi.org/10.1115/FEDSM2003-45122

Vasdekis, A. E., O 'neil, C. P., Hubbell, J. A., & Psaltis, D. (n.d.). Microfluidic Assays for DNA Manipulation Based on a Block Copolymer Immobilization Strategy. http://doi.org/10.1021/bm901453u

Vermette, P., Gengenbach, T., Divisekera, U., Kambouris, P. A., Griesser, H. J., & Meagher, L. (2003). Immobilization and surface characterization of NeutrAvidin biotin-binding protein on different hydrogel interlayers. *Journal of Colloid and Interface Science*, *259*(1), 13–26. http://doi.org/10.1016/S0021-9797(02)00185-6

Vukasinovic, J., Cullen, D. K., LaPlaca, M. C., & Glezer, A. (2009). A microperfused incubator for tissue mimetic 3D cultures. *Biomedical Microdevices*, *11*(6), 1155–1165. http://doi.org/10.1007/s10544-009-9332-6

Waheed, S., Cabot, J. M., Macdonald, N. P., Lewis, T., Guijt, R. M., Paull, B., & Breadmore, M. C. (2016). 3D printed microfluidic devices: enablers and barriers. *Lab Chip*, *16*(11), 1993–2013. http://doi.org/10.1039/C6LC00284F

Walczak, M. M., Chung, C., Stole, S. M., Widrig, C. A., & Porter, M. D. (1991). Structure and Interfacial Properties of Spontaneously Adsorbed n-Alkanethiolate Monolayers on Evaporated Silver Surfaces. *Journal of the American Chemical Society*, *113*(7), 2370–2378. http://doi.org/10.1021/ja00007a004

Wan, Y., Kim, Y. T., Li, N., Cho, S. K., Bachoo, R., Ellington, A. D., & Iqbal, S. M. (2010). Surface-immobilized aptamers for cancer cell isolation and microscopic cytology. *Cancer Research*, *70*(22), 9371–9380. http://doi.org/10.1158/0008-5472.CAN-10-0568

Wan, Y., Liu, Y., Allen, P. B., Asghar, W., Mahmood, M. A. I., Tan, J., … Iqbal, S. M. (2012). Capture, isolation and release of cancer cells with aptamer-functionalized glass bead array. *Lab on a Chip*, *12*(22), 4693–701. http://doi.org/10.1039/c2lc21251j

Watkins, N. N., Hassan, U., Damhorst, G., Ni, H., Vaid, A., Rodriguez, W., & Bashir, R. (2013). Microfluidic CD4+ and CD8+ T lymphocyte counters for point-of-care HIV diagnostics using whole blood. *Science Translational Medicine*, *5*(214), 214ra170. http://doi.org/10.1126/scitranslmed.3006870

Weddell, J. C., & Imoukhuede, P. I. (2014). Quantitative characterization of cellular membrane-receptor heterogeneity through statistical and computational modeling. *PLoS ONE*, *9*. http://doi.org/10.1371/journal.pone.0097271

Weddell, J. C., Kwack, J., Imoukhuede, P. I., & Masud, A. (2015). Hemodynamic analysis in an idealized artery tree: Differences in wall shear stress between Newtonian and non-Newtonian blood models. *PLoS ONE*, *10*(4). http://doi.org/10.1371/journal.pone.0124575

Weickhardt, A. J., Williams, D. S., Lee, C. K., Chionh, F., Simes, J., Murone, C., … Tebbutt, N. C. (2015). Vascular endothelial growth factor D expression is a potential biomarker of bevacizumab benefit in colorectal cancer. *British Journal of Cancer*, *113*(1), 37–45. http://doi.org/10.1038/bjc.2015.209

Welch, N. G., Scoble, J. A., Muir, B. W., & Pigram, P. J. (2017). Orientation and characterization of immobilized antibodies for improved immunoassays (Review). *Biointerphases*, *12*(2), 02D301. http://doi.org/10.1116/1.4978435

Wilchek, M., & Bayer, E. a. (1990). Introduction to Avidin-Biotin technology. *Methods in Enzymology*, *184*, 5–13.

Wilchek, M., & Bayer, E. A. (1987). Applications of Avidin-Biotin Technology: Literature Survey. *Methods in Enzymology*, *152*(1), 183–189.

Willett, C. G., Boucher, Y., di Tomaso, E., Duda, D. G., Munn, L. L., Tong, R. T., … Jain, R. K. (2004). *Direct evidence that the VEGF-specific antibody bevacizumab has antivascular effects in human rectal cancer. Nature medicine* (Vol. 10).

William Chen, H., Medley, C. D., Smith, J. E., Sefah, K., Shangguan, D., Tang, Z., … Tan

Professor, W. (n.d.). Molecular Recognition of Small Cell Lung Cancer Cells Using Aptamers. http://doi.org/10.1002/cmdc.200800030

Wu, H.-W., Lin, C.-C., & Lee, G.-B. (2011). Stem cells in microfluidics. *Biomicrofluidics*, *5*(1), 13401. http://doi.org/10.1063/1.3528299

Wu, L., Guan, G., Hou, H. W., Bhagat, A. A. S., & Han, J. (2012). Separation of leukocytes from blood using spiral channel with trapezoid cross-section. *Analytical Chemistry*, *84*(21), 9324–9331. http://doi.org/10.1021/ac302085y

Wu, L., Wang, Z., Zong, S., & Cui, Y. (2014). Rapid and reproducible analysis of thiocyanate in real human serum and saliva using a droplet SERS-microfluidic chip. *Biosensors and Bioelectronics*, *62*, 13–18. http://doi.org/10.1016/j.bios.2014.06.026

Wynick, D., & Bloom, S. (1990). Magnetic bead separation of anterior pituitary cells. *Neuroendocrinology*. Retrieved from http://scholar.google.com/scholar?hl=en&btnG=Search&q=intitle:No+Title#0

Yamada, N., Okano, T., Sakai, H., Karikusa, F., Sawasaki, Y., & Sakurai, Y. (1990). Thermo-responsive polymeric surfaces; control of attachment and detachment of cultured cells. *Die Makromolekulare Chemie, Rapid Communications*, *11*(11), 571–576. http://doi.org/10.1002/marc.1990.030111109

Ye, X., Zhao, Q., Sun, X., & Li, H. (2009). Enhancement of mesenchymal stem cell attachment to decellularized porcine aortic valve scaffold by in vitro coating with antibody against CD90: a preliminary study on antibody-modified tissue-engineered heart valve. *Tissue Engineering. Part A*, *15*(1), 1–11. http://doi.org/10.1089/ten.tea.2008.0001

Yi-Qiang, F., Mei, W., & ZHANG, Y.-J. (2016). Recent Progress of 3D Printed Microfluidics Technologies. *CHINESE JOURNAL OF ANALYTICAL CHEMISTRY*, *44*(4), 551–561. http://doi.org/10.11895/j.issn.0253-3820.160119

Yousaf, M. N., Houseman, B. T., & Mrksich, M. (2001). Using electroactive substrates to pattern the attachment of two different cell populations. *Proceedings of the National Academy of Sciences*, *98*(11), 5992–5996. http://doi.org/10.1073/pnas.101112898

Yu, C. C., Ho, B. C., Juang, R. S., Hsiao, Y. S., Naidu, R. V. R., Kuo, C. W., … Chen, P. (2017). Poly(3,4-ethylenedioxythiophene)-Based Nanofiber Mats as an Organic Bioelectronic Platform for Programming Multiple Capture/Release Cycles of Circulating Tumor Cells. *ACS Applied Materials and Interfaces*, *9*(36), 30329–30342. http://doi.org/10.1021/acsami.7b07042

Yu, M., Stott, S., Toner, M., Maheswaran, S., & Haber, D. A. (2011). Circulating tumor cells: approaches to isolation and characterization. *The Journal of Cell Biology*, *192*(3), 373–382. http://doi.org/10.1083/jcb.201010021

Zhang, P., Chen, L., Xu, T., Liu, H., Liu, X., Meng, J., … Wang, S. (2013). Programmable fractal nanostructured interfaces for specific recognition and electrochemical release of cancer cells. *Advanced Materials*, *25*(26), 3566–3570.

http://doi.org/10.1002/adma.201300888

Zhu, F., Macdonald, N., Skommer, J., & Wlodkowic, D. (2015). Biological implications of lab-on-a-chip devices fabricated using multi-jet modelling and stereolithography processes. In S. van den Driesche (Ed.), *SPIE Microtechnologies* (p. 951808). International Society for Optics and Photonics. http://doi.org/10.1117/12.2180743

Ziegler, A., Koch, A., Krockenberger, K., & Großhennig, A. (2012). Personalized medicine using DNA biomarkers: A review. *Human Genetics*. http://doi.org/10.1007/s00439-012-1188-9